MAP No.	ASSESSMENT REPORT N. M. E. A. P. CONFIDENTIAL OPEN FILE		TYPE OF WORK: Thesis
115-A,B,G,H		X	

REPORT FILED UNDER	Rec. Study of Granites, SW Yukon DOCUMENT NO. 061641
DATE PERFORMED	DATE FILED: Oct. 31, 1977
LOCATION - LAT.	60°00' - 62°00'N AREA: Southwestern Yukon
LONG.	136°00' - 141°00'W
CLAIM NO.	
VALUE $	
WORK DONE BY	D.C. Way (Queen's University)
WORK DONE FOR	Indian and Northern Affairs
REMARKS	A Reconnaissance Study of Granitoid Plutonism in Southwestern Yukon Territory.

A RECONNAISSANCE STUDY OF GROUNDWATER FEATURES IN SOUTHWESTERN YUKON TERRITORY

DANA CLARK WAY

1977



Government of Canada
Gouvernement du Canada

Industry, Trade and Commerce
Industrie et Commerce

D.C. Way

Iron and Steel Division
Metals and Minerals Group
Resource Industries Branch

Ottawa, Canada
K1A 0H5

(613) 992-0025

A RECONNAISSANCE STUDY OF GRANITOID PLUTONISM IN SOUTHWESTERN YUKON TERRITORY

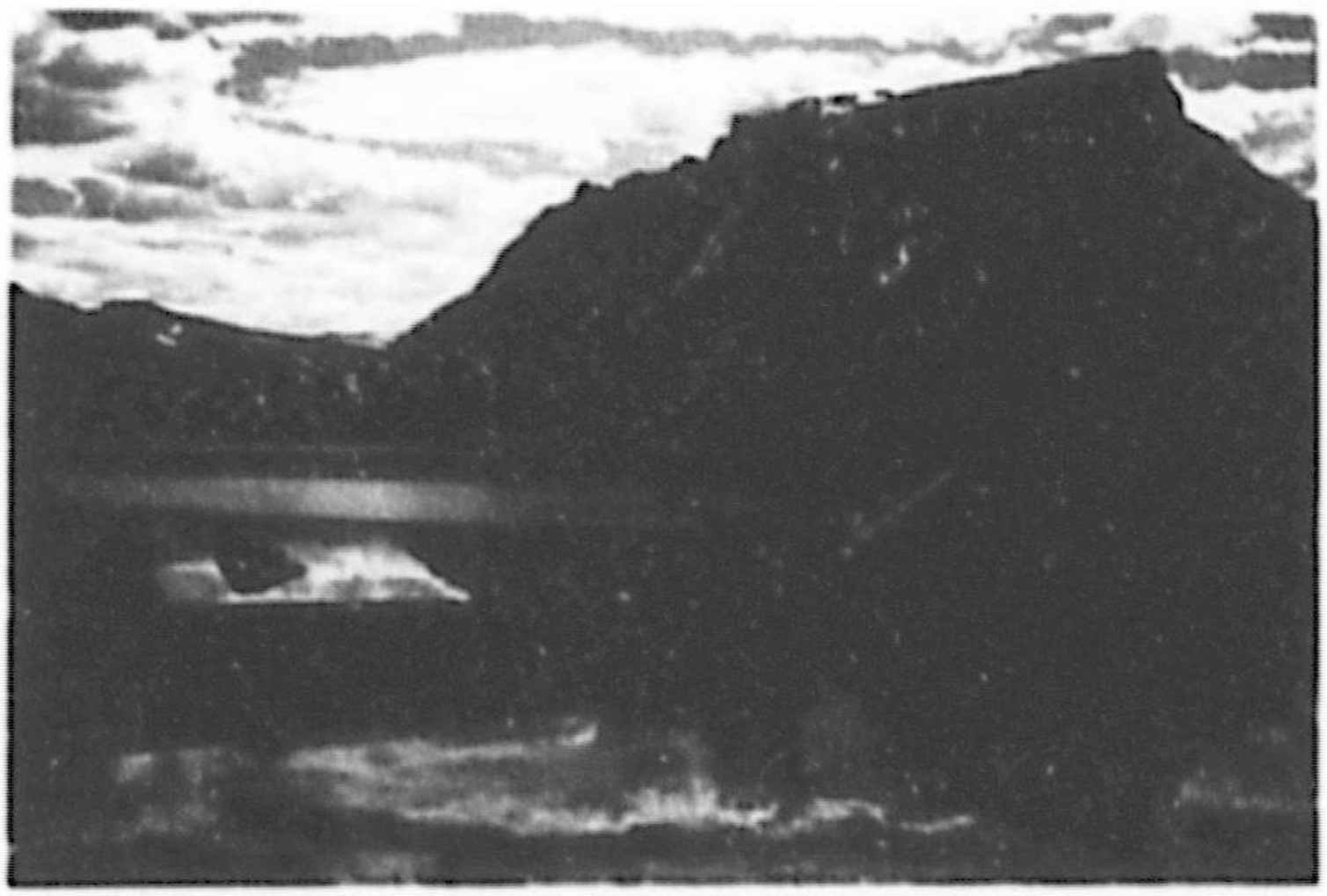
by

Dana Clark Way

A thesis submitted to the
Department of Geological Sciences
in conformity with the requirements
for the degree of Master of Science

Queen's University
Kingston, Ontario, Canada
September, 1977

copyright © Dana Clark Way, 1977



Frontispiece: View of Ark Mountain on Kusawa Lake in the southern part of the Ruby Range Batholith.

TABLE OF CONTENTS

Page

ABSTRACT ----------

ACKNOWLEDGEMENTS ----------

CHAPTER 1 - INTRODUCTION ---------- 1

1.1 Setting ---------- 1
1.2 Previous Geological Work ---------- 3
1.3 Physiography and Topography ---------- 5
1.4 Glaciology ---------- 9
1.5 Purpose of the thesis ---------- 11

CHAPTER 2 - GENERAL GEOLOGY ---------- 14

2.1 Introduction ---------- 14
2.2 Formations Southwest of the Denali-Shakwak Fault ---------- 15
2.3 Formations Northeast of the Denali-Shakwak Fault ---------- 29
2.4 Suite Names for Granitoid Rocks ---------- 37

CHAPTER 3 - REGIONAL TECTONIC FRAMEWORK ---------- 39

3.1 Introduction ---------- 39
3.2 Tectonic Framework Southwest of the Denali-Shakwak Fault ---------- 39
3.3 Tectonic Framework Northeast of the Denali-Shakwak Fault ---------- 49

CHAPTER 4 - GEOCHRONOLOGY OF GRANITOID PLUTONISM ---------- 58

4.1 Introduction ---------- 58
4.2 Geochronology of Plutonism Southwest of the Denali-Shakwak Fault ---------- 59
4.2.1 Alexander Terrane ---------- 62
4.2.2 Gravina-Nutzotin Belt and Taku-Skolai Terrane ---------- 67
4.2.3 Summary ---------- 69
4.3 Geochronology of Plutonism Northeast of the Denali-Shakwak Fault ---------- 71

	Page
CHAPTER 5 - PETROGRAPHY OF GRANITOID ROCKS IN SOUTHWESTERN YUKON	88
5.1 Introduction	88
5.2 Petrography of Granitoid Rocks Southwest of the Denali-Shakwak Fault	89
5.3 Petrography of Granitic Rocks Northeast of the Denali-Shakwak Fault	98
CHAPTER 6 - GEOCHEMISTRY OF GRANITOID PLUTONISM	110
6.1 Introduction	110
6.2 Geochemistry of Granitoid Rocks Southwest of the Denali-Shakwak Fault	110
6.3 Geochemistry of Granitoid Rocks Northeast of the Denali-Shakwak Fault	126
CHAPTER 7 - TECTONIC RECONSTRUCTIONS IN SOUTHWESTERN YUKON	148
7.1 Introduction	148
7.2 Constraints and Tectonic Reconstructions	150
7.2.1 Alexander Terrane and Icefield Range Granite	150
7.2.2 The Taku-Skolai Terrane	152
7.2.3 Interrelationships of Alexander and Taku-Skolai Terranes	156
7.2.4 Post-Triassic Events at the Continental Margin	161
7.3 Summary	168
BIBLIOGRAPHY	171
APPENDIX A - ANALYTICAL METHODS	178
VITA	186
ADDENDUM - Trace Element Analyses	(in pocket)

TABLES

		Page
4.1	Analytical data for K/Ar determinations: Icefield Range Granite, Kluane Range Diorite, Kluane Range Porphyry ----------	60
4.2	Analytical data for K/Ar determinations: Nisling Range Granodiorite, Ruby Range Granodiorite, Nisling Range Alaskite ----------	72
5.1	Modes of granitoid rocks southwest of Denali-Shakwak Fault ----------	91
5.2	Modes of granitoid rocks northeast of Denali-Shakwak Fault ----------	99
6.1	Major and minor element analyses for granitic rocks southwest of Denali-Shakwak Fault ----------	111
6.2	Average trace element values for igneous suites southwest of Denali-Shakwak Fault ----------	123
6.3	Major and minor element analyses for granitic rocks northeast of Denali-Shakwak Fault ----------	127
6.4	Average trace element values for igneous suites northeast of the Denali-Shakwak Fault ----------	146

FIGURES

		Page
Fig. 1.1	Location of project area with respect to major geological and physiographic features and 4-mile scale map areas ----------	2
Fig. 1.2	View looking south over Icefield Ranges -------	7
Fig. 1.3	View looking north to Ruby Ranges from Kluane Lake ----------	8
Fig. 1.4	View looking southwestward up the Kaksawulsh Glacier ----------	10
Fig. 1.5	View looking west across the surface of the Donjek Glacier ----------	10
Fig. 2.1	View looking west across Steele Creek and the terminus of Steele Glacier at flat-lying Wrangell Lavas ----------	28
Fig. 2.2	Exposure of unconsolidated sediments in road cut, South Canol Road ----------	30
Fig. 2.3	View of limestone roof pendant in the Ruby Range Batholith ----------	32
Fig. 2.4	Ruby Range Granodiorite containing mafic xenoliths near contact with Kluane Schist -----	35
Fig. 3.1	Generalized geological map of eastern and southeastern Alaska and southwestern Yukon ----------	40
Fig. 3.2	Sketch map of North American Cordillera -------	51
Fig. 3.3	Plate tectonic interpretation, from Lower Jurassic to Oligocene, in Canadian Cordillera ----------	52
Fig. 3.4	Tectonic subdivisions of the Canadian Cordillera, showing the disposition of the Yukon Crystalline Terrane ----------	53

		Page
Fig. 3.5	Hypothetical restored sections showing evolution of the Yukon Crystalline Terrane ----	56
Fig. 4.1	K/Ar dates from plutonic rocks in St. Elias Mountains compared with ages of granitic rocks from Eastern Alaska Range and southeastern Alaska ----------	65
Fig. 4.2	Comparison of K/Ar dates for Nisling Range Granodiorite, Ruby Range Granodiorite and Nisling Range Alaskite ----------	76
Fig. 4.3	Comparative histogram of new and previously published radiometric dates for Ruby Range Granodiorite and Nisling Range Alaskite ----------	80
Fig. 4.4	Migmatite at contact of Ruby Range Granodiorite and Kluane Schist ----------	81
Fig. 5.1	Quartz-plagioclase-potassium feldspar modal diagram for Icefield Range Granite, Kluane Range Diorite, and Kluane Range Porphyry suites ----------	90
Fig. 5.2	Photographs of Icefield Range Granite specimen showing texture and mineralogy with and without staining for potassium feldspar ---	95
Fig. 5.3	Photographs of Kluane Range Diorite specimen showing texture and mineralogy with and without staining for potassium feldspar -------	96
Fig. 5.4	Photographs of Kluane Range Porphyry specimen showing texture and mineralogy with and without staining for potassium feldspar ----------	97
Fig. 5.5	Quartz-plagioclase-potassium feldspar modal diagram for Nisling Range Granodiorite, Ruby Range Granodiorite and Nisling Range Alaskite suites ----------	102

Page

Fig. 5.6 Photographs of Nisling Range Granodiorite specimen showing texture and mineralogy with and without staining for potassium feldspar ---------- 107

Fig. 5.7 Photographs of Ruby Range Granodiorite specimen showing texture and mineralogy with and without staining for potassium feldspar ------- 108

Fig. 5.8 Photographs of Nisling Range Alaskite specimen showing texture and mineralogy with and without staining for potassium feldspar ---------- 109

Fig. 6.1 AFM plot for Icefield Range Granite, Kluane Range Diorite and Kluane Range Porphyry suites ---------- 118

Fig. 6.2 K_2O vs SiO_2 plot for Icefield Range Granite, Kluane Range Diorite and Kluane Range Porphyry suites ---------- 120

Fig. 6.3 $(K_2O + Na_2O)$ vs SiO_2 plot for Icefield Range Granite, Kluane Range Diorite and Kluane Range Porphyry suites ---------- 122

Fig. 6.4 AFM plot for Nisling Range Granodiorite, Ruby Range Granodiorite and Nisling Range Alaskite suites ---------- 138

Fig. 6.5 K_2O vs SiO_2 plot for Nisling Range Granodiorite, Ruby Range Granodiorite and Nisling Range Alaskite suites ---------- 140

Fig. 6.6 Variation in K_2O across Ruby Range Batholith and Nisling Range ---------- 142

Fig. 6.7 Variation in potash index $[(K_2O/SiO_2-45) \times 10^3]$ across Ruby Range Batholith and Nisling Range ---------- 144

Page

Fig. 7.1 Plate tectonic interpretation from Late Pennsylvanian to Lower Permian ---------- 158

Fig. 7.2 Plate tectonic interpretations from Middle Triassic to Jurassic ---------- 162

Fig. 7.3 Plate tectonic interpretation from Cretaceous to Miocene ---------- 165

MAP (in pocket)

1 Map of project area showing plutons, sample locations, and major structural and physiographic features (scale: 1" = 4 miles).

ABSTRACT

Granitic rocks bordering the Denali-Shakwak Fault in southwestern Yukon are assigned to six distinct plutonic suites using a combination of geochronological, geochemical and petrographical data, as follows:

Suites Southwest of Denali-Shakwak Fault

Icefield Range Granite	140-175 m.y. 260-265 m.y.	calc-alkaline affinity	diorite to alaskite
Kluane Range Diorite	110-120 m.y.	tholeiitic affinity	diorite to quartz diorite
Kluane Range Porphyry	25 m.y.	calc-alkaline affinity	feldspar porphyry

Suites Northeast of Denali-Shakwak Fault

Nisling Range Granodiorite	100 m.y.	calc-alkaline affinity	granodiorite
Ruby Range Granodiorite	55-65 m.y.	calc-alkaline affinity	granodiorite and quartz monzonite
Nisling Range Alaskite	55 m.y.	calc-alkaline affinity	alaskite and quartz monzonite

These observations and published information for contiguous eastern and southeastern Alaska are incorporated into a tentative plate tectonic model for southwestern Yukon for the Late Paleozoic to mid-Tertiary interval. It is suggested that the Alexander and Taku-Skolai terranes had become sutured prior to the Upper Permian, and that this occurred through northeastward overthrusting of Alexander terrane over a Taku-Skolai volcanic arc. Plutonism and ensialic volcanism continued into Upper Jurassic within the resulting microcontinent, as it was carried towards the North American plate through closure of the intervening oceanic basin. An Andean-type magmatic arc is presumed to have been developing at the western margin of the continent at this time.

Following partial clogging of the oceanic basin by clastic debris in the Upper Jurassic and Lower Cretaceous, collision occurred

in the Eocene, causing abrupt uplift of the continental margin and cooling of Paleocene mesozonal plutons. Subduction persisted at the new western margin of the continent; however, the angle of convergence decreased through the mid-Tertiary, ultimately resulting in the Miocene in a cessation of underthrusting and the initiation of major dextral transcurrent faulting, accompanied by rapid uplift and widespread subaerial volcanism.

ACKNOWLEDGEMENTS

The writer wishes to express his appreciation to the Department of Indian and Northern Affairs who provided a generous research grant to support the work presented here and who also provided employment for a number of field seasons. In particular, gratitude is expressed to Dr. D. B. Craig, resident geologist for D.I.N.A. in Whitehorse, who encouraged the writer to undertake graduate work, arranged the necessary financial support, and provided logistical support essential for carrying out a field program in such a large area.

Financial support was also received from Queen's University through a Reinhardt Fellowship, teaching assistantships, and, also in part, through a National Research Council operating grant to Dr. A. H. Clark. This additional support is gratefully acknowledged.

Special thanks are due to Dr. A. H. Clark, Queen's University, for supervising the research program and for providing guidance which was instrumental in the completion of the thesis. The work also benefited from stimulating discussion with Mr. E. Procyshyn, Queen's University.

Dr. E. Farrar and Mr. D. A. Archibald, Queen's University, determined the K/Ar dates presented here which constitute an integral part of this research program. Mr. Frank Dunphy, and the late Mr. Leo Mes, assisted with the major and minor element analyses, respectively.

The Resource Industries Branch, Department of Industry, Trade and Commerce, where the writer is presently employed, permitted a leave-of-absence for the purpose of returning to Queen's University to finish the thesis.

Finally, thanks are extended to Ms. Brenda Mitton, who typed the manuscript, and also to the Examining Committee, who were prepared to undertake their tasks on short notice and permitted the writer to meet certain time constraints.

CHAPTER 1

INTRODUCTION

1.1 Setting

The present thesis summarizes the results of a reconnaissance study of plutonic rocks over an area in excess of 10,000 square miles, in southwestern Yukon Territory. The project area is contained within four, 4-mile scale, map-areas (Kluane Lake, Aishihik Lake, Dezadeash and Kaskawulsh), and is bounded by latitudes 60°N - 62°N and longitudes 136°W - 141°W (see Fig. 1.1). Much of the region is now included within the boundaries of Kluane National Park.

The Alaska Highway and the Haines Road, along with the less-travelled Aishihik Road, provide the main access to this part of the Yukon Territory (see Map 1, in pocket). A number of gravel airstrips are suitable for use by small planes, and floatplanes can make use of many of the lakes, but there are no scheduled air services to this part of the territory. Helicopters are eminently suitable for reaching areas which are otherwise almost inaccessible.

The region is only sparsely populated; most inhabitants live in small settlements along the Alaska Highway. The nearest major population centre is Whitehorse, capital of the territory, which lies about 120 miles east of the study area.

Weather in the summer is generally warm and dry, although

CHAPTER 1

INTRODUCTION

1.1 Setting

The present thesis summarizes the results of a reconnaissance study of plutonic rocks over an area in excess of 10,000 square miles, in southwestern Yukon Territory. The project area is contained within four, 4-mile scale, map-areas (Kluane Lake, Aishihik Lake, Dezadeash and Kaskawulsh), and is bounded by latitudes 60°N - 62°N and longitudes 136°W - 141°W (see Fig. 1.1). Much of the region is now included within the boundaries of Kluane National Park.

The Alaska Highway and the Haines Road, along with the less-travelled Aishihik Road, provide the main access to this part of the Yukon Territory (see Map 1, in pocket). A number of gravel airstrips are suitable for use by small planes, and floatplanes can make use of many of the lakes, but there are no scheduled air services to this part of the territory. Helicopters are eminently suitable for reaching areas which are otherwise almost inaccessible.

The region is only sparsely populated; most inhabitants live in small settlements along the Alaska Highway. The nearest major population centre is Whitehorse, capital of the territory, which lies about 120 miles east of the study area.

Weather in the summer is generally warm and dry, although

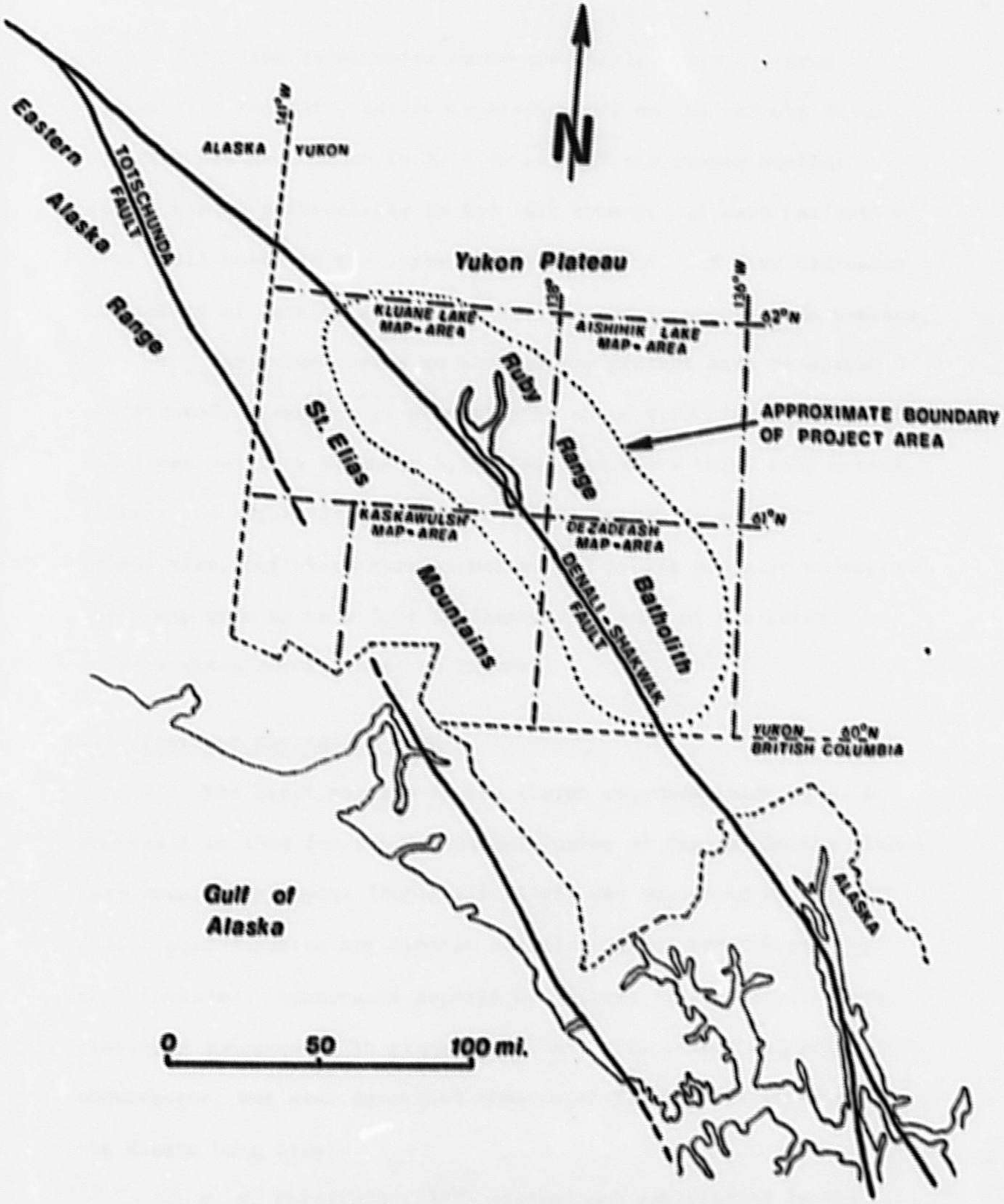


Fig. 1.1. Location of project area with respect to major geological and physiographic features and 4-mile scale map-areas.

brief, localized rainshowers occur frequently. Temperatures are usually moderate, rarely exceeding 30°C on the warmest days, but snow has been known to fall in each of the summer months. Strong winds, particularly in the late summer. can make navigation with small boats on the larger lakes dangerous, and also decreases the safety of working with small helicopters in mountainous terrane.

The forest cover in much of the project area is sparse and stunted. Treeline is generally at about 4,000 feet; scrub willow and alder continue to about 5,500 feet and above this, only mosses, lichens and alpine flowers occur. Black spruce is probably the most common tree, but white spruce, balsam and poplar are also widespread. These may grow up to a foot in diameter in some of the larger valleys where forest cover is thicker.

1.2 Previous Geological Work

The first mapping in the region was undertaken by R. G. McConnell in 1904 for the Geological Survey of Canada, in the Kluane Lake area. His report (McConnell, 1905) was concerned mainly with placer gold deposits but limited descriptions of bedrock geology were included. Subsequent reports by Cairnes (1915a, 1915b) were similarly concerned with placer gold, and with copper and gold occurrences, but also described aspects of the bedrock geology in the Kluane Lake area.

W. E. Cockfield (1927) carried out exploration in the

Aishihik Lake area in 1926 and, in the following year (Cockfield, 1928), mapped rocks along the Dalton trail in the Dezadeash map-area.

In 1941, the geology of Steele Creek in the Kluane map-area was studied by R. P. Sharp (1943). H. S. Bostock of the Geological Survey of Canada later (1945) carried out reconnaissance geological mapping along the Alaska Highway in the Kluane Lake map-area. His report (Bostock, 1952) also summarizes previously-published work.

Systematic geological mapping at the 4-mile scale was carried out in the Kluane Lake, Aishihik Lake, Dezadeash and Kaskawulsh map-areas by the following G.S.C. geologists: Muller (1967); Tempelman-Kluit (1974); Kindle (1952); and Wheeler (1963). Extensive reference will be made to these reports in this thesis.

A number of mineral occurrences are known in the area, but none are presently economic with the possible exception of some placer gold deposits which have been mined intermittently since the turn of the century. No important base metal deposits have been discovered. Copper is known to be associated with Mesozoic volcanics in the St. Elias Mountains and a few, small, high-grade deposits have been worked, but probably not more than a few thousand tons of ore have been produced. Nickel-copper deposits are associated with ultramafic rocks in the Kluane Ranges. The most important of these, the Wellgreen Property, was discovered in the early 1950's and mined by Hudson Bay Mining and Smelting Co. in 1971-1973. Ore reserves proved insufficient to sustain the operation for more than

this brief period. A number of small porphyry type deposits have been explored but have proven sub-economic.

1.3 Physiography and Topography

H. S. Bostock (1948, 1952) has given full descriptions of, and has named, the various physiographic subdivisions in the region. The most important single feature is probably the Shakwak Trench, a wide valley which follows the trace of the Denali-Shakwak Fault (see Map 1, in pocket), and separates two major physiographic divisions, the St. Elias Mountains to the southwest and the Yukon Plateau to the northeast. These two physiographic domains represent two vastly-different geological provinces separated by the Denali-Shakwak Fault. Since the fault bisects the project area, it has imposed a binary format on this thesis, as will become evident, whereby aspects of the rocks on the southwest side of the fault must be discussed separately from those on the northeast.

Southwest of the Shakwak Trench, the Kluane Ranges form the front ranges of the St. Elias Mountains. These rugged peaks rise steeply from the floor of the Shakwak Trench (elev. 2,575 feet a.s.l. at Kluane Lake) to a maximum elevation of about 8,500 feet. The Kluane Range is deeply dissected by V-shaped transverse valleys and broken by several major gaps where rivers drain through to the trench.

South and west of the Kluane Ranges, a chain of valleys

and plateaus, with a maximum elevation of about 5,000 feet, is known as the Duke Depression. For much of its length, it coincides with the Duke River Fault or other southwest-dipping thrust faults (see Map 1, in pocket).

South of the Duke Depression, the Icefield Ranges form the backbone of the St. Elias Mountains (see Fig. 1.2). This region includes some of the highest mountains in North America with eight summits over 15,000 ft., and much of it is covered by permanent snowfields and icefields and large valley glaciers.

The large valley glaciers, and the glacial rivers which flow from them, carry tremendous amounts of silt, sand and rock out of the Icefield Ranges to lower elevations (Figs. 1.4 and 1.5).

The Yukon Plateau, to the northeast of the Shakwak Trench, is an area of more subdued relief, and contrasts sharply with the St. Elias Mountains (see Fig. 1.3). Mountains are here generally in the range 4,000 - 6,000 feet, and have flat or rounded tops often covered with felsenmeer. The area is transected by a reticulate system of valleys that are filled with small lakes, swamps and low-gradient streams. Compared to the St. Elias Mountains, little erosion takes place.

Bostock (1948, 1952) recognized two physiographic subdivisions in this part of the Yukon Plateau. The Ruby Range lies directly north and east of the Shakwak Trench and, in the Kluane Lake and Aishihik Lake map-areas, is flanked to the north by the



Fig. 1.2. View looking south over Icefield Ranges. Peaks are at approximately 8,500 feet elevation.

Fig. 1.3. View looking north to Ruby Ranges from Kluane Lake. Terraced beaches of former glacial lakes are evident in centre portion of photo.



more subdued Nisling Range.

Several large lakes, 40 - 50 miles long and 2 - 4 miles wide, are noteable topographic features in this region (see Map 1, in pocket).

1.4 Glaciology

The region abounds with every sort of glacial phenomenon, both those relict from previous continental glaciation and those associated with current alpine glaciation in the St. Elias Mountains. As a result, most geological reports for the area, in particular those of Muller (1967) and Kindle (1952), contain excellent descriptions of glacial features and history. More recently, the American Geographical Society and Arctic Institute of North America , have sponsored the Icefield Ranges Research Project which has studied many features of alpine glaciation in the St. Elias Mountains. Results of these investigations have been published in a series of volumes by the sponsoring organizations. Figs. 1.4 and 1.5 show two of the larger valley glaciers, the Kaskawulsh and the Donjek, in the St. Elias Mountains.

In the Pleistocene epoch, ice-sheets covered much of the area at least once, and many parts were glaciated several times. Muller (1967) suggests that three separate ice-sheets advanced northwards out of the St. Elias Mountains, the most widespread and earliest advance reaching parts of the Nisling Range. Two later

Fig. 1.4. View looking southwestward up the Kaskawulsh Glacier.





Fig. 1.5. View looking west across the surface of the Donjek Glacier.

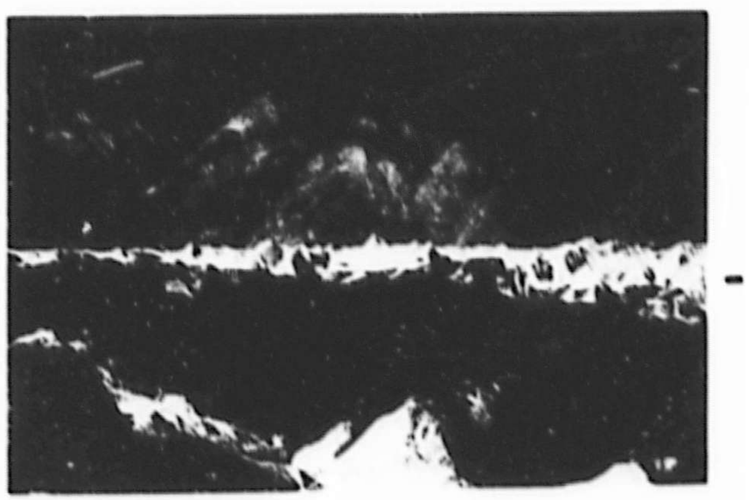
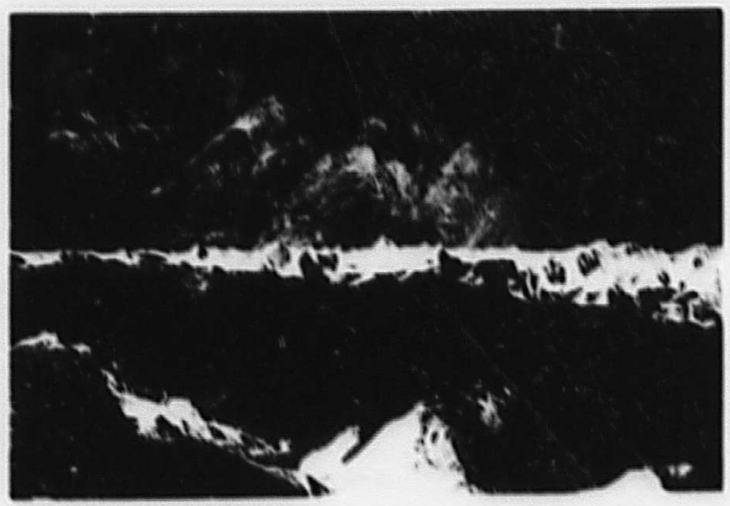




Fig. 1.4. View looking southwestward up the Kaskawulsh Glacier.



Fig. 1.5. . View looking west across the surface of the Donjek Glacier.



advances covered more restricted areas.

However, much of the Nisling Range, in the northeast part of the Kluane Lake map-area and in the northwest part of the Aishihik map-areas, is unglaciated. This accounts in part for the lack of fresh rock exposure in this area.

Muller (1967) and Kindle (1952) describe a number of large post-glacial lakes that occupied parts of the Shakwak Trench and connecting valleys after the waning of the large ice sheets. For example, a well-developed raised beach runs for many miles along the west shore of Kusawa lake about 365 feet above the present lake level. The presence of ice-rafted boulders in lake silts suggests that these lakes must still have been dammed to the southwest by St. Elias ice.

1.5 Purpose of the Thesis

The thesis project was originally conceived in early 1971 as a result of the writer's employment during the previous field season with the resident geologist's office of the Department of Indian and Northern Affairs in Whitehorse, Yukon. The original intent was to carry out a field program in southwestern Yukon with a strong orientation toward economic geology, including a study of some of the known porphyry-copper type deposits.

At the time, a number of exploration companies were carrying out drilling programs on low-grade, disseminated copper-

molybdenum deposits and there was considerable interest in this region as a porphyry-copper type province. However, the results of the exploration programs proved disappointing, and, moreover, much of the St. Elias Mountains was soon to be included within Kluane National Park. The outcome of these events was to bring about a de-emphasis of the economic geology aspect of the project.

Sampling of a number of granitoid plutons had already begun in the 1971 and it was decided, prior to the 1972 field season, to expand the sampling program with the intention of examining as many different plutons as possible. It was the opinion of the writer and his supervisor that a characterization of the plutonic rocks exposed on each side of the Denali-Shakwak Fault in southwestern Yukon, through a combination of geochronological, geochemical and petrographical analyses would lead to a more complete understanding of the geological evolution of this little-studied area. It is also hoped that this contribution, although indirect, will by expanding the geological information about the region, ultimately be of benefit to the mineral industry of the territory. With this in mind, an addendum to this thesis has been prepared for the Department of Indian and Northern Affairs which lists a number of trace element analyses of possible metallogenetic interest.

Reconnaissance sampling of the plutonic rocks was based on short traverses to plutons within walking distance of roads, sampling along the shores of large lakes by freighter canoe, and,

where other modes of transport were not feasible, sampling from helicopter. Outcrop in the immediate area of sample sites was examined to ensure sample representivity. The logistical support provided by Dr. D. B. Craig, resident geologist with Department of Indian and Northern Affairs in Whitehorse, made the collection of specimens from such a large area possible. In two summers, a total of about 14 weeks was spent in the field on this project.

At Queen's University, thin sections were made from many of the specimens and rock slabs were prepared for modal analyses. A number of biotite and hornblende mineral separates were prepared for K/Ar age determinations. Portions of all of the specimens were crushed (to -100 mesh) and analyzed for major and minor elements by X-ray fluorescence and emission spectroscopy respectively. Analyses for volatile content in small number of specimens were also carried out.

CHAPTER 2

GENERAL GEOLOGY

2.1 Introduction

Southwestern Yukon Territory is transected by the Denali-Shakwak Fault, a major crustal lineament which extends northwestward from Chatham Strait and Lynn Canal in southeastern Alaska, through British Columbia and the southwestern corner of Yukon Territory, and into the Eastern Alaska Range. Thence, the fault swings southwestward to meet the Bering Sea north of the Aleutian Peninsula.

In southwestern Yukon, the fault separates two distinct major tectonic belts. Southwest of the fault, rocks in the St. Elias Mountains comprise a eugeosynclinal assemblage including low-grade metamorphic rocks, carbonate and clastic sediments, volcanics of basaltic to rhyolitic composition, and intrusive rocks which include peridotite, dunite, and a complete compositional gradation from gabbro and diorite to alaskite.

The region has been mapped at 4-mile scale by the Geological Survey of Canada, and reports by Kindle (1952), Wheeler (1963) and Muller (1967) describe this work. More recently, in 1973 and 1974, the G.S.C. carried out a program known as Operation Saint Elias which investigated selected aspects of the geology of this area. The results of this work are reported in a number of short papers (in G.S.C. Papers 74-1, 75-1, 76-1).

The portion of the study area lying immediately northeast of the Denali-Shakwak Fault is the northwestward limit of the Coast Plutonic Complex, one of the five major tectonic elements which comprise the Canadian Cordillera. This area is almost completely underlain by plutonic rocks of granodioritic and quartz monzonitic composition, and by older metamorphic rocks, some of which may be Cretaceous in age (Eisbacher, 1976), and others which may be Proterozoic or Cambrian (Muller, 1967; Tempelman-Kluit, 1976).

This area has been mapped at the 4-mile scale by Kindle (1952) and Muller (1967), and,more recently, Tempelman-Kluit (1974). In addition, a number of papers have appeared recently in the literature, particularly those by Tempelman-Kluit and Wanless (1975), Tempelman-Kluit (1976) and LeCouteur and Tempelman-Kluit (1976) which, while mainly concerned with the area northeast of the Ruby Range Batholith, have a bearing on the rocks within the study area of this thesis.

The major structural and physiographic features which will be referred to in this chapter are shown on Map 1 (in pocket).

2.2 Formations Southwest of the Denali-Shakwak Fault

Kaskawulsh Group. The oldest rocks exposed in the St. Elias Mountains belong to the Devonian Kaskawulsh Group, which consists largely of

marble intercalated with slate, quartzite and argillite. The stratigraphy of these rocks is characterized by rapid facies changes and discontinuity of beds along strike. This formation has not been found in contact with older sedimentary or volcanic rocks, or lying upon a crystalline basement. Exposure conforms to the northwestward regional trend of the geology, and is confined to the upthrown, or southwestern, side of the Duke River thrust fault. The southerly extension of these rocks into the higher peaks of the St. Elias Mountains, is not known.

This group was originally defined by Kindle (1952), in the Dezadeash map-area and assigned a Carboniferous age. Subsequent work by Wheeler (1963) and Muller (1967), based on more complete and diagnostic fossil collections, redefined the age as Middle and Upper Devonian.

Greenschist Complex. The Kaskawulsh Group is overlain with apparent conformity by a sequence of metasediments and metavolcanics referred to as the Greenschist Complex by Muller (1967). This unit, generally metamorphosed to the greenschist facies, is comprised mainly of greenstone and chlorite schist, with subordinate metagreywacke, slate, phyllite, conglomerate and marble. The greenstones are massive in form, extensively saussuritized and locally show structures inherited from the original basaltic or andesitic lavas. The metamorphosed greywacke is derived from a wide range of original source rocks, as evidenced by its composition of fragments of quartz, chert, plagioclase,

volcanic and granitic rocks, slate and earlier greywacke. Conglomerates in this formation are highly-deformed, and contain pebbles and cobbles of limestone and argillite flattened in the plane of schistosity.

The Greenschist Complex is spatially associated with the Kaskawulsh Group, and likewise is exposed only on the southwest side of the Duke River Thrust. The unit is unfossiliferous, and the assignment of a Devonian-Mississippian age is based on tentative correlations with geographically-remote units of similar lithology (Muller, 1967).

In a report of the Operation St. Elias program, Read (1976) reports the occurrence of Cambrian or Early Ordovician volcanic rocks in the southeast part of the Dezadeash map-area, west of the Duke River Fault. Unfortunately, he fails to mention the basis for this age assignment (presumably radiometric?), or an affiliation with the previously-described Kaskawulsh and Greenschist formations. Heretofore, the Devonian Kaskawulsh Group was the oldest-known formation in the region.

The Kaskawulsh Group and Greenschist Complex in southwestern Yukon form the northwestern part of the Alexander terrane, a tectonic element defined by Berg et al. (1972), and which is discussed in more detail in Chapter 3.

Icefield Range Granite. This name is used by the writer (see section 2.4) to describe a suite of plutonic rocks of widely-ranging

fabric and composition. The geochronology, petrography and chemistry of this suite are described in Chapters 4, 5, and 6, respectively.

Icefield Range granites show intrusive contacts only against rocks of the Kaskawulsh Group and Greenschist Complex, and similarly only occur in the Alexander terrane southwest of the Duke River thrust (see Map 1, in pocket).

The three formations described to this point are not known to have depositional or intrusive contacts with rocks older than Tertiary. Where the former and the latter are in juxtaposition, they are in fault contact along the Duke River thrust.

In the Kaskawulsh and Dezadeash map-areas, Kaskawulsh Group, Greenschist Complex and Icefield Range Granite rocks are overlain by Tertiary sedimentary and volcanic rocks of the Amphitheatre Formation and St. Clare Group, generally within close proximity to the Duke River Fault.

The remainder of the formations described here, of Permian and Mesozoic age, are exposed only to the northeast of the Duke River Fault, whereas Tertiary formations are exposed mainly northeast of the fault.

Cache Creek Group. This Permian formation was named by Muller (1967) after rocks of similar age and lithology which occur in central British Columbia. Muller divided the group into lower, volcanic, and upper, sedimentary divisions, which he mapped as separate units. The

contact between the two divisions is a transitional zone of intercalated volcanic and sedimentary rocks.

Rocks of the lower volcanic division are pyroclastics, including tuffs and breccias, and altered basic lavas of andesitic and basaltic composition. The tuffs are mostly light-coloured, fine- to medium-grained, and show rhythmic graded beds ranging in thickness from one inch to one foot. Breccias contain angular and sub-rounded fragments up to one foot in size. The lavas show flow-banding, chilled flow tops, and pillows.

The sedimentary division includes fossiliferous clastic and carbonate sedimentary rocks. Within this sequence, Muller (1967) has noted a 2500 ft. section ranging from a basal member of dark brown, coarse-grained greywacke and chert-pebble conglomerate to several units of lighter-coloured, medium- to coarse-grained, greywacke and chert-pebble conglomerate. The succession is topped by about 650 ft. of limestone and cherty limestone. Fossils collected from these sediments date the group as Permian.

Cache Creek rocks show their greatest areal extent in the Kluane Lake map-area, where they form much of the rugged Kluane Ranges adjacent to the Denali-Shakwak Fault. These rocks pinch out to the southwest in the Kaskawulsh map-area, which may be due, in part, to covering by the Duke River thrust fault which reaches closest to the Denali-Shakwak Fault (about 4 miles) in this area.

Cache Creek rocks have not been described in the Dezadeash

map-area, possibly because they were mistakenly assigned by Kindle (1952) to the Triassic Mush Lake Group. Muller (1967) remarked on the difficulty of distinguishing between Cache Creek and Mush Lake rocks, and assigned all volcanic rocks occurring above Permian sediments to the latter group, while recognizing that, in highly disturbed areas, errors in assignment could be made.

Mafic and Ultramafic Rocks. The Cache Creek Group was succeeded by a suite of mafic and ultramafic rocks, whose age may range from early Permian to Cretaceous. In the Kluane map-area, gabbro and peridotite occur as long, narrow, tabular bodies which show an intimate spatial association with both divisions of the Cache Creek Group, the only rocks with which they show intrusive contacts. Muller (1967) describes these bodies as steep-to-vertical sills, a few hundred feet thick, which are roughly concordant with the intruded Cache Creek Group. Many of the bodies outcrop close to, and parallel with, the surface expressions of thrust faults, both northeast and southwest dipping. Gabbro and peridotite are often juxtaposed along mutual sharp contacts.

Mafic and ultramafic rocks are not widespread in the Kaskawulsh map-area, probably because Cache Creek rocks are also scarce. Occurrences are confined to a few, small, serpentinized peridotite and serpentinite lenses which intrude Cache Creek and older rocks adjacent to the Duke River Fault.

In the Dezadeash map-area, this suite is not as widespread as in the Kluane Lake map-area, although, where exposed, individual exposures tend to be more aerially-extensive. In the northwestern part of this map-area, two large, partly serpentinized, ultramafic masses intrude lower Cretaceous strata; the larger of these measures 12 miles by 1 to 2 miles, and is elongated parallel to the Denali-Shakwak and Duke River faults. Eisbacher (1976) reports K/Ar ages of 118 m.y. and 107 m.y. for hornblende and biotite from the smaller of the ultramafic intrusions. Gabbro occurs in two small intrusions, separated from the ultramafic bodies, where it also cuts Lower Cretaceous strata.

Mush Lake Group. Another major episode of volcanism is represented by the Triassic Mush Lake Group, a thick assemblage of volcanic and sedimentary rocks first described by Kindle (1952) in the Dezadeash map-area. This group, along with Cache Creek rocks, underlies much of the Kluane Ranges and is prominent in all three map-areas southwest of the Denali-Shakwak Fault.

Muller (1967) has separated the group into volcanic and sedimentary divisions. The volcanics consist of lava flows and pyroclastics, which are distinguished in the field from the Paleozoic volcanics by their dark-green and purple colours. Minor beds of argillite and tuffaceous limestone also occur in this unit. The lavas are commonly amygdaloidal and contain small plagioclase

phenocrysts. In thin-section, these rocks are seen to consist largely of altered plagioclase and diopside showing ophitic texture (Muller, 1967). Pyroclastic rocks consist of fine-grained tuffs and breccias containing subangular fragments several inches in size, set in a tuffaceous matrix. These rocks show pervasive spilitic alteration assemblages of albitized plagioclase, epidote, chlorite, carbonates and prehnite.

The sedimentary division of the Mush Lake Group is comprised of two parts: a lower massive limestone unit; and an upper unit of thinly-bedded, shaly limestone and shale. The limestone unit is massive, jointed, finely crystalline and brecciated in places, and has indistinct bedding. The upper limestone-shale unit is highly deformed due to its incompetency. Individual layers of shaly limestone range in thickness from six to twelve inches; the interbedded silty shale layers vary from one half- to two inches-thick.

Fossil collections identify the Mush Lake Group as Middle or Upper Triassic in age. Muller (1967) suggests that these rocks disconformably overlie the Cache Creek Group, citing the lack of Upper Permian and Lower Triassic beds.

The Cache Creek and Mush Lake Groups and associated ultramafics comprise a part of another tectonic element known as the Taku-Skolai terrane (Berg et al., 1972), which will be discussed in Chapter 3.

Dezadeash Group. Mush Lake rocks are disconformably overlain by the Dezadeash Group, a name proposed by Kindle (1952) for a thick assemblage of flysch sediments, which show their greatest development in the Dezadeash map-area. These rocks are also exposed in the Kluane Ranges, farther to the northwest, in the Kaskawulsh and Kluane Lake map-areas, but are much more restricted in their exposure there.

Dezadeash and Mush Lake Group rocks shown in the southwest corner of the Dezadeash map-area, southwest of the Duke River Fault, were misinterpreted by Kindle (1952), and properly belong to the Kaskawulsh Group, Greenschist Complex or older rocks (Campbell and Dodds, 1975; Read, 1976). This reassignment is important since it preserves the Duke River thrust fault as a boundary between pre-Permian metasediments and metavolcanics, on its southwest side, and Permian and Mesozoic rocks to the northeast.

The group is comprised of a sequence of slate, greywacke, argillite, quartzite, chert, impure limestone, grit, conglomerate, tuffaceous sandstone, and volcanic tuffs many thousands of feet thick. Argillite and greywacke are the major components. Metamorphism is locally intense, and in many places a strong cleavage has been imposed which obscures the original bedding, although graded bedding, load-casts, fluting, and slump bedding can be observed locally. Where discernible, beds are generally seen to range from one to six inches-thick. Muller (1967) describes occurrences of Dezadeash Group

basal conglomerates which contain cobbles of limestone and pebbles of volcanic rocks, granodiorite and leucogranite, the latter clearly derived from older granitic intrusions.

Fossil collections date these rocks as Late Jurassic to Lower Cretaceous.

Some recent work of the Operation Saint Elias program has revised the position of the Denali-Shakwak Fault in the Dezadeash map-area. Whereas previous work (Kindle, 1952) showed the fault trace to the east of the Dezadeash Group, with a sharp bend at Dezadeash Lake, Campbell and Eisbacher (1974) suggest that this part of the Denali-Shakwak fault system, which they have named the Dalton Fault, passes to the west of the Dezadeash Group (see Map 1, in pocket). For most of its length, from near the south end of Kluane Lake to the Yukon-British Columbia border, the Dalton Fault separates the Dezadeash Group from Mush Lake rocks, a boundary which Kindle (1952) previously interpreted as a disconformity.

In southwestern Yukon, the Dezadeash Group represents another tectonic element known as the Gravina-Nutzotin Belt (Berg et al., 1972). This unit, and rocks of the Alexander and Taku-Skolai terranes, are discussed in the following chapter in terms of their comprising a regional tectonic framework.

Kluane Range Diorite. This term is used by the writer (see section 2.4) to describe a suite of intermediate intrusive rocks, mainly diorites, which forms a series of plutons in the Kluane Ranges. These

rocks show intrusive contacts only against rocks of the Cache Creek, Mush Lake and Dezadeash Groups, and are exposed only in the area between the Duke River Fault and the Denali-Shakwak Fault. This suite is discussed in more detail in subsequent chapters.

Amphitheatre Formation. Muller (1967) proposed this name to designate continental, clastic sediments of early Tertiary age. These rocks do not have great areal extent, but occur in scattered areas in the Kluane Lake and Dezadeash map-areas in close proximity to the Duke Depression, a topographic feature which generally trends parallel to, and approximately 5 to 20 miles southwest of, the Denali-Shakwak Fault.

These rocks are often loosely-consolidated and consist, in approximate order of abundance, of sandstone and sand, conglomerate and gravel, shale, coaly shale, coal and clay, and tuff. Muller (1967) notes apparent cyclicity in the sedimentary succession with a single cycle consisting of conglomerate at the bottom, ranging through pebbly sandstone and sandstone, to shale with clay and coal at the top. Fossil plants indicate a Paleocene or Eocene age for this formation.

Wrangell Lavas (St. Clare Group). Muller (1967) originally proposed the name St. Clare Group for this sequence of Tertiary, sub-aerial lavas and pyroclastic rocks, but, more recently, Souther and Stanciu (1975) named these rocks the Wrangell Lavas, after similar, coeval,

volcanics extensively exposed in eastern Alaska. These represent the fourth major period of volcanism in the St. Elias Mountains, and their age is bracketed between Paleocene and Miocene on the basis of conformable contacts with the older Amphitheatre Formation and intrusion by hypabyssal felsites of Miocene age.

Wrangell Lavas have considerable areal extent in the St. Elias Mountains, particularly in the Kluane Lake map-area. The distribution of this group is unlike that of Mesozoic and older rocks: the outcrop does not conform to the northwesterly trend of the geology, and the rocks are exposed on both sides of the Duke River Fault.

Muller (1967) has divided these rocks into lower volcanic and upper sedimentary formations. The lower consists mainly of massive basalt flows which range in thickness from 10 to 200 feet. Flow tops are commonly vesicular, brecciated and oxidized. Columnar jointing is observed in the lower parts of some flows. These rocks are distinguished in the field from earlier volcanics by their reddish to rusty brown colour and relative freshness. In thin section, feldspar is generally unaltered and occurs with augite in both ophitic and granular textures.

The upper formation is made up largely of boulder conglomerate, with some beds of breccia, flow breccia and tuff. Clasts in the conglomerate are derived mainly from the lower volcanic formation and range up to 3 ft. in size in some beds.

Both Muller (1967) and Souther and Stanciu (1975) have

remarked on the lack of deformation in these rocks. Generally, they lie in relatively flat, undisturbed piles over large areas. Fig. 2.1 shows a section of these rocks on the north side of Steele Glacier.

Kluane Range Porphyry. The youngest consolidated rocks exposed in the St. Elias Mountains are sills, dykes, and small felsite stocks of probable Miocene age. Muller (1967) reports that these rocks are mainly latites, but that rhyolite and trachyte are also prominent. This suite is well represented in the Kluane Lake map-area, has a limited distribution in the Dezadeash map-area, and occurs only in two small stocks in the Kaskawulsh map-area.

The writer prefers the name 'Kluane Range Porphyry' for these rocks for reasons which are outlined in section 2.4 and also in Chapter 5.

Muller (1967) describes two small, olivine gabbro bodies which he believes are contemporaneous with the above-mentioned felsic rocks. The olivine gabbro intrudes Tertiary volcanic rocks but has no contact with the felsic intrusives. These rocks are difficult to distinguish in the field from older mafic and ultramafic intrusives, but microscopically are characterized by their general freshness, and the presence of pink augite and unaltered olivine (Muller, 1967).

Volcanic Ash. The most recent evidence of igneous activity in the area is a layer of volcanic ash which is widespread across southern Yukon. The eruption centre is generally believed to lie close to the

Fig. 2.1. View looking west across Steele Creek and the terminus of Steele Glacier at flat-lying Wrangell Lavas.



Alaska-Yukon border along the western edge of the Kluane Lake map-area. Prevailing winds dispersed the ash in two large lobes, one extending about 300 miles to the north and the other about 450 miles to the east (Bostock, 1952). Fig. 2.2 shows a layer of the white ash in a road cut approximately 270 miles east of the eruption centre.

Throughout most of its area, the ash has the texture of a coarse, unlithified sand. It is best seen in road cuts where it is usually overlain by loess, gravel or humus up to a few feet thick.

The most accurate estimates of the age of the ash are by Fernald (1962), who dated, by the radiocarbon method, layered peat underlying and overlying the ash layer. The age of the ash was bracketed between 1520 and 1750 yrs.

2.3 Formations Northeast of the Denali-Shakwak Fault

Yukon Group (Biotite Schist, Kluane Schist). The name Yukon Group was introduced by Cairnes (1914) to refer to an assemblage of generally low-grade metamorphic rocks, of probable Precambrian age, which underlies much of the Yukon Plateau between the Denali-Shakwak and Tintina Faults. More recently, Muller (1967) and Tempelman-Kluit (1976) have advanced modifications to this name, on the basis that it is too loosely defined, and includes units which are not all part of one stratigraphic sequence. Tempelman-Kluit (1976) has proposed the use of informal names for sub-units of Cairne's (1914) original group. Two of these, the Biotite Schist and Kluane Schist, are

Fig. 2.2. Exposure of unconsolidated sediments in road cut showing succession, from bottom to top, of glacial till, loess, white ash, loess and humus, South Canol Road.



exposed within the study area and so, for convenience and to avoid ambiguity inherent in the terms Yukon Group or Yukon Complex (Muller, 1967), these more restrictive, but informal, terms will be adopted here.

The Biotite Schist unit is exposed along the northern flank of the Ruby Range Batholith, and marks the southern limit of a complex tectonic element called the Yukon Crystalline Terrane (Tempelman-Kluit, 1976; see section 3 in following chapter for discussion). These rocks are an assemblage of micaceous quartzite and coarsely-crystalline garnet-muscovite-biotite quartz schist, metamorphosed to the amphibolite facies. Schistosity is generally well-developed and coincident with primary compositional layering. Thick marble lenses are contained within this unit, and form roof pendants in the western part of the Ruby Range Batholith (see Fig. 2.3). Tempelman-Kluit (1976) suggests that this sequence was derived from original fine-grained, fairly uniform, clean shale and sandstone with interbedded limestone.

The age of these rocks is difficult to establish since they lack fossils and are not physically connected to dateable stratigraphic equivalents. Tempelman-Kluit (1976) tentatively places the age at Proterozoic, based on a similarity with the metamorphosed Windermere sequence exposed in the Omineca Crystalline Belt.

The age of metamorphism of these rocks is also difficult

Fig. 2.3. View of limestone roof pendant in the Ruby Range Batholith, east shore of Talbot Arm, Kluane Lake.



to establish and no radiometric dates are available. Tempelman-Kluit (1976) suggests a single metamorphic event in Early or Middle Triassic time, contemporaneous with that defined in metamorphic units farther to the north.

The Kluane Schists lie along the southwestern flank of the Ruby Range Batholith and separate it, for most of its length, from the Denali-Shakwak Fault. The batholith intervenes between Biotite Schist and Kluane Schist units, so no transition or gradation between the two rocks is known.

These rocks are coarsely-crystalline quartz-biotite-muscovite schists, with cordierite and staurolite. Poor compositional layering is paralleled by a well-developed, uniformly northeast-dipping, schistosity. These rocks have also been regionally metamorphosed to amphibolite facies. These rocks are presumably the metamorphic products of a thick, uniform sequence of fine-grained, thin-bedded clastic rocks.

The age of these rocks is again not known with certainty, but Eisbacher (1976) recently suggested that they are the metamorphosed equivalent of the Upper Jurassic and Lower Cretaceous Dezadeash Group. In the Dezadeash map-area, these two units are mainly juxtaposed in fault contact, but local gradation from unmetamorphosed shale and siltstone to Kluane Schist rocks is observable (Kindle, 1952).

Radiometric dates from these rocks (this thesis; Eisbacher,

1976) are in the range 40 m.y. to 70 m.y., and suggest metamorphism in the early Tertiary, essentially coeval with intrusion of the Ruby Range Batholith (see below).

Nisling Range Granodiorite. These plutonic rocks are exposed only along the northern fringe of the study area in the Kluane Lake map-area, and are known to occur only in two small batholiths in the southern part of the Yukon Crystalline Terrane where they intrude the Biotite Schist unit and the Nasina Quartzite (Tempelman-Kluit, 1976). Generally, these rocks are biotite-hornblende granodiorites and quartz monzonites. This suite represents one of a number of plutonic events which occurred during the Cretaceous and Tertiary in the area immediately northeast of the Denali-Shakwak Fault.

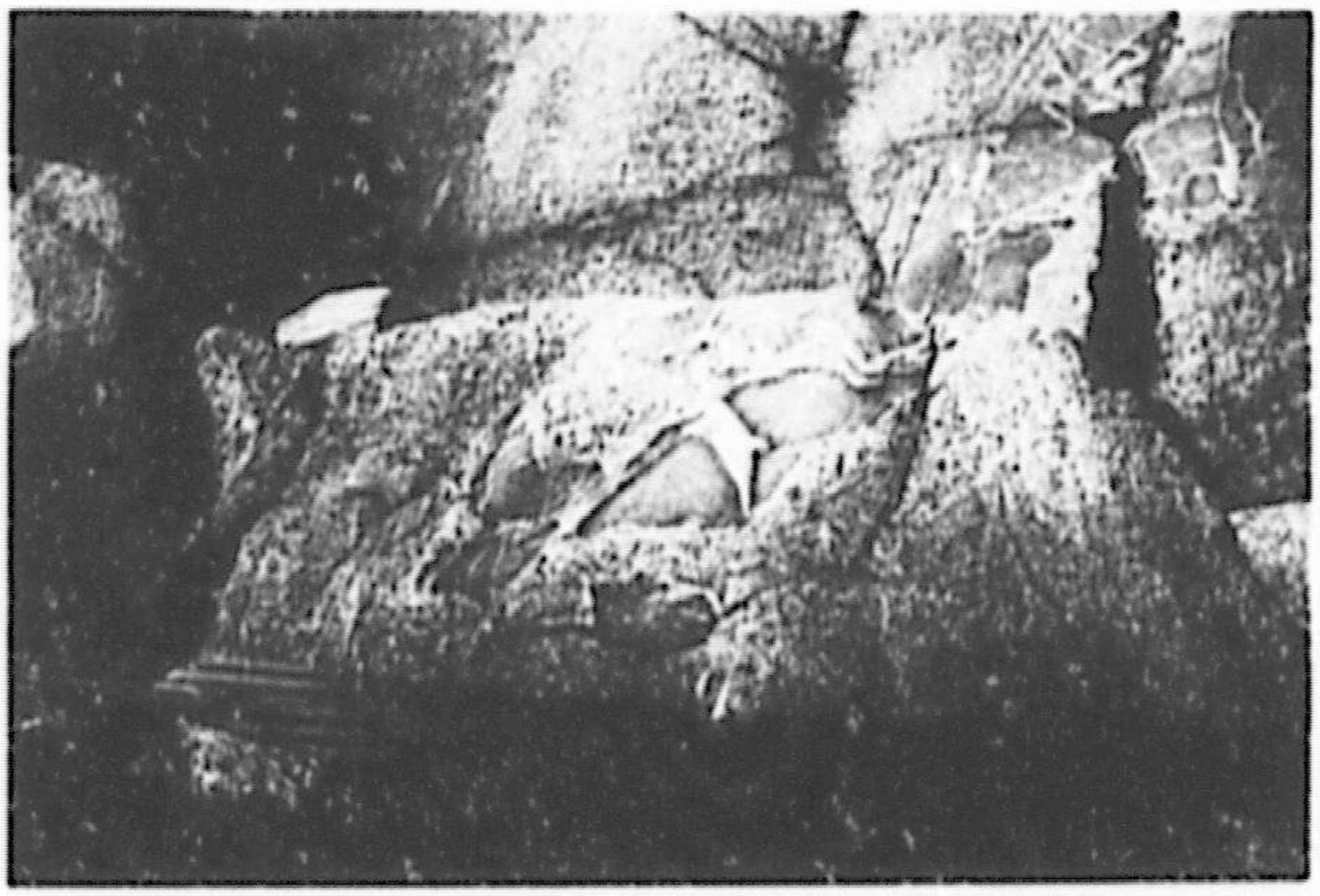
This suite, and the Ruby Range Granodiorite and Nisling Range Alaskite suites which will be subsequently described, were first named by Muller (1967). Each will be described in more detail in Chapters 4, 5 and 6.

Ruby Range Granodiorite. These extensively-exposed rocks are mainly hornblende-biotite granodiorites and quartz monzonites, which are broadly similar to rocks of the Nisling Range Granodiorite suite in gross fabric, mineralogy, and chemistry. Fig. 2.4 shows part of an outcrop of Ruby Range granodiorite containing xenolithic material.

These rocks form the Ruby Range Batholith, the northern part of the Coast Plutonic Complex, and underlie much of the study



Fig. 2.4. Ruby Range Granodiorite containing mafic xenoliths near contact with Kluane Schist, west shore of Talbot Arm, Kluane Lake.



area to the northeast of the Denali-Shakwak Fault.

Nisling Range Alaskite. This suite is comprised of leucocratic, hypabyssal, granitic rocks which occur in small stocks intruded mainly into the Biotite Schist unit to the north of the Ruby Range Batholith. However, cross-cutting relationships with the older Nisling Range Granodiorite and Ruby Range Granodiorite suites are also observed in the field.

Mount Nansen Group. The name Mt. Nansen Group was originally used by Bostock (1936), and later given a more restricted meaning by Tempelman-Kluit (1974). These rocks are dark-green tuffs and breccias of intermediate to acidic composition. Textures are mainly aphanitic, but some rocks are porphyritic with small plagioclase phenocrysts. Pyroclastic facies also occur, and display angular fragments, similar in composition to the matrix, up to several inches in size.

These rocks do not have great areal extent within the thesis area, but rather are distributed in a series of isolated exposures, often overlying the Biotite Schist unit to the north of the Ruby Range Batholith.

Tempelman-Kluit (1974) describes Mount Nansen Group rocks overlying Nisling Range Alaskite in places. Elsewhere, apophyses of the alaskite intrude the volcanics. These field relationships suggest that the Mount Nansen Group is coeval with, or perhaps slightly younger than, the Nisling Range Alaskite suite.

2.4 Suite Names for Granitoid Rocks

The names used here for the plutonic suites southwest of the Denali-Shakwak Fault, i.e., "Icefield Range Granite", "Kluane Range Diorite", and "Kluane Range Porphyry", are particular to this study and have not been used in the literature. For the purposes of this work, the writer found previously-used expressions to be either too restrictive, as in "Donjek Range intrusions" (Muller, 1967), or too general, as in "undifferentiated granitic rocks" (Wheeler, 1963).

The name Icefield Range Granite is used to designate a suite of plutonic rocks which occurs mainly in that range. "Granite" is used here in the widest possible sense, as in "granitic rocks", since this suite shows a great range in modal composition although few, if any, of these rocks are true granites. This suite includes that described by Muller (1967) as "Donjek Range intrusions".

"Kluane Range Diorite" designates a suite of plutonic rocks which is exposed mainly in the Kluane Ranges, and is comprised mostly of diorite. Muller (1967) referred to this suite as "Kluane Range intrusions".

"Kluane Range Porphyry" refers to a suite of hypabyssal felsic rocks which occur in the Kluane Ranges. These rocks generally display porphyritic textures and the writer prefers to call them feldspar porphyries, rather than latites, trachytes or rhyolites, for reasons which are developed in more detail in Chapter 5.

The names used here for the three plutonic suites on the

northeast side of the Denali-Shakwak Fault ("Nisling Range Granodiorite", "Ruby Range Granodiorite" and "Nisling Range Alaskite") have all been used previously in the literature (Muller, 1967; Tempelman-Kluit, 1974, 1976), and are acceptably descriptive for purposes of this thesis.

CHAPTER 3

REGIONAL TECTONIC FRAMEWORK

3.1 Introduction

Plate tectonic concepts have recently been used to unravel the tectonic history of northwestern North America in the region bordering the Gulf of Alaska. Much of the recent work has been carried out by geologists of the United States Geological Survey working in southern and southeastern Alaska. Most of the tectonic relationships which have been described to date are broad in scope, and have contributed greatly to the understanding of the evolution of a geologically-complex area. However, large tracts of this region, which includes some of the highest mountains on the North American continent, are unmapped geologically. This has impeded the development of a detailed tectonic synthesis. To a large extent, the first section of this chapter is based on several publications of the U.S.G.S., and the second on papers by Monger, Souther and Gabrielse (1972) and Tempelman-Kluit (1976).

3.2 Tectonic Framework Southwest of the Denali-Shakwak Fault

Berg, Jones and Richter (1972) have grouped the geological formations of southeastern Alaska and contiguous southwestern Yukon into tectonic elements, or "terranes" (Fig. 3.1). The oldest of these, lying south and west of the Denali-Shakwak Fault, is the

CHAPTER 3

REGIONAL TECTONIC FRAMEWORK

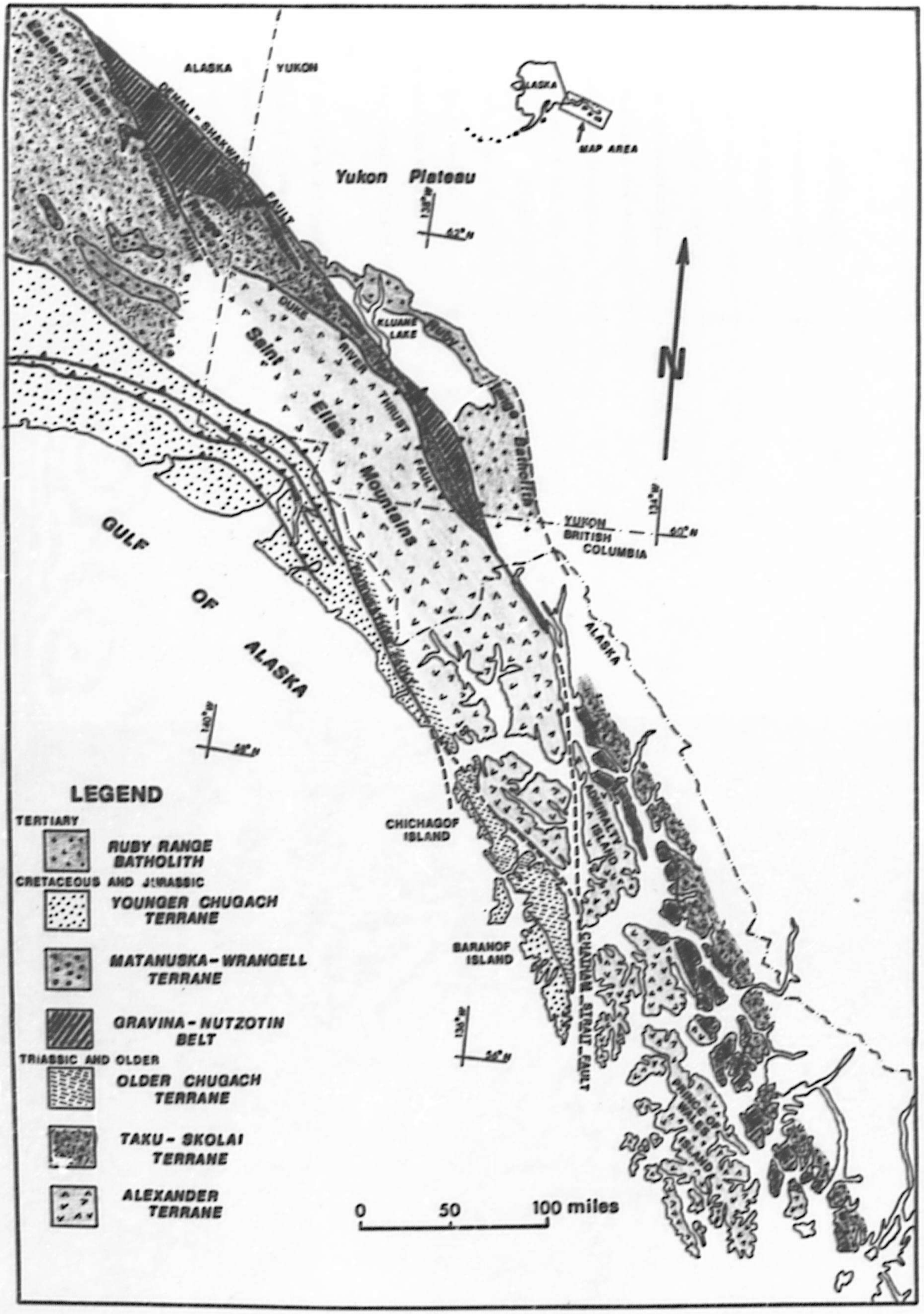
3.1 Introduction

Plate tectonic concepts have recently been used to unravel the tectonic history of northwestern North America in the region bordering the Gulf of Alaska. Much of the recent work has been carried out by geologists of the United States Geological Survey working in southern and southeastern Alaska. Most of the tectonic relationships which have been described to date are broad in scope, and have contributed greatly to the understanding of the evolution of a geologically-complex area. However, large tracts of this region, which includes some of the highest mountains on the North American continent, are unmapped geologically. This has impeded the development of a detailed tectonic synthesis. To a large extent, the first section of this chapter is based on several publications of the U.S.G.S., and the second on papers by Monger, Souther and Gabrielse (1972) and Tempelman-Kluit (1976).

3.2 Tectonic Framework Southwest of the Denali-Shakwak Fault

Berg, Jones and Richter (1972) have grouped the geological formations of southeastern Alaska and contiguous southwestern Yukon into tectonic elements, or "terranes" (Fig. 3.1). The oldest of these, lying south and west of the Denali-Shakwak Fault, is the

Fig. 3.1. Generalized geological map of eastern and southeastern Alaska and southwestern Yukon, showing major structural features and tectonic terranes. Modified from Berg et al. (1972).


ALASKA
YUKON
ALASKA
MAP AREA
Yukon Plateau
Eastern Alaska
DENALI - SHAKWAK FAULT
DUKE RIVER FAULT
KLUANE LAKE
Ruby Range
Saint Elias Mountains
DUKE RIVER THRUST FAULT
Dalton Post
YUKON
BRITISH
COLUMBIA
ALASKA
GULF OF ALASKA
CHICHAGOF ISLAND
ADMIRALTY ISLAND
BARANOF ISLAND
CHATHAM STRAIT FAULT
PRINCE OF WALES ISLAND
LEGEND
TERTIARY
RUBY RANGE BATHOLITH
CRETACEOUS AND JURASSIC
YOUNGER CHUGACH TERRANE
MATANUSKA - WRANGELL TERRANE
GRAVINA - NUTZOTIN BELT
TRIASSIC AND OLDER
OLDER CHUGACH TERRANE
TAKU - SKOLAI TERRANE
ALEXANDER TERRANE
0
50
100 miles

Alexander terrane, an heterogeneous assemblage of sedimentary, volcanic and metamorphic rocks. In southeastern Alaska, these rocks range in age from Precambrian to Late Triassic and are cut by granitoid rocks as old as Silurian and as young as Cretaceous. Ordovician and Silurian ultramafic plutons also intrude Alexander terrane near its southern termination on Prince of Wales Island.

The Alexander terrane extends northwestward as far as the Alaska-Yukon international border (longitude 141°W) where it pinches out against the Totschunda fault and the Duke River thrust fault (Fig. 3.1). In Yukon Territory, the Alexander terrane underlies much of the area southwest of the Duke River thrust fault and includes the Kaskawulsh Group and the Greenschist Complex, which were described in Chapter 2. These units range in age from Middle Devonian to, possibly, Mississippian, and are intruded by granitoid stocks.

The Alexander terrane is bounded on all sides by high-angle or thrust faults, except in the region southeast of the Chatham Strait fault, where the eastern margin of this unit is in depositional contact with the Mesozoic Gravina-Nutzotin belt, a flysch-like assemblage of sedimentary and intercalated volcanic rocks. Berg et al. (1972) show the Alexander terrane and an isolated outlier of the Gravina-Nutzotin belt (represented in the Yukon by the Dezadeash Group) in depositional contact west of the Duke River thrust fault in the Dezadeash map-area. A more recent examination

of this area by Campbell and Eisbacher (1974) indicated that rocks of this "outlier", previously assigned to the Cretaceous Dezadeash Group (Kindle, 1952; Berg et al., 1972), are probably Paleozoic in age, and do not belong to that group. The significance of this is that all of the Alexander terrane northwest of the Chatham Strait fault, along which a right-lateral displacement of 120 miles is postulated (Lathram, 1964; Ovenshine and Brew, 1972), is fault-bounded and shows no depositional contacts with rocks older than Tertiary.

A number of geologists support the concept that the Alexander terrane is allochthonous with respect to northwestern North America. This terrane is anomalous in that rocks of comparable age and lithology do not occur along the western North American continental margin, except in California. Jones et al. (1972) have speculated that California was the source for the Alexander terrane. Their hypothesis is based on a comparison of truncated Silurian facies trends in carbonate and clastic rocks in California with similar trends in the Alexander terrane. The proposed mechanism for this displacement is right-lateral transcurrent faulting, but the evidence in support of this model is not conclusive.

In a recent survey of the "borderland terranes" of Precambrian to Paleozoic age now enclosed within the North American Cordillera, Churkin and Eberlein (1977) recognize the Alexander terrane as one such allochthonous unit. However, they provide no new stratigraphic information on its northerly portion in southwestern

Yukon or contiguous Alaska. Indeed, they do not record the known intrusive bodies in this region in a tabular summary of igneous activity (their Fig. 5). They emphasize that numerous micro-continental plates and volcanic arcs probably existed off western North America over this time span, and that these may be presumed to have moved outwards and inwards to accommodate a succession of marginal basins opening and closing behind migrating arcs (op. cit., p. 769).

In southwestern Yukon, the northern margin of the Alexander terrane is juxtaposed (Fig. 3.1) along the Duke River thrust fault with late Paleozoic (mainly Permian) and early Mesozoic rocks belonging to the Taku-Skolai terrane. The latter terrane includes the units previously described as the Cache Creek and Mush Lake Groups, each of which may represent an episode of island arc activity. The Permian rocks of the Cache Creek Group comprise andesitic and basaltic volcanics and pyroclastics, succeeded by younger clastic and carbonate sedimentary rocks. The Triassic Mush Lake Group, largely basalt, andesite and limestone, is similarly composed of volcanic and younger sedimentary rocks.

The Permian rocks are associated with mafic and ultramafic rocks and banded chert. In the west-central Alaska Range, assemblages of serpentine, gabbro, basalt, and banded chert have been interpreted as ophiolite suites (Clark, Clark, and Hawley, 1972). It is suggested that these rocks represent oceanic crust upon which island

arcs (represented by later basalts and andesites) were developed, with concomitant and subsequent deposition of marine sedimentary rocks.

The Alaska ophiolite assemblages are similar in age, lithology and structural setting to the ultramafic and mafic rocks associated with the Cache Creek Group in the Kluane map-area (Muller, 1967). In Yukon, the Permian and Triassic tectonic history may parallel the sequence of events in west-central Alaska Range, except that the Cache Creek group and the Mush Lake group may each represent a complete cycle of island arc development.

There is some evidence that the Taku-Skolai terrane, and in particular the Permian assemblages, is also allochthonous with respect to continental northwestern North America. Monger and Ross (1971) draw attention to the distribution of fusulinacean faunas in the Upper Paleozoic rocks of the western Canadian Cordillera. The fauna form two assemblages: one is dominated by genera of the family Schwagerinidae which occur in Permian limestones with intercalated clastic and volcanic rocks; and the other by genera of the family Verbeekinidae, which occur in regionally-extensive Permian limestones associated with cherts, basalts and ultramafic rocks. Schwagerinidae are distributed in two belts in the eastern and western Cordillera, respectively. Verbeekinidae occupy a central belt between the two Schwagerinidae domains. Schwagerinidae are present in limestone members of the Cache Creek group in the

Kluane and Kaskawulsh map-areas.

A number of models are proposed by Monger and Ross (1971) to account for this pattern of faunal belts. An ecological model explains the distribution of the different fauna by differences in local environment. Other models, favoured by the authors, are tectonic. The most reasonable tectonic model involves the oblique cutting of paired ecological belts - a continent-ward Schwagerinid belt and an ocean-ward Verbeekinid belt - by a major, northwest-trending, right-lateral transcurrent fault so that part of the eastern Schwagerinid belt came to lie west of the central Verbeekinid belt. This type of crustal movement would be somewhat analogous to the present-day truncation of southwestern California by the San Andreas fault. Jones et al. (1972) expanded on this model of right-lateral transcurrent faulting as a mechanism for moving the older Alexander terrane into place.

However, in spite of substantial evidence suggesting that Alexander and other borderland terranes are allochthonous relative to the North American craton, it should be recognized, as Churkin and Eberlein (1977) point out, that there is little agreement on the amount, direction and type of movement undergone by these terranes. In this light, the mechanisms proposed by Jones et al. (1972) and Monger and Ross (1971) for moving the Alexander and Taku-Skolai terranes into their current positions should be regarded as tenuous and speculative.

The third major tectonic element in the region (Fig. 3.1) has been called the Gravina-Nutzotin belt (Berg, Jones and Richter, 1972), after geographical features at its two extremities. The rocks comprising this belt are mainly marine, flysch-like, argillites and greywackes, minor non-marine strata, granitoid and ultramafic rocks, and subordinate interbedded andesitic and pyroclastic rocks. This unit is represented in southwest Yukon by the Dezadeash Group. Fossils establish the age of these rocks as Late Jurassic (Oxfordian) to Middle Cretaceous (Albian).

In Eastern Alaska Range and in southwestern Yukon, the Gravina-Nutzotin belt is a long, narrow, area lying between the northeastern flanks of the Alexander and Taku-Skolai terranes and the Denali-Shakwak fault system. In this region, Gravina-Nutzotin rocks depositionally overlie Taku-Skolai terrane strata. In the Kluane Lake map-area, for example, Muller (1967) reported a basal conglomerate of the Dezadeash Group overlying limestone of the Triassic Mush Lake Group, part of the Taku-Skolai terrane.

In southeastern Alaska, southeast of the Chatham Strait fault, Gravina-Nutzotin rocks are in depositional contact with Alexander terrane rocks and the elsewhere-intervening Taku-Skolai terrane is absent. Instead, the Taku-Skolai terrane, whose character and distribution are poorly-known in southeastern Alaska, is exposed in an overthrust east of the Gravina-Nutzotin belt, across a postulated eastward-dipping thrust fault. Here, depositional contact between

Gravina-Nutzotin and Taku-Skolai rocks in unknown. Gravina-Nutzotin rocks, as well as the Taku-Skolai rocks, are highly-deformed and regionally metamorphosed to the greenschist facies in this region. In the northern part of the Gravina-Nutzotin belt, the strata are only moderately deformed and metamorphosed.

Two other tectonic elements described by Berg, Jones and Richter (1972) are of lesser importance to the tectonic history of southwestern Yukon than those described previously: the Matanuska-Wrangell and the Chugach terranes. These are coeval with the Gravina-Nutzotin belt but are lithologically dissimilar, in spite of their present close proximity to Gravina-Nutzotin rocks in some areas (Fig. 3.1).

The Matanuska-Wrangell terrane is an arcuate belt that parallels the Gulf of Alaska coast from approximately the international border at 141°W Longitude to approximately 162°W in the Aleutian Peninsula. These rocks are comprised of thick sequences of Lower Jurassic sedimentary and volcanic rocks and Middle Jurassic to Upper Cretaceous shallow marine deposits. In the eastern part of the belt, the Upper Jurassic (Oxfordian) to Lower Cretaceous (Albian) sequences are quite different from the contemporaneous Gravina-Nutzotin rocks which lie to the north. The Matanuska-Wrangell terrane rocks, mainly mudstone and siltstone with minor shale, sandstone and conglomerate, are believed to have been deposited in a moderately-shallow marine environment (MacKevett, 1971). They are

characterized by rapid facies changes and abundant local disconformities, which may be indicative of an unstable continental shelf. Within this sequence, flysch-type rocks are rare, fossils are abundant and volcanic rocks are absent.

The Chugach terrane lies oceanward of the Matanuska-Wrangell terrane and follows the same arcuate path around the Gulf of Alaska. However, the Chugach terrane is more extensive and is continuous into southeastern Alaska as far as the Chatham Strait fault. Chugach terrane rocks have been divided into older and younger units. The older Chugach terrane occurs as a wedge between younger Chugach terrane and Alexander terrane, mainly on Baranof and Chichogof Islands in southeastern Alaska. These rocks are regionally metamorphosed and highly-deformed phyllites, metagreywackes, quartzites, metacherts, greenstones, amphibolites and ultramafic rocks. The assemblage is locally intruded by Middle Jurassic and younger granitoid plutons. Older Chugach rocks also occur across the Fairweather fault, along the southern margin of the St. Elias Mountains. Plafker (1972) believes that the older Chugach terrane rocks on either side of the Fairweather fault were once continuous but have been separated by about 150 miles of Cenozoic right-lateral slip on the fault. Definitive evidence is lacking for the age of these rocks, but they may be as old as Triassic or Permian.

Younger Chugach terrane rocks comprise the remainder of the belt. These are Upper Paleozoic and Mesozoic in age and include

greywacke, argillite, slate, conglomerate, volcanic rocks, chaotic mélanges and granitoid plutons. Deformation is complex and the rocks are regionally metamorphosed. In southeastern Alaska, some of the units belonging to this terrane bear the same Buchia fossil assemblages as occur in some rocks of the Gravina-Nutzotin belt.

Rocks of the younger Chugach terrane were apparently deposited in a deep marine trench (Berg, Jones and Richter, 1971). Older Chugach rocks, as indicated by the presence of alpine-type ultramafic rocks with chert, greenstone, amphibolite and gabbro, may have been deposited directly on oceanic crust. No depositional contacts between younger Chugach terrane, older Chugach terrane or Alexander terrane are inferred. Instead, where any two of the elements are juxtaposed, they are believed to be in fault contact.

3.3 Tectonic Framework Northeast of the Denali-Shakwak Fault System

The region to the north and east of the Denali-Shakwak fault system, in Yukon Territory, is probably the northwestward limit of the Coast Plutonic Complex of British Columbia, although some recent work in this area proposes a different origin and tectonic regime (Tempelman-Kluit, 1976). The area under consideration extends northwestwards from the Yukon-British Columbia border (60°N latitude) as a 200 by 50 mile strip along the northeast flank of the Denali-Shakwak fault. It is underlain by greenschist and amphibolite facies metamorphic rocks, described in the previous chapter as the Biotite

Schist and Kluane Schist units, and by late Mesozoic to early Tertiary plutonic rocks of granodiorite and quartz monzonitic composition.

Monger et al. (1972) include this area in the northern part of the Coast Plutonic Complex, one of the five major geological and physiographic belts of the Canadian Cordillera (Fig. 3.2). These authors envisage the early development of the Coast Plutonic Complex as an island arc in upper Paleozoic times, separated from the western edge of the continent by an oceanic ridge. By Upper Triassic or Lower Jurassic times, the oceanic ridge had disappeared and the system of island arcs had evolved (by oceanward stepping of successive subduction zones) into an eastward-dipping, continental margin, subduction zone approximately coincident with the present-day margin of northwestern North America (Fig. 3.3). This evolution affected events in all parts of the Cordillera but, in particular, led to the intrusion of great volumes of granitoid magmas in the Coast Plutonic Complex, beginning in the Cretaceous. In the Coast Range, uplift, metamorphism and granitic intrusion were broadly coeval. In the northern part of the range, uplift took place during the Jurassic, attended by metamorphism which persisted into the Cretaceous, and by intrusion which continued until the late Tertiary.

Tempelman-Kluit (1976) has proposed an alternative grouping of tectonic elements in southwestern Yukon Territory (Fig. 3.4), which will be outlined in the succeeding paragraphs. In this

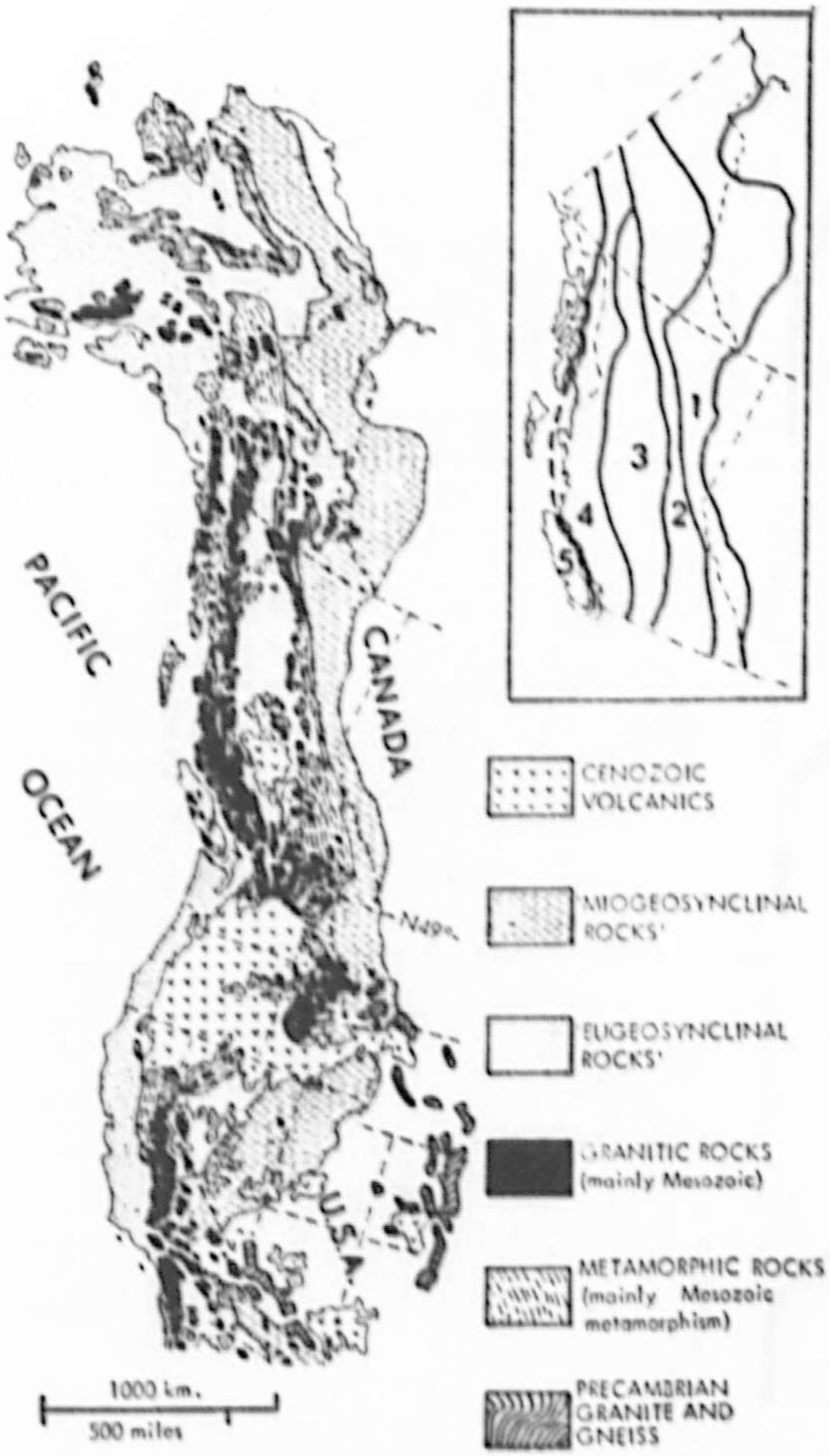


Fig. 3.2. Sketch map of the North American Cordillera. The inset map shows the location of the geological and physiographic belts of the Canadian Cordillera. These are (1) Rocky Mountain Belt, (2) Omineca Crystalline Belt, (3) Intermontane Belt, (4) Coast Plutonic Complex, and (5) Insular Belt (from Monger et al., 1972).

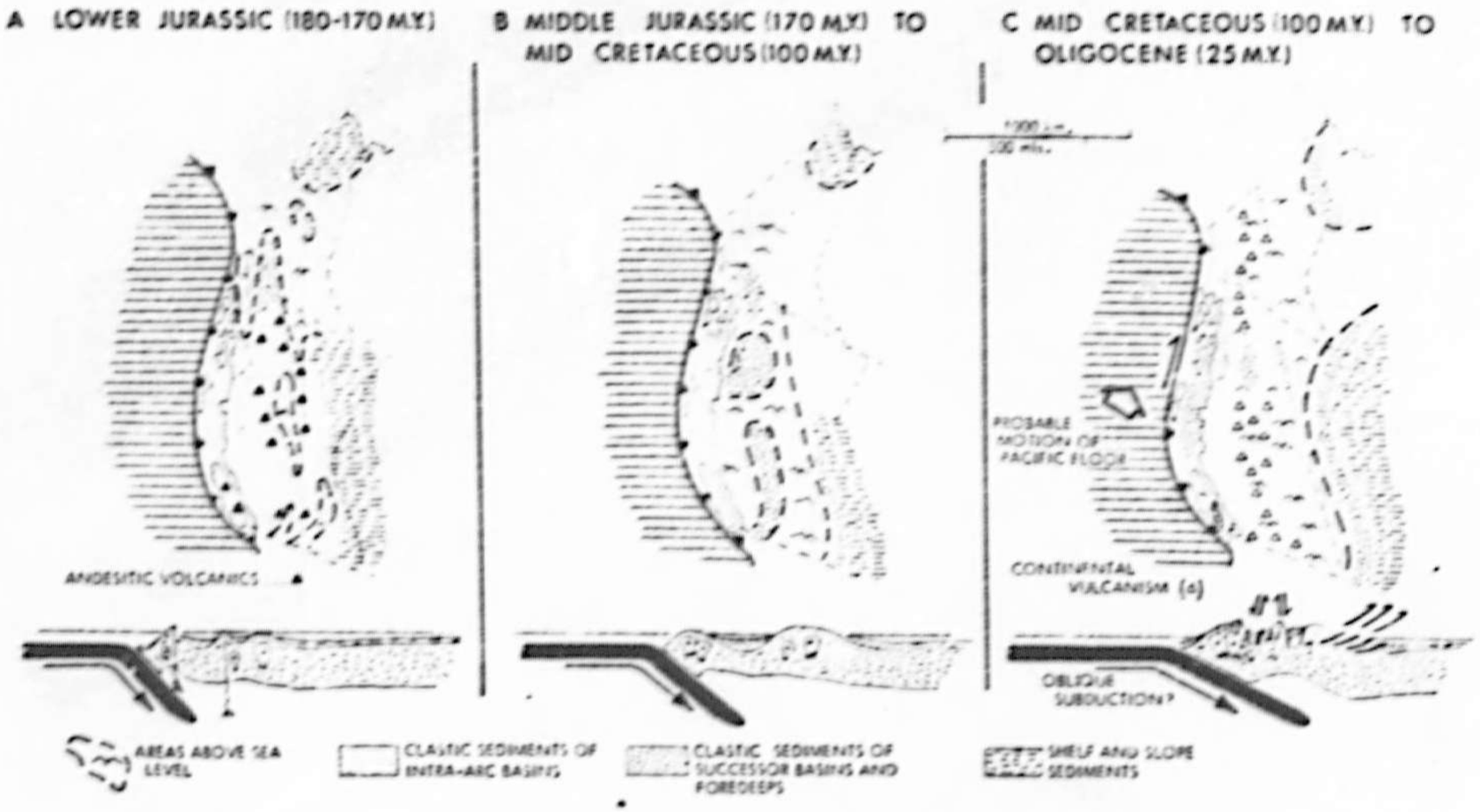


Fig. 3.3. Plate tectonic interpretations, from Lower Jurassic to Oligocene, in Canadian Cordillera (from Monger et al., 1972).

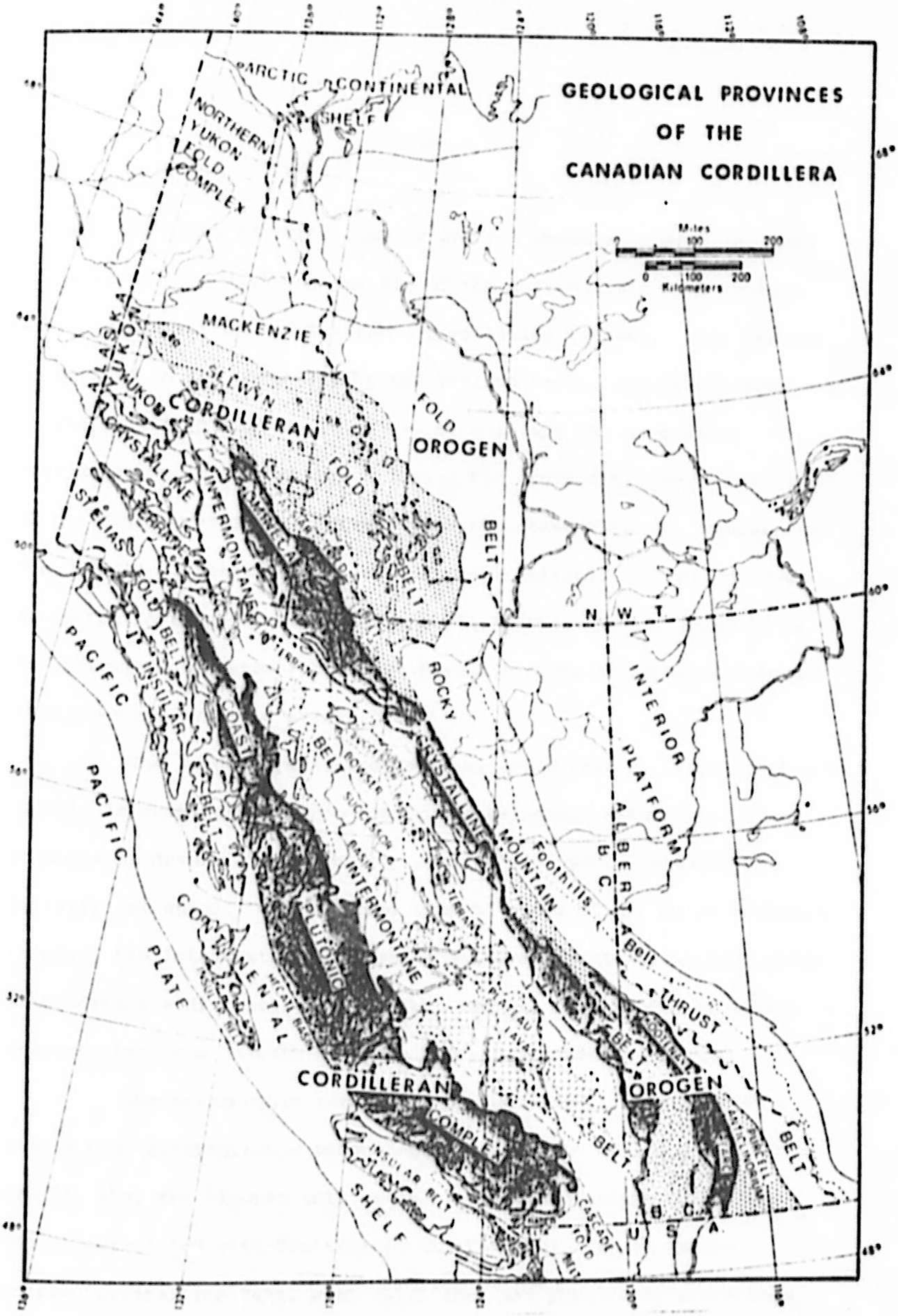


Fig. 3.4. Tectonic subdivisions of the Canadian Cordillera, showing the disposition of the Yukon Crystalline Terrane relative to the Omineca Crystalline Belt, the Intermontane Belt, and the Coast Plutonic Complex (from Tempelman-Kluit, 1976).

scheme, the Coast Plutonic Complex and the Omineca Crystalline Belt merge around the northwestern tip of the Intermontane Belt to form a hybrid element called the Yukon Crystalline Terrane. This terrane is bounded on the northeast by the Tintina Fault, and on the southwest by the Denali-Shakwak Fault, where it overlaps the area under consideration in this thesis. Toward the southeast, the boundaries of the Yukon Crystalline Terrane with the Coast Plutonic Complex and the Omineca Crystalline Belt are not well-defined. To the northwest, in central Alaska, the Yukon Crystalline Terrane passes into, or is faulted against, metamorphosed Proterozoic rocks and unmetamorphosed Paleozoic and Mesozoic strata.

The Yukon Crystalline Terrane, as defined by Tempelman-Kluit (1976), is comprised of Proterozoic and Paleozoic metamorphic rocks intruded by Mesozoic and Tertiary plutons and partly covered by Tertuary volcanics. The superposition of rocks of the Coast Plutonic Complex, the Intermontane Belt and the Omineca Crystalline Belt gives this terrane a distinctive character, as well as a number of shared characteristics with each of three component tectonic elements.

The metamorphic rocks are not considered to be part of a single time-stratigraphic assemblage, as previous work has suggested. Rather, they are grouped into crude lithological assemblages which can be correlated with Proterozoic and Paleozoic strata of the Omineca Crystalline Belt, with which they are physically continuous, at least in part, through facies changes.

The plutonic rocks in the Yukon Crystalline Terrane are divided by Tempelman-Kluit (1976) into four suites. The two oldest (of Late Triassic and mid-Jurassic ages) are correlated with similar plutons in the Intermontane Belt and mark the continuation of the latter through the central part of the Yukon Crystalline Terrane. A younger, mid-Cretaceous, suite in the northern part of the terrane is considered to be a westward continuation of the plutonic rocks of the Omineca Crystalline Belt. The youngest, early Eocene, alaskite suite marks the superposition of Coast Plutonic Complex rocks on the southern part of the Yukon Crystalline Terrane.

Two groups of subaerial, tholeiitic basalts cover parts of the central Yukon Crystalline Terrane. The older, and more widespread, Carmacks Group may be as old as Eocene or as young as Pliocene. The Selkirk Group is more confined in its distribution, and has an apparent Pleistocene or Holocene age.

Tempelman-Kluit (1976) proposes that the evolution of the southern part of the Yukon Crystalline Terrane, adjacent to the Denali-Shakwak Fault, commenced in late Proterozoic or early Paleozoic times with the deposition of fine clastic rocks with minor intercalated volcanics (Fig. 3.5). This stable depositional regime was terminated in the Late Devonian, when greywacke and shale were deposited over the Lower Paleozoic strata. Whereas the former sequence was probably derived from the craton to the east, the (?) Late Devonian and younger rocks may have had a southwestern source. The southern part of the

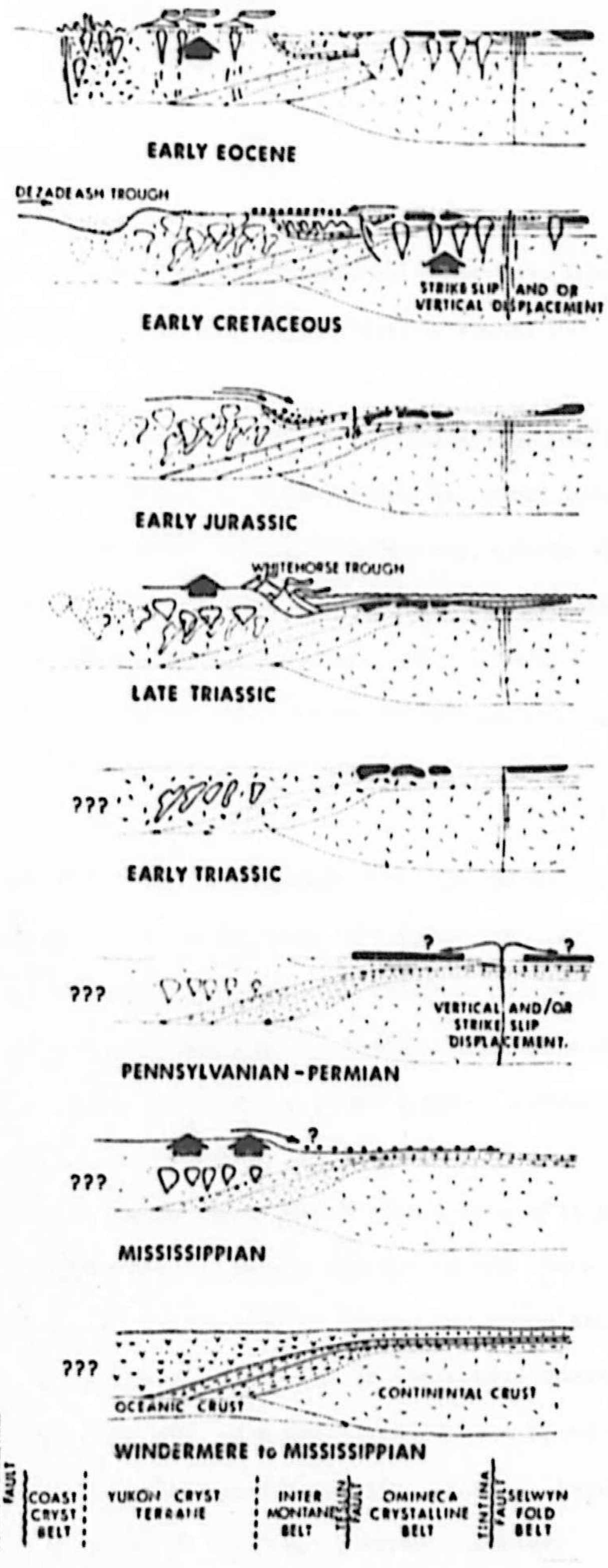


Fig. 3.5. Hypothetical restored sections showing evolution of Yukon Crystalline Terrane (from Tempelman-Kluit, 1976).

Yukon Crystalline Terrane thereafter remained relatively inactive until Early Triassic time, although more complex events were taking place to the north.

In Early Triassic time, the entire assemblage was metamorphosed. By the Late Triassic, metamorphism had waned and, in the southwestern part of the Yukon Crystalline Terrane, quartz diorite and granodiorite batholiths intruded the metasedimentary assemblage. The area stabilized during the Jurassic but, in the Early Cretaceous, southwestwardly-derived flysch began to accumulate rapidly in the Dezadeash Trough on the southwestern flank of the Yukon Crystalline Terrane.

Tempelman-Kluit (1976) suggests that, in the early Eocene, the Ruby Range Batholith was produced by the remobilization of pre-existing rocks, in particular the Late Triassic plutonic rocks. This Eocene plutonism was accompanied by regional metamorphism and deformation, and was followed by major right-lateral movement on the Dalton-Shakwak segment of the Denali fault system.

In later chapters of this thesis, the writer will present evidence which suggests that, while the concept of the Yukon Crystalline Terrane may be valid, it is erroneous to define the southwestern boundary of the Yukon Crystalline Terrane as the Denali-Shakwak Fault system. The boundary may more appropriately lie along the northeastern flank of the Ruby Range Batholith, which is legitimately the northwestward extension of the Coast Plutonic Complex.

CHAPTER 4

GEOCHRONOLOGY OF GRANITOID PLUTONISM

4.1 Introduction

Twenty-eight new K/Ar ages are presented in this chapter as a basis for the definition of plutonic episodes on each side of the Denali-Shakwak Fault. Southwest of the fault, in the Kluane and Icefield Ranges, the rock samples dated yield some of the youngest and oldest ages reported for plutonic rocks in the western part of the Canadian Cordillera. To the northeast, the age of the Ruby Range Batholith is clearly defined, and field evidence for two additional plutonic events is substantiated. The distribution of the dated samples is shown on Map 1 (in pocket).

The radiometric analyses were carried out by Dr. E. Farrar and Mr. D. A. Archibald in the geochronology laboratory of the Department of Geological Sciences, Queen's University. Argon extractions from minerals and whole-rock specimens were carried out in a high-vacuum line by induction heating in a niobium crucible, follcwing baking at about 150°C for 16 hours. Argon isotope ratios were determined in an AEI MS-10 mass spectrometer, operated statically, using ^{38}Ar as the tracer. A bulb tracer system was used to release aliquots of ^{38}Ar, which were periodically calibrated against known volumes of air argon and against geological standards.

At least two aliquots of each sample were taken into

solution through digestion in HF and H_2SO_4. Potassium concentrations were measured with an IL-143 flame photometer, using lithium as an internal standard. The solutions were buffered with sodium to overcome interference effects.

The analytical data are presented in Tables 4.1 and 4.2. The quoted errors in the apparent ages were calculated after the procedure of Baksi et al. (1967), and represent the analytical precisions at the 95 percent confidence levels. The radiometric ages reported in this thesis have been referred to the geological time scale of Van Eysinga (1975).

4.2 Geochronology of Plutonism Southwest of the Denali-Shakwak Fault

Nine K/Ar age determinations from eight separate plutons in the Kluane and Icefield Ranges range from 26.2 to 266.3 million years, a temporal span for Paleozoic and Mesozoic intrusive rocks unequalled in any other part of the Canadian Cordillera. Significantly, these ages show a consistent northeastward younging across a short, 20 mile transect perpendicular to the Denali-Shakwak Fault. The geological complexity of this area, as described in the previous chapters, is reflected in the widely-ranging K/Ar ages of the granitic rocks. The radiometric dating of these rocks is a key element in unravelling the geological history of this area, but comprehensive dating programmes are unfortunately prohibitively expensive due to the inaccessibility of much of the region.

Table 4.1. Analytical data for K/Ar age determinations.

Sample Number	Location	Rock Type	Material Dated	% K	^{40}Ar rad. (10^{-6} cm^3 STP/g)	% Atmospheric Contamination	Apparent Age and Error (m.y.)
Icefield Range Granite (Alexander Terrane)							
115	Lat. 60°18'N Long.137°38'W	Hornblende Granodiorite	Hornblende	1.009	6.115	5.0	145.8 ± 4.4
127	Lat. 61°04'N Long.139°17'W	Bio.-Hb. Quartz Monzonite	Hornblende	0.787	4.541	6.8	139.1 ± 4.4
128	Lat. 61°07'N. Long.139°34'N	Hb.-Bio. Granodiorite	Biotite	7.346	54.68	3.4	176.8 ± 5.4
134	Lat. 61°14'N Long.140°03'W	Hb.-Bio. Quartz Monzonite	Biotite	7.116	79.38	2.1	260.2 ± 10.6
136	Lat. 61°14'N Long.140°03'W	Bio.-Hb. Quartz Monzonite	Hornblende	0.863	9.870	10.1	266.3 ± 8.2
Kluane Range Diorite (Gravina-Nutzotin Belt and Taku-Skolai Terrane)							
144	Lat. 61°21'N Long.139°25'W	Hornblende Diorite	Hornblende	0.389	1.970	28.3	111.7 ± 3.8
167	Lat. 61°44'N. Long.140°19'W	Bio.Hb. Granodiorite	Biotite	6.214	30.97	9.1	120.8 ± 3.6
169	Lat. 61°56'N Long.140°35'W	Hornblende Granodiorite	Hornblende	0.620	3.030	20.6	118.4 ± 3.6

Table 4.1 (cont'd.)

Sample Number	Location	Rock Type	Material Dated	% K	^{40}Ar rad. (10^{-6} cm^3 STP/g)	% Atmospheric Contamination	Apparent Age and Error (m.y.)
Kluane Range Porphyry (Gravina-Nutzotin Belt and Taku-Skolai Terrane)							
145	Lat. 61°22'N Long.139°26'W	Latite Porphyry	Biotite	7.400	7.802	16.0	26.2 ± 0.8

Constants used: $\lambda e = 0.585 \times 10^{-10}\ yr^{-1}$

$\lambda\beta = 4.72 \times 10^{-10}\ yr^{-1}$

$^{40}K/K = 0.0119$ atom percent

All of the dates presented here are consistent with observed stratigraphic contact relations. Further, biotite-hornblende pairs from coeval rocks in the Eastern Alaska Range (Richter et al., 1975) show strong concordance. These data are therefore taken tentatively to represent the times of crystallization of the plutonic rocks.

4.2.1 Alexander Terrane

The subdivisions of Chapter Three will be retained here, since the tectonic elements previously described provide a convenient framework for the discussion of the K/Ar dates. The data classified in Table 4.1 under the heading "Icefield Range Granite", are representative of the ages of plutonic rocks at the northwestward extremity of the Alexander terrane. The five dated samples show a spread in age from 139 m.y. to 266 m.y., and probably represent two plutonic episodes, one from Late Pennsylvanian to mid-Permian in age, and the other spanning much of the Jurassic.

The two oldest ages of 260 (biotite) and 266 (hornblende) m.y. (sample nos. 134 and 136) are for rocks from a small stock about 8 mi. in diameter adjacent to Steele Glacier. This Permian pluton can be considered to be the most northwestern exposure of granitoid rocks in the Alexander terrane. In spite of the concordant ages of the two samples, the stock has a diverse multiphase composition. In the small area examined by this writer, rocks were observed which

range in fabric and composition from aplite to pegmatite and from diorite to quartz monzonite. Samples 134 and 136 are from two different phases of quartz monzonitic composition which, from the evidence available, are the predominant igneous phases. The modal compositions of dated specimens are shown on Figs. 5.1 and 5.5 in Chapter 5.

Part of this stock was staked as a molybdenum porphyry prospect in the 1960's on the basis of some molybdenite float found in the moraines of Steele Glacier, and on reports of minor molybdenum in place by R. P. Sharp (1943). No serious exploration has ever been carried out on the prospect, known as the Steele Creek showing, most of the area lying under ice. News of the existence of molybdenum in this stock found its way into the literature (Clark, 1972) where it is mentioned in an inventory of stockwork molybdenum deposits in the western Cordillera.

Each of three other dated samples from the Alexander terrane represents an individual pluton situated close to the north-eastern margin of this tectonic element, where it is juxtaposed along the Duke River thrust fault against the Taku-Skolai terrane. These intrusions are considerably younger than the Steele Glacier stock, and yield Jurassic ages that range from 139 m.y. to 177 m.y. Their composition is mainly granodioritic or quartz monzonitic and, when compared to the dated Steele Glacier samples on a modal diagram, they show an enrichment in plagioclase at the expense of

potassium feldspar (see Fig. 5.1).

The distribution of these five ages with respect to the boundary of the Alexander terrane suggests a migration of plutonism across the terrane from southwest to northeast. However, the geometry of the specimen locations with respect to the terrane boundaries is such that this observation must be regarded as very tentative.

The plutonic style of these stocks corresponds to Hutchison's (1969) allochthonous-intrusive type. For the most part, they are sub-circular in plan (Muller, 1967) and show marked discordance with the Paleozoic country rocks. However, considerable heterogeneity exists along their margins owing to intimate intermixing of granite and metasediments and incorporation of xenolithic material.

In addition to the data presented here, there is other, indirect, evidence which supports the existence of two pulses of plutonic activity in the Alexander terrane. In Eastern Alaska Range, immediately south of the juncture of the Totschunda and Denali faults, Richter et al. (1975) report K/Ar ages from two plutons, known as the Diorite Complex and the Ahtell Pluton, which have ages ranging from 163 to 199 m.y. and from 282 to 285 m.y., respectively (Fig. 4.1). The geographic distribution of these dates show the same southwest-to-northeast younging evident in the St. Elias Mountains of Yukon Territory.

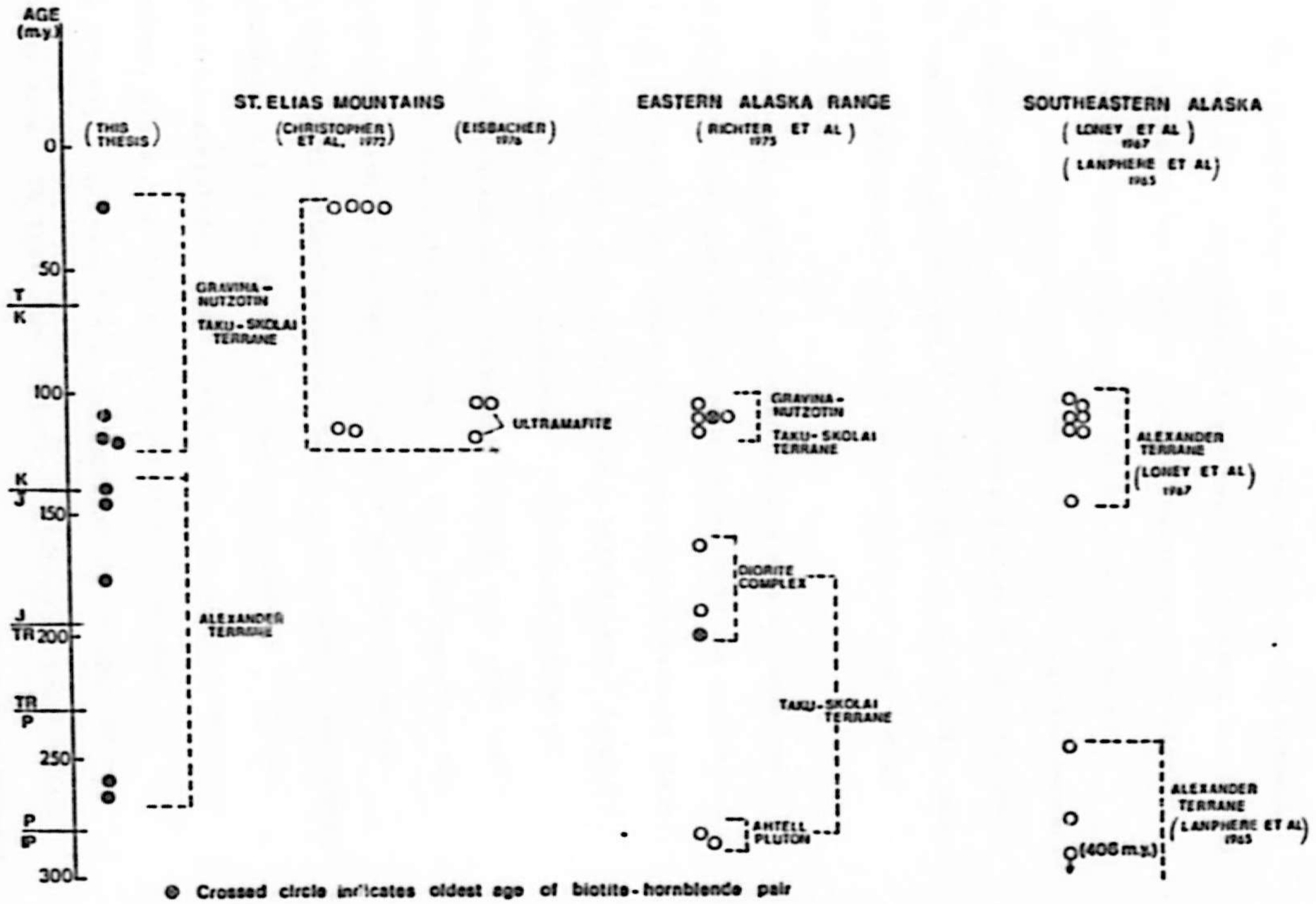


Fig. 4.1. K/Ar dates from plutonic rocks in St. Elias Mountains compared with ages of granitic rocks from Eastern Alaska Range and southwestern Alaska.

Petrographically, these rocks are similar to the Alexander terrane intrusives; in particular, the Ahtell Pluton bears a striking resemblance to the Steele Glacier pluton. Relative to the Steele Glacier pluton, the Ahtell Pluton and the Diorite Complex are displaced about 180 miles northwestward (in the right-lateral sense), along the Totschunda Fault. However, these plutons do not intrude Alexander terrane as it has been defined by Berg et al (1972), and their evolution may bear a different relationship to the country rocks they invade.

There are no other published potassium-argon ages for granitic rocks in the Alexander terrane except near its southeastern extremity on Chichagof and Admiralty Islands in southeastern Alaska. These data do not match closely the dates reported here. Lanphere et al. (1964, 1965) describe intrusion by granitoid bodies of Ordovician and Silurian ages, considerably older than even the metasediments in the Icefield Ranges. There is evidence for two periods of plutonism in the Mesozoic, one in the late Jurassic and the other in the mid-Cretaceous (Loney et al., 1967), the younger of which postdates intrusion in the northwestern Alexander terrane. This lack of correlation is not unexpected: the distance between the northwestern and southeastern limits of the Alexander terrane exceeds 300 miles and very little is known of the geology of the intervening area. Further, the geological history of the Alexander terrane, if it did evolve as an element allochthonous to northwestern

North America, is not well understood.

4.2.2 Gravina-Nutzotin Belt and Taku-Skolai Terrane

Strata of the Gravina-Nutzotin belt and the Taku-Skolai terrane are in depositional contact in Eastern Alaska and southwestern Yukon, where they show their greatest areal extent. Both units have been intruded by plutons ascribable to a single, well-defined phase of mid-Cretaceous intrusive activity which lasted for about 10 m.y., according to evidence from radiometric dating.

In the Kluane Range, these rocks are diorites, quartz diorites and granodiorites of rather basic composition; much of the diorite, which is the dominant phase, is undersaturated with respect to silica and contains no free quartz. On a modal diagram (Fig. 5.1), these rocks are seen to be poor in potassium feldspar when compared to the intrusive rocks of the Alexander terrane.

Three samples from separate plutons (shown as Kluane Range Diorite in Table 4.1) range in age from 112 m.y. to 121 m.y., in close agreement with previously published dates. Christopher et al. (1972) have dated the same pluton from which sample 144 (112 m.y.) was taken and determined two, essentially identical, ages of 115 m.y. and 117 m.y. Recently, Eisbacher (1976) has reported three K/Ar dates of 106 m.y., 107 m.y. and 118 m.y., although the two older ages are from a pyroxenite intrusion which may be synchronous, but not necessarily consanguinious with, the Kluane

Range Diorite suite.

The plutonic style of these intrusive rocks is similar to that described for the plutons in the Alexander terrane. However, in comparison, intrusive contacts, though irregular, tend to be more distinct, and there is less intermixing with the country rock. In plan, these plutons tend to be elongated from northwest to southeast, parallel to the grain of the geology.

Outside of Yukon Territory, these rocks have received the closest examination in the Eastern Alaska Range along the northwestward extension of the St. Elias Mountains. The triangular area bounded by the Denali and Totschunda Faults and the Alaska-Yukon border (see Fig. 3.1) is underlain entirely by Gravina-Nutzotin and Taku-Skolai terranes. Within these boundaries, Richter et al. (1975) have dated four plutons which define a period of intrusive activity from 117 to 105 m.y., synchronous with the mid-Cretaceous activity in the Kluane Ranges. These rocks are similar to their counterparts in Yukon; modal analyses indicate predominant dioritic and granodioritic compositions, with a significant proportion of syenodiorites and monzonites, consistent with the silica undersaturation characteristic mentioned previously.

The most recent plutonic event in the St. Elias Mountains is represented by a series of small, hypabyssal, felsite (i.e., rhyolite, latite, dacite and trachyte) stocks. These rocks, herein grouped as the Kluane Range Porphyry suite, mainly intrude Gravina-

Nutzotin and Taku-Skolai terrane as dykes, sills and small stocks, but also occur along the northeastern edge of the Alexander terrane within a few miles of the Duke River Thrust. They appear to have been emplaced in the early Miocene, as is indicated by the age of 26 m.y. for sample 145 (Table 4.1); this age is coincident with those reported by Christopher et al. (1972). There is some field evidence to suggest that these felsic intrusions are genetically related to the subaerial suite of Tertiary volcanic rocks defined by Muller (1967) as the St. Clare Group. Souther and Stanciu (1975) note that the lower and middle units of that volcanic pile are cut by felsic intrusions, and offer as evidence for a genetic relationship the occurrence of stream-rounded felsite clasts in conglomerates associated with air-fall pumice interlayered with lavas in the middle unit.

Similar hypabyssal rocks have been described in the Eastern Alaska Range (Richter and Jones, 1973), where they show comparable structural relationships to the Wrangell Lavas. This suite of Miocene felsic intrusives is not known to occur in south-eastern Alaska.

4.2.3 Summary

The K/Ar ages reported in this thesis, for plutonic rocks in the Alexander terrane, as well as previously published dates, Gravina-Nutzotin Belt and Taku-Skolai terrane are graphically compared in Fig. 4.1. The radiometric data appear to define four

distinct plutonic episodes in the region bordering the southwest side of the Denali-Shakwak fault system and extending from the Eastern Alaska Range through the St. Elias Mountains to southeastern Alaska.

The oldest of these epochs began in the late Pennsylvanian or early Permian, and persisted to about the mid-Permian, approximately from 290 m.y. to 260 m.y. ago. The second epoch embraced much of the Jurassic, and was followed, after a hiatus of about 20 m.y., by a brief but widespread pulse of mid-Cretaceous plutonism. Finally, a Miocene age has been defined for a suite of hypabyssal felsic intrusives which may be related to a period of extensive subaerial volcanism.

A fifth plutonic event, which has not been delimited by radiometric dating, is represented by large dykes and sills of gabbro and peridotite which are inferred to have been emplaced in the interval from Permian to Cretaceous on the basis of stratigraphic evidence. In the St. Elias Mountains, these rocks are confined to the Taku-Skolai terrane where they generally occur in close proximity to thrust faults. This suite also occurs in the Eastern Alaska Range (Richter and Jones, 1973).

Although radiometric dating appears to define four phases of granitic plutonism in contiguous geographic regions considered in this discussion (i.e., Eastern Alaska Range, St. Elias Mountains and southeastern Alaska), there seems to be less

consistency in associating plutonic epochs with tectonic elements by region (see Fig. 4.1). Furthermore, each phase of plutonism, in the St. Elias Mountains at least, appears to be considerably younger than the country rocks which it invades. These observations imply that the granitic rocks have evolved independently from, and much later than, the tectonic stratigraphic elements in which they occur.

4.3 Geochronology of Plutonism Northeast of the Denali-Shakwak Fault

Nineteen new K/Ar dates, presented herein, from the area northeast of the Denali-Shakwak Fault are considered to define three phases of plutonic activity during the Cretaceous and Tertiary. Most of these data are from the Ruby Range Batholith, but five dates represent two other plutonic suites which are exposed to the north of the batholith.

The oldest recognized plutonic rocks in this region are the Nisling Range granodiorites, a suite first defined by Muller (1967). Three samples dated here, a granodiorite and two quartz monzonites (see Fig. 5.2), gave Cretaceous ages of 101, 99 and 67 m.y. (see Table 4.2). The two mid-Cretaceous ages of 101 and 99 m.y. are taken to represent times of crystallization, but the date of 67 m.y. is almost certainly too young, perhaps due to degassing by a later thermal event. This sample (#24) was taken from drill-core from a small porphyry copper prospect on Rhyolite Creek in the Nisling Range. This small, sparsely-mineralized, stock has been

Table 4.2. Analytical data for K/Ar age determinations.

Sample Number	Location	Rock Type	Material Dated	% K	^{40}Ar rad. (10^{-6} cm^3 STP/g)	% Atmospheric Contamination	Apparent Age and Error (m.y.)
Nisling Range Granodiorite							
1	Lat. 61°53'N Long.140°05'W	Hb.-Bio. Grano-diorite	Biotite	7.179	29.21	12.1	99.1 ± 3.0
2	Lat. 61°59'N Long.139°43'W	Bio.-Hb. Quartz Monzonite	Biotite	5.777	23.91	10.3	100.8 ± 3.2
24	Lat. 61°50'N Long.138°31'W	Hb.-Bio. Quartz Monzonite	Biotite	7.440	20.38	10.8	67.3 ± 2.2
Ruby Range Granodiorite							
7	Lat. 61°46'N Long.139°58'W	Hb.-Bio. Granodiorite	Biotite	7.697	17.03	16.6	54.6 ± 1.6
13	Lat. 61°37'N Long.139°21'W	Biotite Quartz Monzonite	Biotite	7.112	15.60	25.5	54.1 ± 1.6
18	Lat. 61°41'N Long.138°56'W	Biotite Quartz Monzonite	Biotite	7.403	16.34	14.5	54.4 ± 1.6

Table 4.2 (cont'd.)

Sample Number	Location	Rock Type	Material Dated	% K	^{40}Ar rad. (10^{-6} cm^3 STP/g)	% Atmospheric Contamination	Apparent Age and Error (m.y.)
32	Lat. 61°36'W Long.138°25'N	Hb.-Bio. Granodiorite	Biotite	6.323	15.77	11.5	61.4 ± 1.8
48	Lat. 61°31'N Long.138°39'W	Hb.-Bio. Quartz Diorite	Biotite	7.572	16.69	23.2	54.3 ± 1.6
54	Lat. 61°23'N Long.138°44'W	Hb.-Bio. Quartz Diorite	Biotite	7.489	16.44	23.4	54.1 ± 1.6
61	Lat. 60°49'N Long.137°29'W	Biotite Granodiorite	Biotite	6.997	13.96	19.7	49.3 ± 1.6
77	Lat. 60°35'N Long.136°07'W	Biotite Quartz Monzonite	Biotite	6.982	15.73	12.7	55.5 ± 1.8
90	Lat. 60°21'N Long.136°21'W	Hb.-Bio. Quartz Diorite	Biotite	7.402	16.52	18.7	55.0 ± 1.8
103	Lat. 60°08'N Long.136°07'W	Bio.-Hb. Granodiorite	Biotite	7.086	15.66	20.1	54.5 ± 1.6
104	Lat. 60°03'N Long.136°53'W	Bio.-Hb. Quartz Diorite	Biotite	7.447	19.69	15.8	65.0 ± 2.0

Table 4.2 (cont'd.)

Sample Number	Location	Rock Type	Material Dated	% K	^{40}Ar rad. (10^{-6} cm^3 STP/g)	% Atmospheric Contamination	Apparent Age and Error (m.y.)
Kluane Schist							
KLL-1-1	Lat. 61°22'N Long.138°40'W	Quartz-Bio. Schist	Biotite	7.060	15.30	7.8	53.4 ± 1.6
KLL-2-5	Lat. 61°21'N	Quartz-Bio. Schist	Whole Rock	2.668	5.363	27.7	49.6 ± 1.6
KLL-2-1	Lat. 61°10'N Long.138°27'W	Quartz-Sericite Schist	Whole Rock	2.149	3.596	23.7	41.4 ± 1.4
Nisling Range Alaskite							
28	Lat. 61°49'N Long.138°33'W	Biotite Quartz Monzonite	Biotite	6.162	13.82	14.4	55.3 ± 1.8
36	Lat. 61°28'N Long.138°07'N	Biotite Quartz Monzonite	Biotite	6.540	13.47	19.1	50.8 ± 1.6

Constants used: $\lambda e = 0.585 \times 10^{-10}$ yr^{-1}

$\lambda\beta = 4.72 \times 10^{-10}$ yr^{-1}

$^{40}K/K = 0.0119$ atom percent

invaded by at least two sets of later quartz veins, probably associated with dyke swarms of the Eocene Nisling Range Alaskite in this part of the claim group (Hassard and Woollett, 1971).

The Nisling Range Granodiorite suite is not extensively developed in the Yukon, where it forms only two elongated plutons in the southern part of the Yukon Crystalline Terrane (Tempelman-Kluit, 1976). Furthermore, these plutons only encroach upon the northernmost part of the area under consideration in this thesis, so they were not sampled in detail. However, Tempelman-Kluit and Wanless (1975) report four K/Ar age determinations for these rocks. One sample pair gave ages for coexisting biotite and hornblende of 85 m.y. and 92 m.y.; another pair gave coincident ages of 94 m.y. All four ages are slightly younger than the two valid biotite dates reported here.

In the Eastern Alaska Range, there is exposed a suite of plutonic rocks which is probably coeval with the Nisling Range granodiorites. These rocks occur as elongated plutons lying close to the Denali Fault on its northern side. They display a wider range of composition than do the Nisling Range rocks, with a greater relative abundance of quartz monzonites. Richter et al. (1975) report K/Ar ages ranging from 89 to 94 m.y. for these rocks, corresponding closely to the age determinations of Tempelman-Kluit and Wanless (1975). These dates are compared in Fig. 4.2. The broadly concordant dates are tentatively inferred to represent a mid-Cretaceous age of

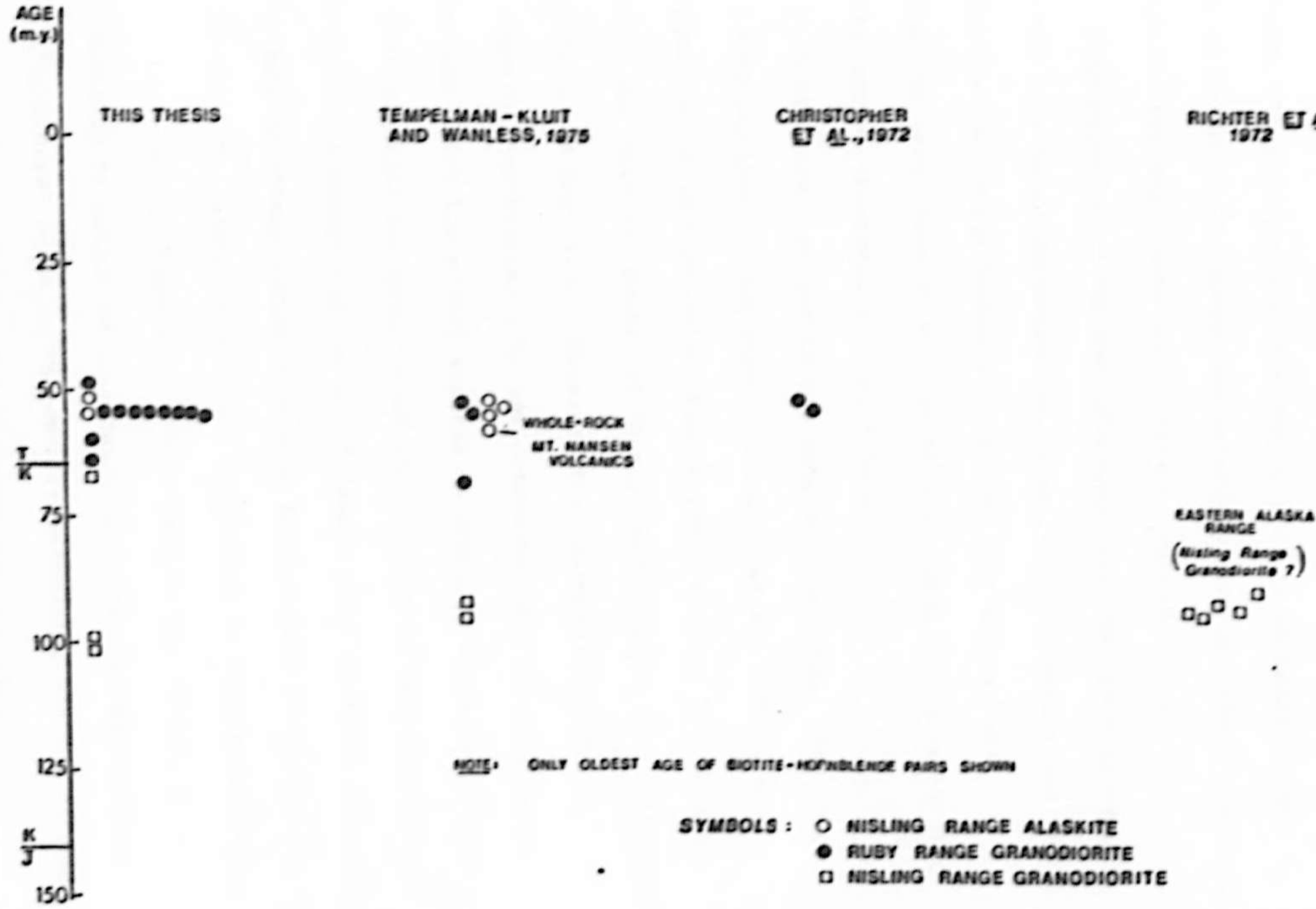


Fig. 4.2. Comparison of K/Ar dates for Nisling Range Granodiorite, Ruby Range Granodiorite and Nisling Range Alaskite.

emplacement. They contradict no stratigraphic relationships and there is no evidence of thermal overprinting, such as widely scattered radiometric dates and discordant biotite-hornblende pairs.

The majority of the new K/Ar dates reported in this section are for the Ruby Range granodiorites, a suite of plutonic rocks which comprises the Ruby Range Batholith. Eleven K-Ar mineral age determinations range from 49 m.y. to 65 m.y., eight of these falling within the narrow interval, 53 m.y. - 56 m.y.

These Paleocene and Eocene ages are consistent with other recent determinations by Tempelman-Kluit and Wanless (1975), who report ages for three biotite-hornblende pairs ranging from 49 m.y. to 68 m.y., and with two dates, of 52 m.y. and 54 m.y., by Christopher et al. (1972; see Fig. 4.2). However, the Geological Survey of Canada reports four earlier K/Ar age determinations for Ruby Range granodiorites which the writer regards as probably erroneous. There may be justification for questioning the validity of many K/Ar dates determined at the Geological Survey of Canada prior to 1965, including the four determinations referred to here (nos. G.S.C. 59-12, 59-13, 60-31, 60-32). The evidence for this contention is summarized below:

i) In G.S.C. Paper 67-2 (1967, part A, pp. 35-38), a brief discussion is presented concerning discrepancies between two sets of K/Ar mineral dates on the Guichon Batholith, one set of ages done at the University of British Columbia and the other at the G.S.C. prior to 1965. The U.B.C. determinations averaged approximately

200 m.y. as compared to the G.S.C. dates of approximately 245 m.y. After some changes were made in analytical equipment at the G.S.C. (in late-1964 or early-1965), some of the G.S.C. dates were repeated and found to agree closely with the U.B.C. determinations. In this same paper, the closing comment (in the discussion of sample 66-40) lists ten G.S.C. determinations, done prior to 1965, which were considered to be too high. This is the only published statement the writer is aware of which suggests that pre-1965 G.S.C. K/Ar age determinations might be unreliable.

ii) In another instance, J. C. Roddick (1970) obtained K/Ar ages for the Eagle granodiorite of about 104 m.y., which may be compared to a G.S.C. date of 143 m.y. (G.S.C. 62-56). A more recent G.S.C. age determination gave an age of 98 m.y. (G.S.C. 65-9) in close agreement with some of Roddick's dates.

iii) G.S.C. sample 59-10, with a reported age of 225 m.y., from the Whitehorse area, Yukon, is described as having 100% radiogenic argon (G.S.C. Paper 60-17, p. 7), which is virtually impossible. This determination is quoted in the literature (e.g., Roddick and Hutchison, 1974; Tempelman-Kluit, 1976) as evidence for the occurrence of Triassic plutonism in southern Yukon Territory.

There is other evidence, some of it more circumstantial, which does not bear repetition here. The modifications to the apparatus at the G.S.C. (in 1965?) involved the addition of an electron multiplier to the mass spectrometer which significantly increased the

sensitivity of the instrument in the measurement of ^{36}Ar. This, in turn, permitted a more accurate determination of the atmospheric ^{40}Ar content. Previous estimates of this quantity were low and, when subtracted from the total ^{40}Ar content, gave values of radiogenic ^{40}Ar which were high, thereby resulting in apparent ages which were too high.

Unfortunately, one of the analyses under consideration (G.S.C. 59-12), with a reported age of 176 m.y., has been cited in the recent literature (e.g., Tempelman-Kluit, 1976) as representing the true age of the Ruby Range Batholith.

The new and previously-published radiometric ages for the Ruby Range granodiorites and the adjacent Nisling Range alaskites, excluding the G.S.C. dates, are presented in the form of histograms in Fig. 4.3.

Any interpretation of the age data must take into account the markedly gradational nature of at least part of the Ruby Range Batholith contact. Where well exposed, as along the shores of Talbot Arm, the outer zones of the batholith are observed to contain very numerous inclusions and screens of metasedimentary rocks, often in an agmatitic or migmatitic association (see Fig. 4.4). The gneissic appearance of such contacts argues for the assimilation of metasedimentary host rock by the granodioritic magma. Further, in passing outwards from the contact, the metasediments of the envelope grade from gneissic, through schistose to phyllitic in texture.

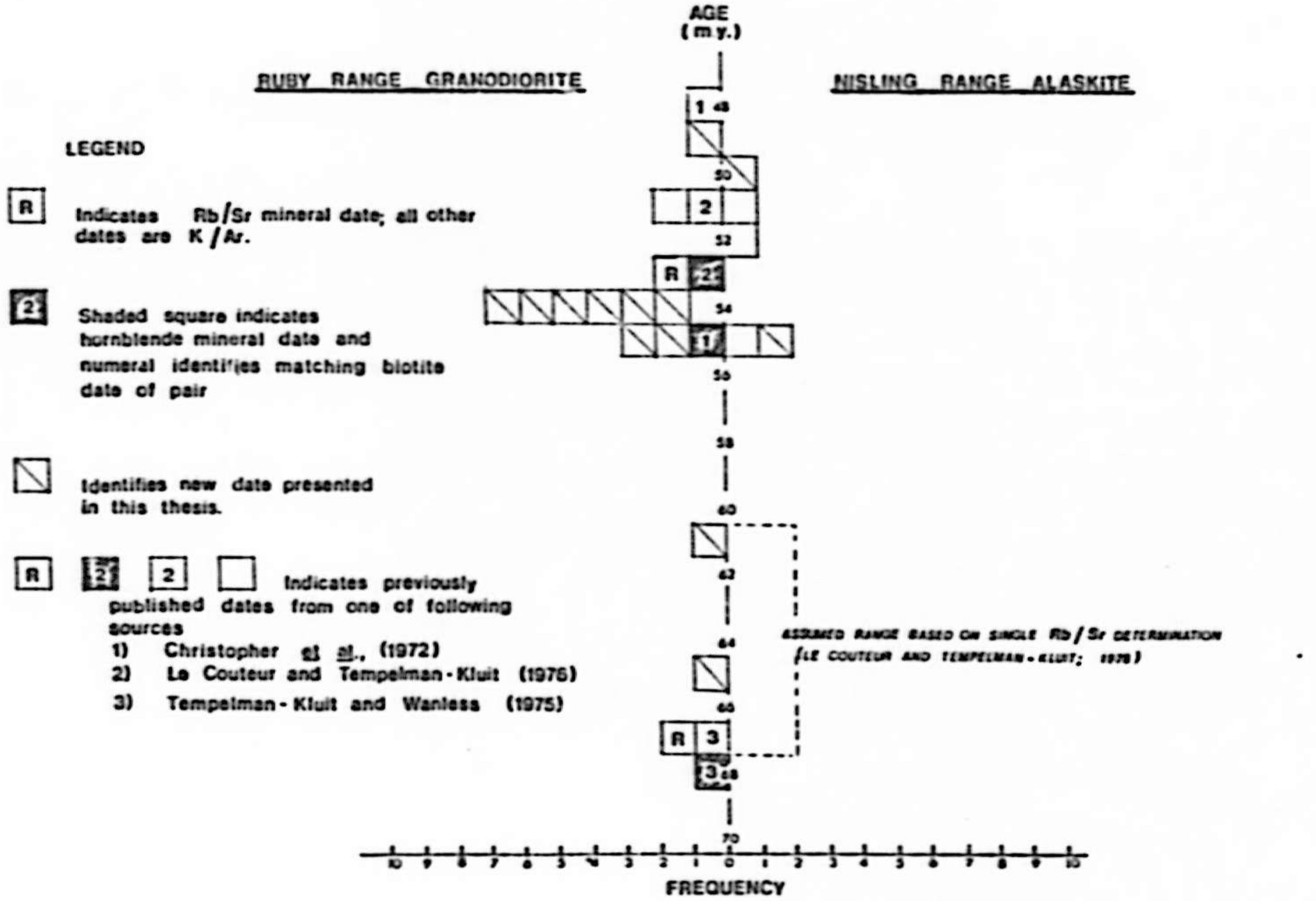
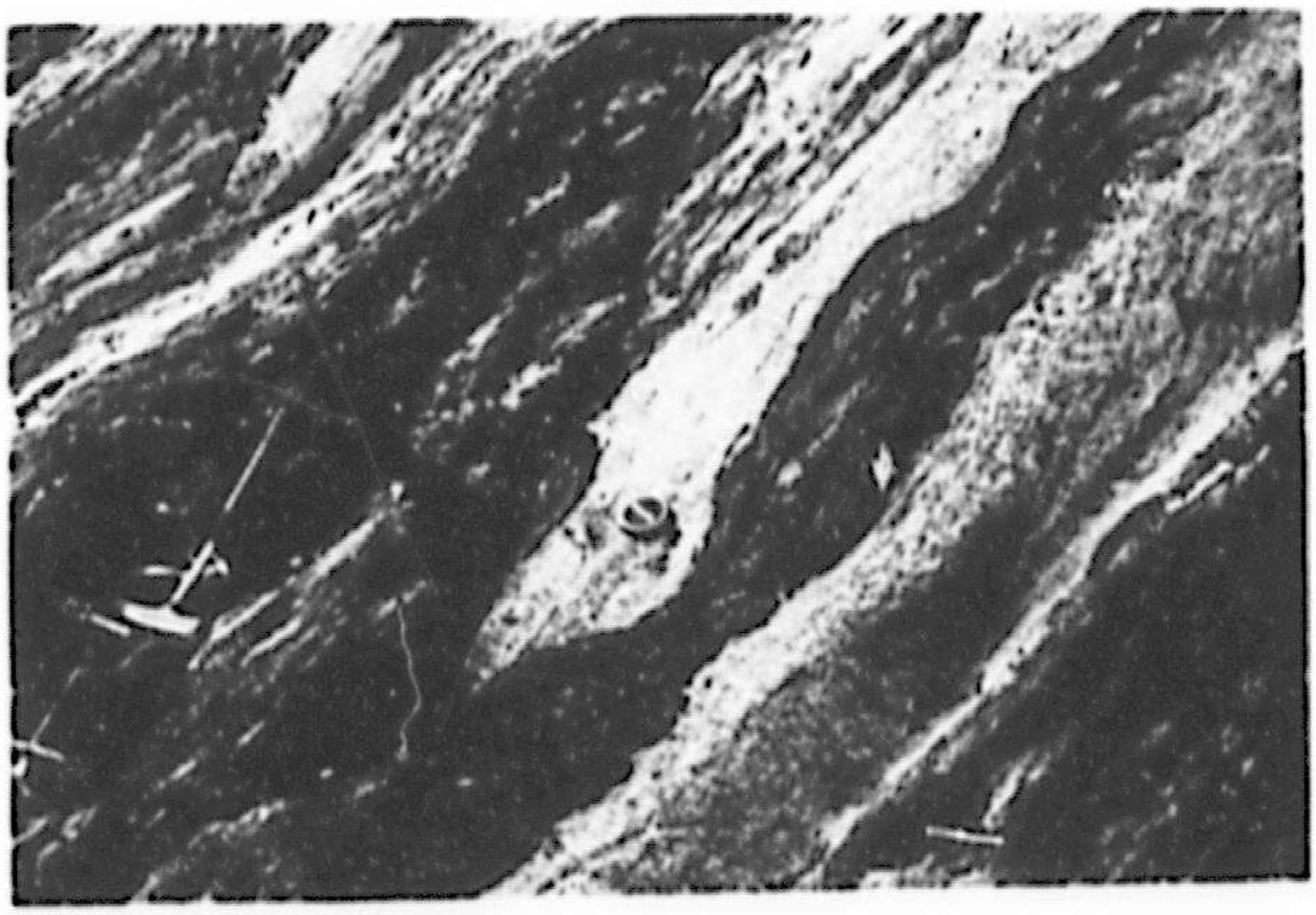


Fig. 4.3. Comparative histogram of new and previously published radiometric dates for Ruby Range Granodiorite and Nisling Range Alaskite.

Fig. 4.4. Migmatite at contact of Ruby Range Granodiorite and Kluane Schist, west shore of Talbot Arm, Kluane Lake.



These relationships correspond to Hutchison's (1970) "autochthonous-migmatitic" style, and are suggestive of a relatively deep-seated, probably mesozonal, emplacement of the batholith. Thus, a spectrum of K/Ar mineral ages, reflecting progressive cooling during erosional unroofing and uplift, would be expected. Indeed, the available ages cover a time span of ca. 20 m.y. However, the apparently bimodal distribution of the ages (Fig. 4.3) implies the occurrence of two, distinct, events or stages in the cooling history of this large intrusion: one at ca. 65 m.y.; and the later at ca. 54 m.y. The older and younger ages display no systematic analytical differences (e.g., K% in biotite) which would permit their distinction. They are all, therefore, considered to reflect the times of cooling of the biotites to below the argon retention temperature, following intrusion.

Field observations and petrographic (Chap. 5) and chemical (Chap. 6) data lend no support to the hypothesis that the two maxima in the K-Ar age distribution reflect two distinct episodes of intrusion in a polyphase batholith. Sharp contacts between lithologically-different intrusion planes have not been observed, while "older" and "younger" rocks are essentially identical in their mineral assemblages, textures, and compositions.

In this context it is significant that all of the older ages are for rocks located very close to the margins of the batholith (see Map 1). In view of the gradational nature of the batholith

contacts, the possibility has been considered that these older, Paleocene, ages reflect the incorporation of radiogenic argon of metasedimentary origin in the magmas. However, the lack of older ages in all specimens dated from the well-exposed, gradational, Talbot Arm contact zone, including both granodiorite and meta-sediment, argues strongly against such an interpretation.

It is considered, therefore, that, following initial emplacement at comparatively great depths, at which ambient temperatures exceeded those required for the retention of argon in biotite and hornblende, moderate uplift and erosion in the Paleocene, and more rapid heat transfer to country rocks in the thermal aureole of the intrusion, caused the preferential cooling of portions of the margins of this batholith. Alternatively, the topography generated above the batholith during its emplacement may have been sufficiently great to permit the earlier cooling of such marginal areas.

Subsequently, following a period of relative stability that lasted for some 10 m.y., further, abrupt, uplift and erosion caused the entire batholith to move through the argon retention "isotherm". It is noteworthy that this Eocene event is indistinguishable in its age from the cooling age indicated for the Nisling Range alaskites (see below; and Fig. 4.3). It is thus reasonable to ascribe the final uplift of the Ruby Range Batholith and the high-level (epizonal) emplacement of the Nisling Range alaskites to the same, Eocene, event.

Tempelman-Kluit (1974, 1976) considers the true age of the Ruby Range granodiorites to be Triassic, on the basis of its compositional similarity to the Triassic Klotassin quartz diorite suite which is exposed in the northern part of the Yukon Crystalline Terrane, and on a single K/Ar date (G.S.C. 59-12) of 176 m.y. which, he suggests, is close to the true age of these rocks. This contention is difficult to support, for a number of reasons. Firstly, there is reason to doubt the validity of pre-1965 K/Ar determinations by the G.S.C., as outlined above. Secondly, this single date differs markedly from twenty other radiometric dates (Fig. 4.3) which establish the age of the Ruby Range granodiorites as early Tertiary. Finally, to suggest that Ruby Range granodiorites are Triassic when they are observed to intrude Upper Jurassic and Lower Cretaceous Kluane Schist rocks (Eisbacher, 1976), is contradictory.

The argument has also been advanced by Tempelman-Kluit (1974, 1976) and by Tempelman-Kluit and Wanless (1975) that "The preponderance of 50- to 60-m.y. ages in the [Ruby Range] granodiorite is thought to result from widespread argon loss of the rocks during intrusion by the Nisling Range alaskite" (Tempelman-Kluit, 1976; p. 1352). Again, this contention is difficult to support in the face of a number of serious objections, not the least of which is that the vast bulk of the Ruby Range Batholith is not spatially contiguous with Nisling Range Alaskite. In the Talbot Arm-Kluane Lake area, the Kluane Schists appear to have equilibrated thermally

with the intrusion in the Eocene (see age determinations for Kluane Schist in Table 4.2), and Eisbacher (1976) has mentioned that ages of up to 70 m.y. have been found for biotites in these metasediments in proximity to the batholith (unpubl. data, Univ. Alaska). By implication, Tempelman-Kluit suggests that intrusion by Nisling Range alaskites and not Ruby Range granodiorites is responsible for thermally-resetting the age of the Kluane Schists, yet it is difficult to see how this could be so, when the entire Ruby Range Batholith intervenes between the Nisling Range Alaskite and the Kluane Schist. Moreover, thermal resetting of Ruby Range granodiorites by intrusion of Nisling Range alaskites could reasonably be expected to produce a scatter of ages but, although apparently bimodally distributed, the radiometric dates for the Ruby Range granodiorites' cannot be said to be scattered. Indeed, Le Couteur and Tempelman-Kluit (1976) report two Rb/Sr mineral ages for the Ruby Range Batholith (Fig. 4.3) which lend additional support to the "reality" of the older and younger ages outlined by the K/Ar dates.

The early Tertiary age of emplacement of the Ruby Range Batholith, inferred from the present work, is matched by many rocks from the eastern parts of the Coast Plutonic Complex of British Columbia (Roddick and Hutchison, 1974; Peto, 1974). Such young ages were originally interpreted by Hutchison (1970) as resulting from late unroofing of the Complex, but, more recently (talk presented at informal Circum-Pacific Plutonism Conference, Vancouver,

1975) he has tentatively regarded them as indicating actual ages of intrusion. The broad contemporaneity of the Ruby Range Batholith and the eastern part of the Coast Plutonic Complex supports the hypothesis that they represent two segments of one major intrusive system.

The youngest plutonic rock suite in the region northeast of the Denali-Shakwak Fault is the Nisling Range Alaskite (Muller, 1967). This suite forms a series of hypabyssal plutons, often associated with dyke swarms, that are presumed to represent feeders to the intermediate and acid pyroclastics of the Mount Nansen Group (Tempelman-Kluit, 1974). For the most part, the Nisling Range alaskites lie to the north and east of the Ruby Range Batholith and there is little areal overlap. However, where these two units are contiguous, the alaskites are observed to cut the Ruby Range Granodiorite, indicating that they are younger (Tempelman-Kluit, 1974, 1976).

Radiometric ages from Nisling Range alaskites coincide closely with those of Ruby Range Granodiorite (Fig. 4.3), as noted above, and offer no basis for distinguishing Nisling Range Alaskite as a younger intrusive event as is revealed by the field relationships.

The two age determinations for these rocks presented here (Table 4.2, Fig. 4.3), give ages of 51 m.y. and 55 m.y. Tempelman-Kluit and Wanless (1975) report three very similar K/Ar

1975) he has tentatively regarded them as indicating actual ages of intrusion. The broad contemporaneity of the Ruby Range Batholith and the eastern part of the Coast Plutonic Complex supports the hypothesis that they represent two segments of one major intrusive system.

The youngest plutonic rock suite in the region northeast of the Denali-Shakwak Fault is the Nisling Range Alaskite (Muller, 1967). This suite forms a series of hypabyssal plutons, often associated with dyke swarms, that are presumed to represent feeders to the intermediate and acid pyroclastics of the Mount Nansen Group (Tempelman-Kluit, 1974). For the most part, the Nisling Range alaskites lie to the north and east of the Ruby Range Batholith and there is little areal overlap. However, where these two units are contiguous, the alaskites are observed to cut the Ruby Range Granodiorite, indicating that they are younger (Tempelman-Kluit, 1974, 1976).

Radiometric ages from Nisling Range alaskites coincide closely with those of Ruby Range Granodiorite (Fig. 4.3), as noted above, and offer no basis for distinguishing Nisling Range Alaskite as a younger intrusive event as is revealed by the field relationships.

The two age determinations for these rocks presented here (Table 4.2, Fig. 4.3), give ages of 51 m.y. and 55 m.y. Tempelman-Kluit and Wanless (1975) report three very similar K/Ar

determinations from Nisling Range alaskites that range from 52 m.y. to 56 m.y. as well as a 58 m.y. whole-rock date for a tuff from the Mt. Nansen Group. A single Rb/Sr whole-rock determination by Le Couteur and Tempelman-Kluit (1976), assuming an initial Sr^{87}/Sr^{86} ratio of 0.704 - 0.708, gave a range of 61 to 67 m.y. but should not be regarded as sufficiently accurate to contradict the K/Ar data. Thus, the Nisling Range Alaskite and Ruby Range Granodiorite can be defined as separate plutonic events on the basis of location, chemistry and mineralogy (to be shown in following chapters), plutonic style, and cross-cutting relationships, but not on the basis of radiometric dating.

CHAPTER 5

PETROGRAPHY OF GRANITOID ROCKS IN SOUTHWESTERN YUKON

5.1 Introduction

This chapter presents the results of petrographical studies of rock samples from the plutonic suites occurring in the thesis area. Ninety-one modal analyses were carried out on stained slabs, using Chayes' (1956) replication schedules to control analytical error. The analytical techniques are described in Appendix A. The difference between the number of modal analyses reported in this chapter and the number of chemical analyses (122) reported in the following chapter is accounted for mainly by porphyritic rocks whose texture made them unsuitable for the analytical technique used here.

The modal classification scheme used in this chapter is shown in Figs. 5.1 and 5.5. This system is used by the United States Geological Survey and the Geological Survey of Canada and is the one most frequently used in the literature on Cordilleran geology. The reconnaissance scale nature of this study, and the need to correlate with previous work, argued for the retention of a common nomenclature system, rather than the adoption of more recent, and perhaps better-founded, classification systems.

5.2 Petrography of Granitoid Rocks Southwest of the Denali-Shakwak Fault

The major mineral modes of individual samples are presented in Table 5.1, and are plotted on the quartz-plagioclase-potassium feldspar diagram in Fig. 5.1. No modal analyses of the Kluane Range Porphyry suite were done owing to the generally aphanitic matrix of these rocks.

It is apparent from Fig. 5.1 that the Icefield Range granites show a wide range of modal composition and, as will be later shown (Chapter 6), of chemical composition as well. Muller (1967) performed modal analyses on eight samples from this suite, four of which were shown to be alaskite in composition, with no more than 10% plagioclase. Taking Muller's analyses into account, the field defined by this suite would show a wide range from 0-50% quartz, 0-100% plagioclase, and 0-65% orthoclase.

The limited sampling of this suite by this writer and others makes it difficult to make conclusions about the variability of rock compositions in Icefield Range granites. However, there are apparently significant differences in modal composition from pluton to pluton. Furthermore, there is no correlation of rock type with age: it is evident from Fig. 5.1 that the Permian Steele Glacier pluton shows more variation in mineralogy than occurs between all the Jurassic plutons.

In a limited area of the Steele Glacier pluton examined by

Table 5.1. Modes of granitoid rocks southwest of Denali-Shakwak Fault.

Sample	Quartz	Orthoclase	Plagioclase	Total Mafics	Rock
Icefield Range Granite					
115	5	18	50	27	GDT
127	17	26	50	7	Q-M
128	4	8	58	30	GDT
132					Q-M
133	-	-	61	39	D
134	25	29	41	5	Q-M
136	6	48	41	5	Q-M
138	-	-	69	31	D
Kluane Range Diorite					
105					D
110	--	-	47	53	D
111	-	-	63	37	D
112	16	-	55	29	Q-D
113					Q-D
114	33	1	59	7	Q-D
119	-	-	61	39	D
120	1	1	59	39	D
121	1	1	64	34	D
122	8	1	54	37	Q-D
123					D
124	-	-	52	48	D
125	-	-	55	45	D
144	2	1	68	29	D
167	21	17	40	22	GDT
168	32	30	31	8	Q-M
169	6	6	61	27	GDT

Symbols: D - diorite; GDT - granodiorite; Q-D - quartz diorite; Q-M - quartz monzonite; FP - feldspar porphyry

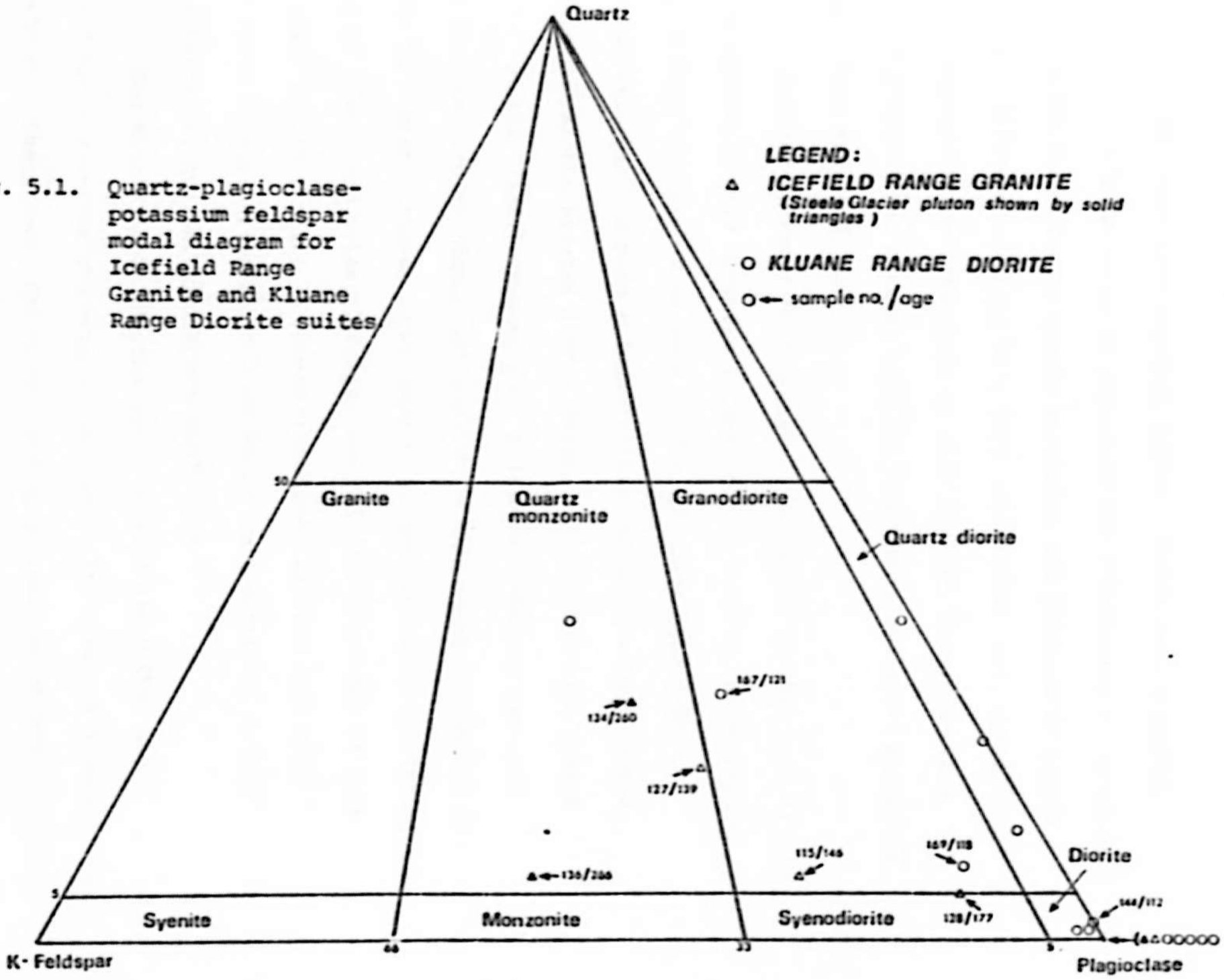


Fig. 5.1. Quartz-plagioclase-potassium feldspar modal diagram for Icefield Range Granite and Kluane Range Diorite suites.

this writer, at least five distinct igneous phases were observed. These range from large veins of pegmatite and aplogranite to hornblende diorite, hornblende-biotite quartz monzonite and porphyritic quartz monzonite. This latter phase is a very distinctive rock, containing abundant megacrysts of orthoclase as much as 2 in. long, set in a matrix of plagioclase, quartz, biotite, hornblende and minor potassium feldspar (see Fig. 5.2, p. 95).

Another interesting feature of this suite is that many of the samples are relatively depleted in quartz. Five of the seven samples shown on Fig. 5.1 have 7% or less quartz yet range from 0-50% in potassium feldspar. A more extensive sampling of this suite would probably reveal the existence of syenodiorite and monzonite phases.

Muller (1967) reports thin section analyses of two rock types from the Donjek Ranges not sampled in this study. Alaskite is a fine- to medium-grained, light grey or salmon pink rock consisting mainly of quartz and potash feldspar and only a few percent of dark minerals. Albite granite is a medium-grained, darkish rock with phenocrysts of microcline up to 5 mm across in a matrix of mainly potash feldspar, quartz, albite and hornblende.

The Kluane Range Diorite suite is more basic than the Icefield Range granites and more restricted in its range of mineralogical composition. These rocks are mainly medium-grained, hornblende diorites and quartz diorites (see Fig. 5.3, p. 96), which exhibit hypidiomorphic-equigranular textures in thin section. Hornblende is the dominant mafic

mineral, with biotite usually subordinate or absent. The occurrence of inclusions of augite in the cores of hornblende crystals was noted in a number of thin sections. Quartz typically occurs in small, fine-grained, anhedral crystals, interstitial between plagioclase and mafic minerals. Plagioclase is the major component of these rocks and, according to Muller (1967), has a composition in the range oligoclase-andesine.

Throughout much of the Kluane Ranges, rocks of this suite contain very little, if any, potassium feldspar. The exception is a series of plutons which lie west of the Donjek River in the north-western part of the field area. These rocks contain considerable potassium feldspar, and approach the Icefield Range granites in modal composition. On Fig. 5.1, samples from these plutons (#167 - 169) account for the three points which fall in the quartz monzonite and granodiorite fields.

In the Kluane Lake map-area, these more acidic plutons constitute almost all of the exposures of the Kluane Range diorites, and probably led Muller (1967) to conclude that granodiorite forms a major component of this suite. However, on the basis of more widespread sampling, this writer believes that diorite and quartz diorite are the major phases, with granodiorite being relatively less important.

The Tertiary Kluane Range Porphyry suite has a distinctive megascopic appearance and is easily distinguished in the field from

rocks belonging to the two older suites. These rocks typically show white, subhedral phenocrysts of sodic plagioclase, up to 5 mm in length, set in a grey- or buff-coloured, aphanitic matrix. Biotite is often the only other recognizable mineral in hand-specimen, and forms small, dark, euhedral crystals which usually comprise less than 1% by volume of the rock. Only rarely do quartz and potassium feldspar form phenocrysts, and when these occur, they are sparse and form small, anhedral crystals (see Fig. 5.4, p. 97).

Muller (1967) has suggested that latite is the most common rock-type of this suite and, farther to the southeast in the Dezadeash map-area, Kindle (1952) has named this suite "soda syenite". Perhaps the lack of quartz phenocrysts in these rocks led these writers to believe that this suite displays only intermediate values of SiO_2 (say 55-60 wt.%). However, the chemical analyses presented in Chapter 6 show that these rocks typically contain SiO_2 in excess of 70 wt.%, and therefore are rhyodacites, quartz latites or rhyolites in chemical composition. To avoid using rock names which imply a certain chemical composition, this writer prefers to use the term "feldspar porphyry" to describe this suite. Not only is this term more descriptive of the texture of the rock, but it embraces a wider range of chemical composition.

Fig. 5.2. Photographs of Icefield Range Granite specimen showing texture and mineralogy with, and without, staining for potassium feldspar.

Rock is a porphyritic, hornblende-biotite quartz monzonite with xenomorphic-granular texture. Subhedral, orthoclase megacrysts (stained yellow in lower photograph) are set in a medium- to coarse-grained matrix of plagioclase, quartz, potassium feldspar, biotite and hornblende, in approximate order of abundance. Scale is in millimetres.

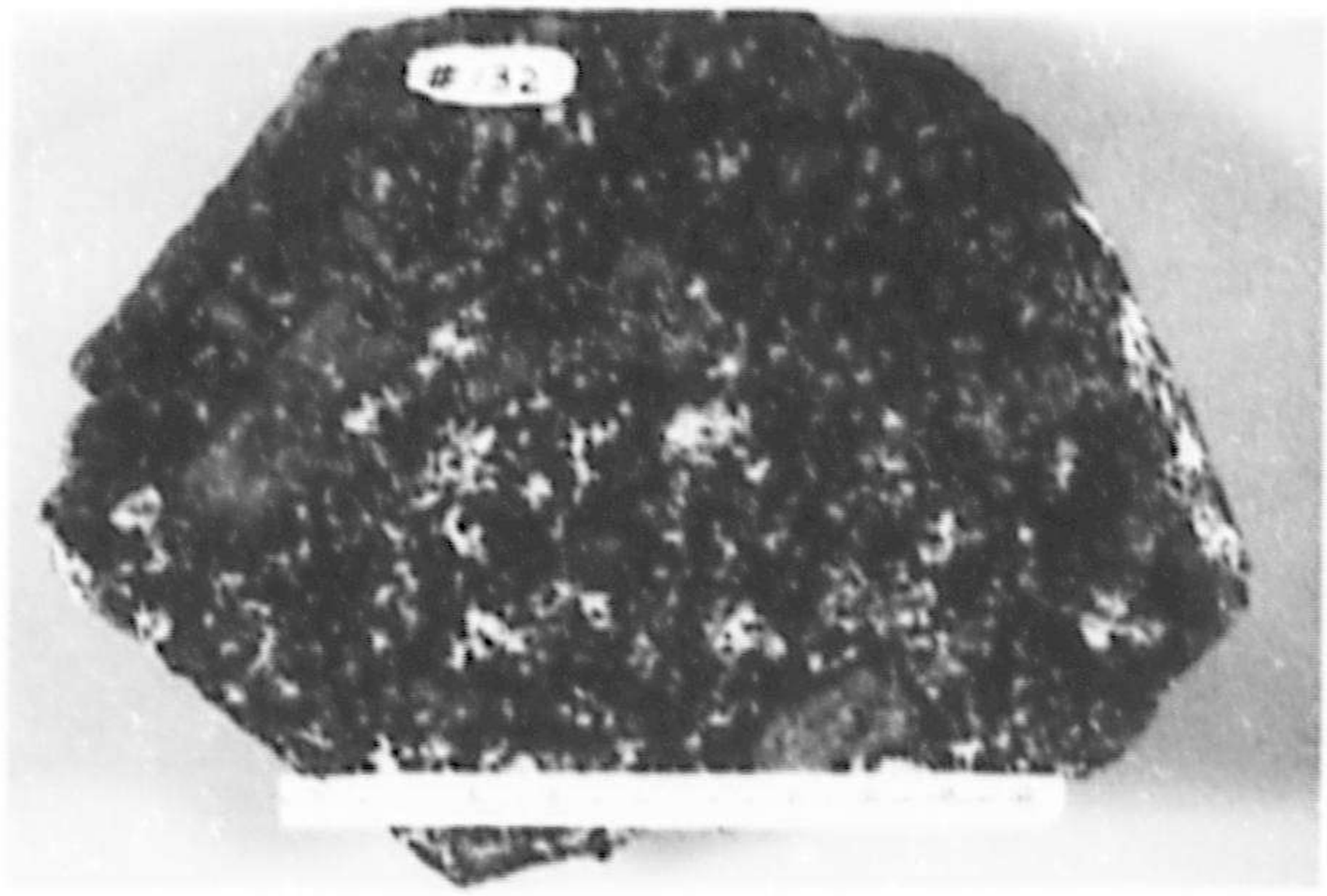
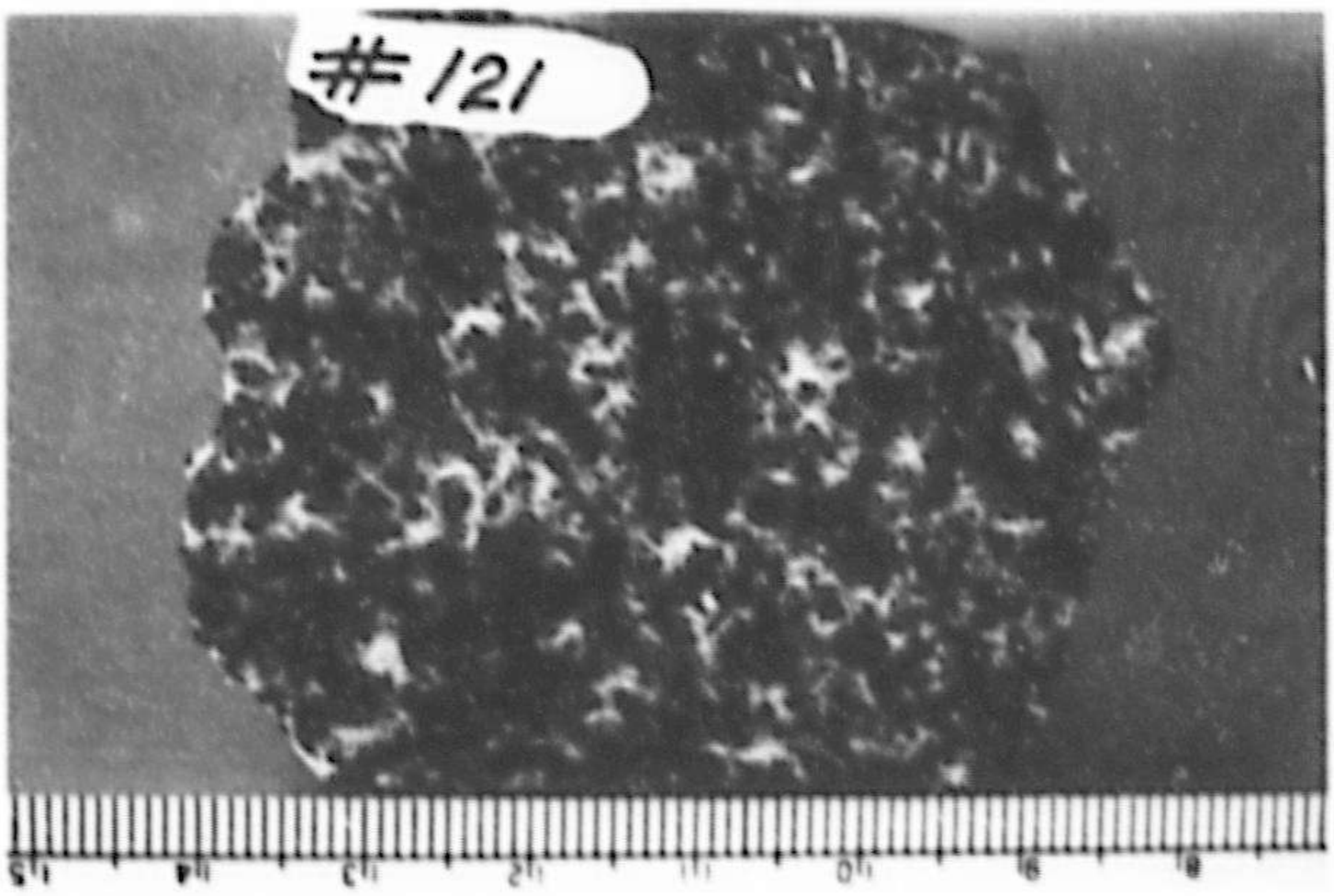


Fig. 5.3. Photographs of Kluane Range Diorite specimen showing texture and mineralogy with, and without, staining for potassium feldspar.

Rock is a medium-grained, hornblende diorite with hypidiomorphic-granular texture. The modal composition is about 65% plagioclase and 34% hornblende. Potassium feldspar comprises 1% or less of the rock (by volume) as is evident in the lower photograph. Scale is in millimetres.




#121

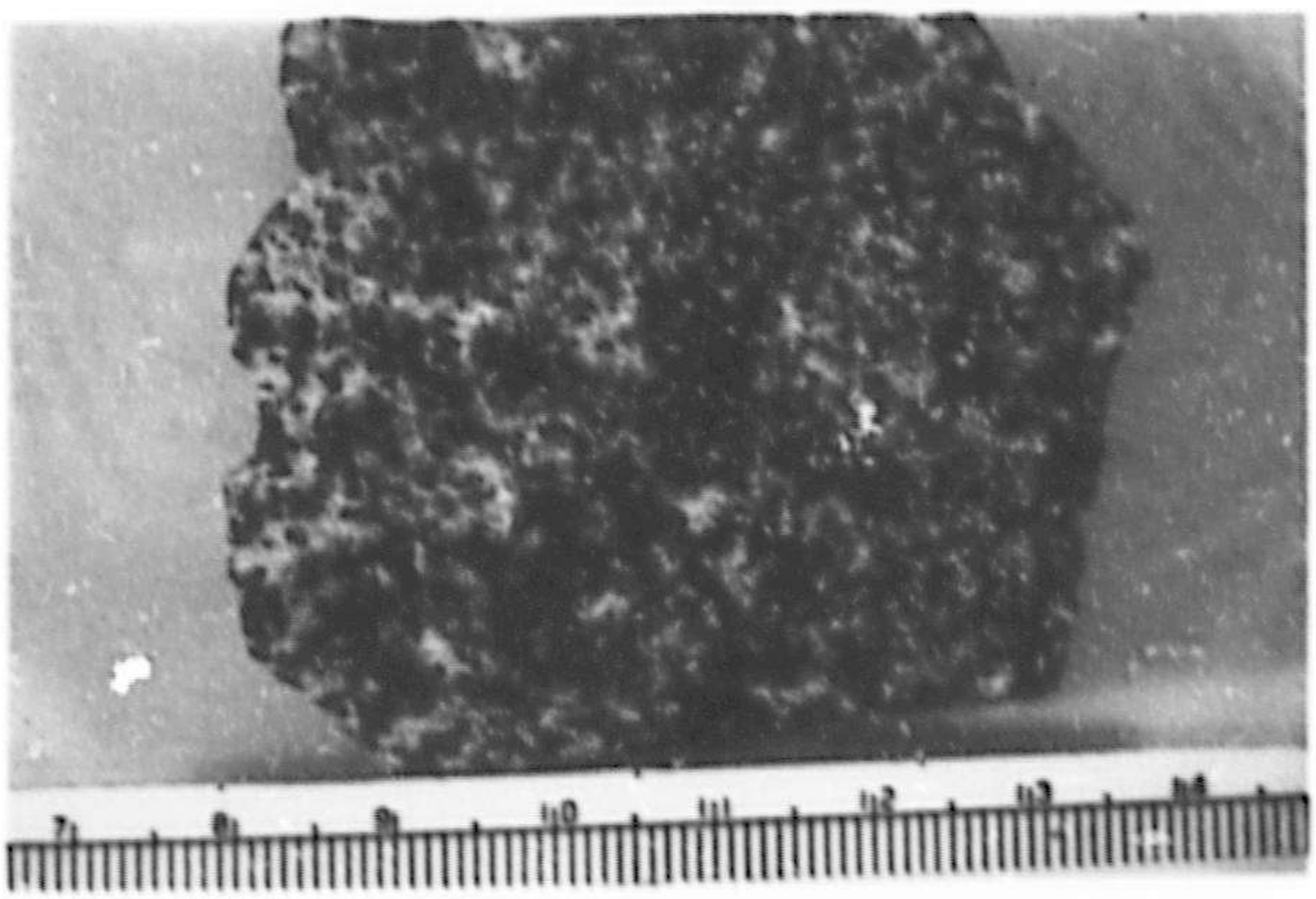
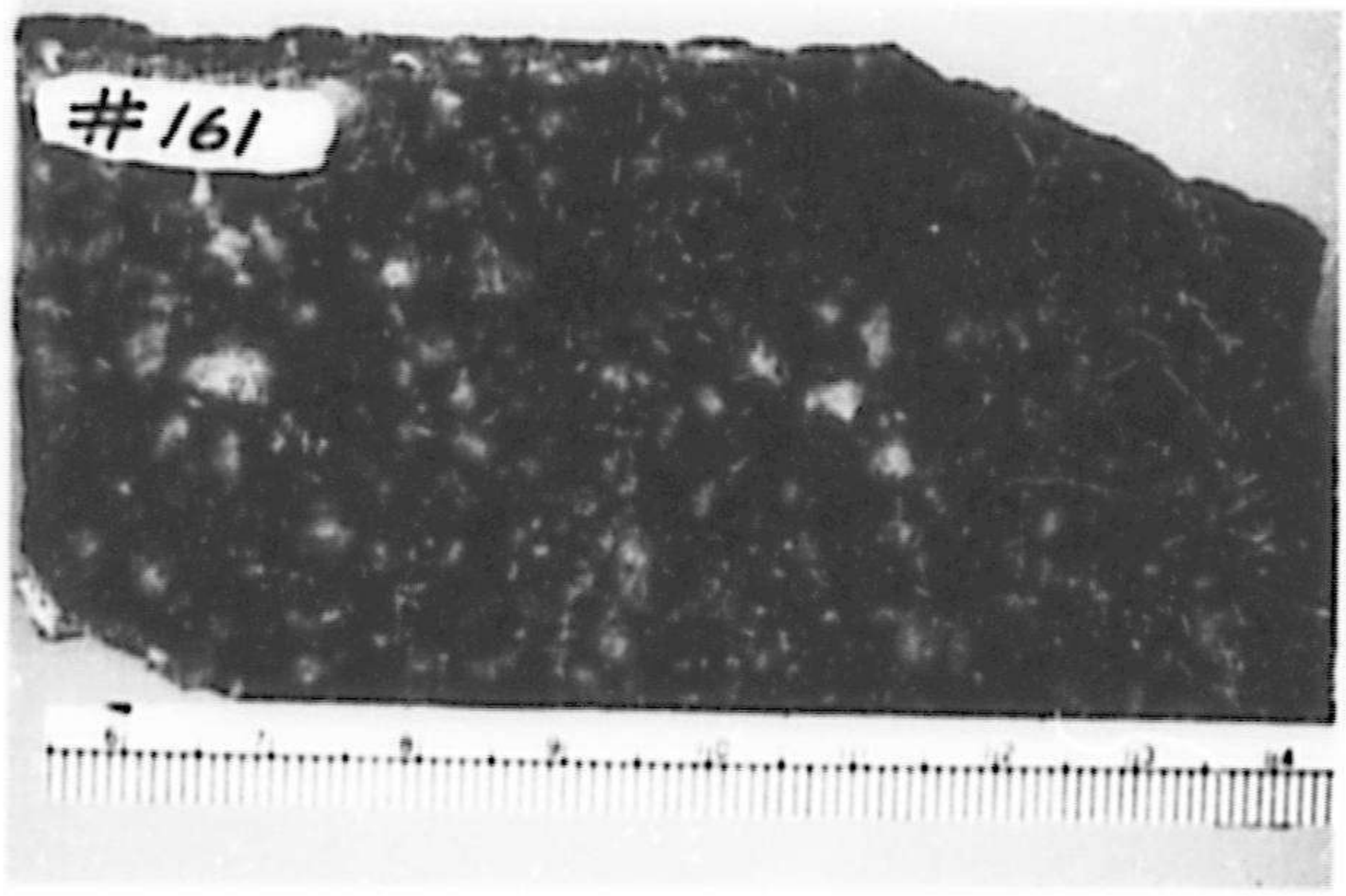
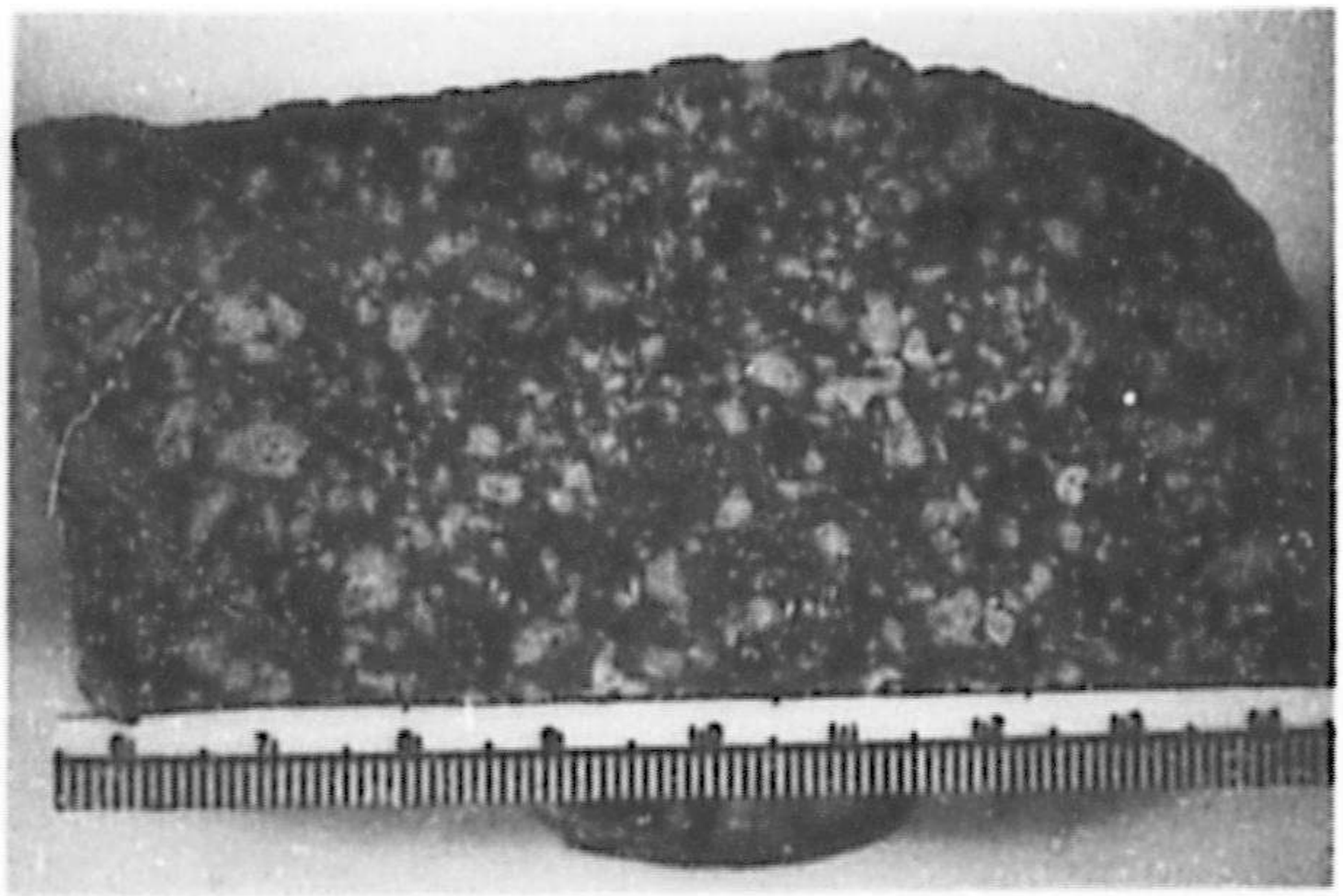


Fig. 5.4. Photographs of Kluane Range Porphyry specimen showing texture and mineralogy with, and without, staining for potassium feldspar.

Rock is a feldspar porphyry of rhyodacitic to rhyolytic composition. Subhedral phenocrysts of sodic plagioclase, up to 5 mm., and small, euhedral biotite and subordinate subhedral hornblende phenocrysts are set in an aphanitic matrix. Not evident in the photograph is finely-disseminated pyrite. Yellow staining of the matrix in the lower photograph is produced by reaction of the staining chemical (sodium cobaltinitrate) with very fine-grained potassium-bearing minerals. Scale is in millimetres.


#161



5.3 Petrography of Granitoid Rocks Northeast of the Denali-Shakwak Fault

The modal compositions of the Nisling Range Granodiorite, Ruby Range Granodiorite, and Nisling Range Alaskite suites are shown in Table 5.2, and are plotted on the quartz-plagioclase-potassium feldspar diagram in Fig. 5.5. Compared to the plutonic rocks on the southwest side of the Denali-Shakwak Fault, these suites constitute a more homogeneous group in terms of modal composition, with fewer diagnostic characteristics to distinguish one from another.

The Nisling Range Granodiorite suite is not extensively exposed in southwestern Yukon, being limited to two small batholiths which only slightly overlap the northwestern boundary of the study area. From Fig. 5.5, it is seen that these rocks are mainly granodiorites. However, quartz monzonites are also prominent in this suite, and Tempelman-Kluit (1974) reports rocks of quartz diorite composition. It is apparent however, from the modal diagram, that the field defined by this suite is a restricted subset of that of the Ruby Range Granodiorite suite. Thus, modal composition alone is not a useful diagnostic feature in distinguishing these two suites.

Nisling Range granodiorites are generally medium- to coarse-grained, and equigranular, with a diagnostic mottled green and purplish appearance. The mottled green appearance is due in part to patches of mafic minerals set against a pinkish or purplish background of plagioclase, orthoclase and quartz (see Fig. 5.6, p. 107). Mafic

Table 5.2. Modes of granitoid rocks northeast of Denali-Shakwak Fault.

Sample	Quartz	Orthoclase	Plagioclase	Total Mafics	Rock
Nisling Range Granodiorite					
1	15	4	47	34	GDT
2	31	34	26	9	Q-M
3	20	20	44	16	GDT
4					GDT
23	22	20	49	9	GDT
24	26	22	43	9	Q-M
25					GDT
26					GDT
27					GDT
31	26	20	48	6	GDT
Ruby Range Granodiorite					
5	6	-	61	33	Q-D
6	13	28	38	20	Q-M
7	12	9	53	26	GDT
8					GDT
9	25	33	37	5	Q-M
11	26	20	41	13	GDT
12	22	25	36	17	Q-M
13	23	24	43	10	Q-M
14	26	19	46	8	GDT
18	29	26	37	8	Q-M
32	31	21	43	5	GDT
41	24	15	53	8	GDT
42	22	21	45	12	GDT
46	8	7	53	32	GDT
48	11	2	55	32	Q-D

Table 5.2 (cont'd.)

Sample	Quartz	Orthoclase	Plagioclase	Total Mafics	Rock
50	26	3	58	13	GDT
52	22	2	51	25	Q-D
53	10	-	55	34	Q-D
54	13	-	69	18	Q-D
56	21	-	62	17	Q-D
57	29	8	49	13	GDT
58	33	23	37	7	Q-M
59	24	27	41	8	Q-M
60	33	12	46	9	GDT
61	24	14	51	10	GDT
62	29	10	51	9	GDT
64	11	32	45	12	Q-M
67	22	18	48	12	GDT
68	8	-	55	36	Q-D
69	15	21	52	12	GDT
70	33	28	35	4	Q-M
72					Q-M
73	23	9	57	11	GDT
74	31	34	28	6	Q-M
75	15	10	58	17	GDT
76	22	20	48	9	GDT
77	33	30	32	6	Q-M
79					Q-M
81	35	6	45	14	GDT
82	32	28	36	4	Q-M
83	31	32	30	7	Q-M
84	43	25	27	5	Q-M
85					GDT
86	26	33	34	6	Q-M

Table 5.2 (cont'd.)

Sample	Quartz	Orthoclase	Plagioclase	Total Mafics	Rock
87	29	31	33	7	Q-M
88	24	25	43	8	Q-M
90	19	-	61	21	Q-D
91	34	27	32	6	Q-M
92	31	35	30	5	Q-M
93	32	26	37	6	Q-M
94	30	29	33	7	Q-M
95	31	29	35	5	Q-M
96	29	30	36	5	Q-M
97	30	20	41	8	GDT
98	36	21	35	7	Q-M
99	25	4	51	20	GDT
100	26	15	51	8	GDT
101	27	2	53	17	Q-D
102	28	18	44	10	GDT
103	8	4	52	36	GDT
104	18	3	55	24	GDT
<u>Nisling Range Alaskite</u>					
28	33	32	33	2	Q-M
29					A
30	34	58	9	-	A
36	32	37	28	3	Q-M
37	30	36	29	5	Q-M
38	32	36	29	3	Q-M
39	25	37	30	8	Q-M
40					Q-M

<u>Symbols</u>: A - alaskite
GDT - granodiorite
Q-D - quartz diorite
Q-M - quartz monzonite

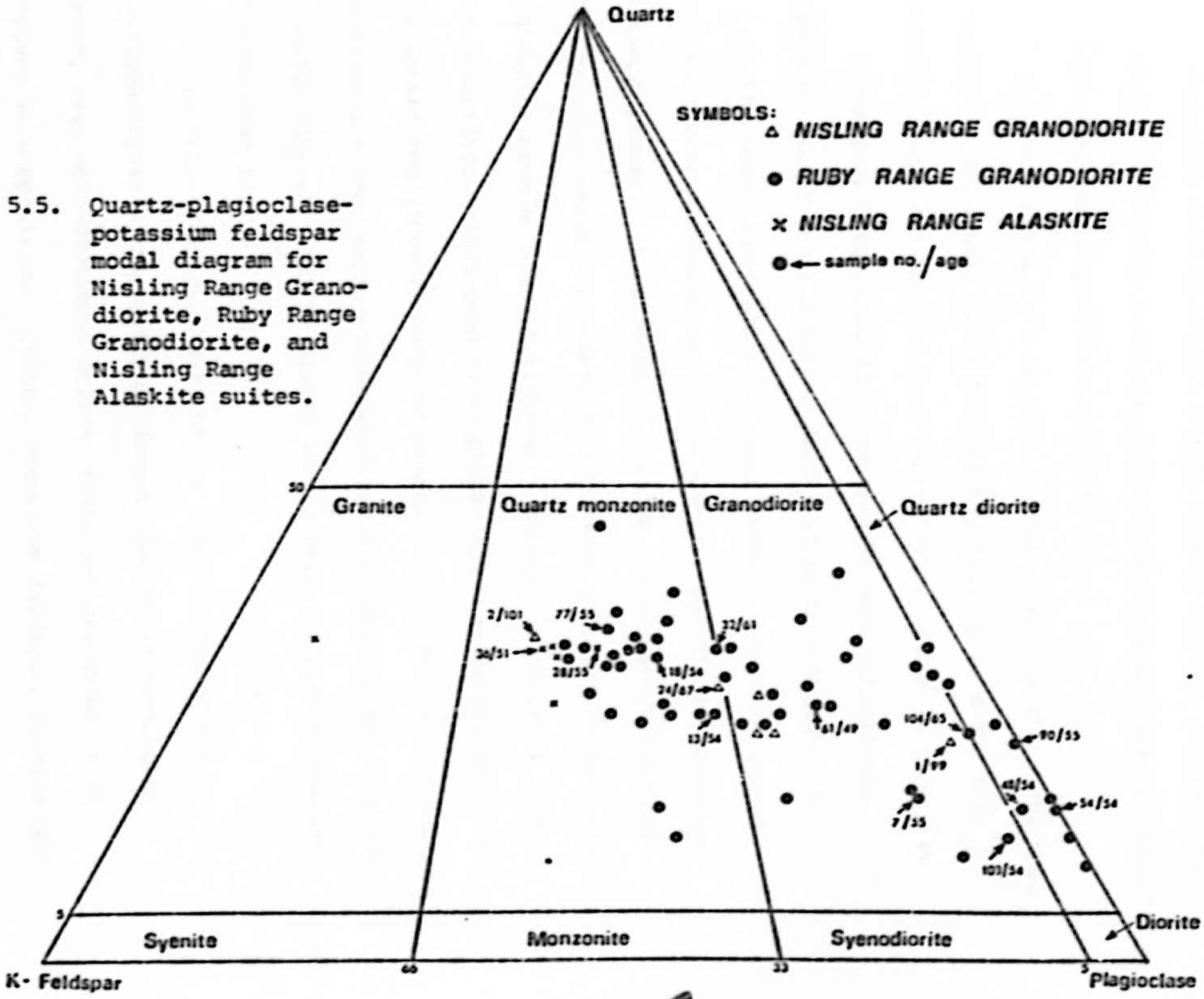


Fig. 5.5. Quartz-plagioclase-potassium feldspar modal diagram for Nisling Range Granodiorite, Ruby Range Granodiorite, and Nisling Range Alaskite suites.

minerals generally make up 15-20% of the rock by volume. Muller (1967) reports that thin-section analyses show that the plagioclase is commonly sericitized, and has compositions close to An_{50}.

A second diagnostic feature of these rocks is the occurrence of conspicuous hexagonal, fresh biotite crystals up to about 5 mm in diameter; these are not observed in the other suites in this area.

The Ruby Range granodiorites are the most extensively sampled rocks among the six suites described in this thesis. On Fig. 5.5, the modal composition of these rocks ranges from quartz diorite to quartz monzonite, with granodiorite and quartz monzonite as dominant phases. These rocks are medium- to coarse-grained and exhibit textures which are generally hypidiomorphic and equigranular. Granodiorites have an overall light-grey colour, in contrast to the quartz monzonites, which tend to be pinker and coarser-grained, and with a lesser abundance of mafic minerals. In contrast to the Nisling Range granodiorites, where either biotite or hornblende may form the major mafic mineral, biotite almost always tends to predominate over hornblende (see Fig. 5.7, p. 108).

In thin-section, the rocks are fresh in appearance. Plagioclase crystals are typically larger than other components of the rock, have well-developed crystal form, and are andesine or oligoclase in composition. Quartz, potassium feldspar, biotite and hornblende form anhedral grains in the interstices between plagioclase crystals.

Samples taken from the transition zone between the batholith and the metamorphic country rocks exhibit gneissic foliation in hand-specimen, defined by a preferred orientation of the mafic minerals. In thin-sections of such foliated rocks, Muller (1967) notes mortared or sutured grain boundaries, which he suggests are indicative of recrystallization or movement within crystalline rock.

Among the samples collected for this study, there is a geographical bias among the quartz diorite, granodiorite and quartz monzonite phases; the latter are more abundant in the Kusawa Lake area, but quartz diorite and granodiorite are predominant in the more northerly Kluane Lake area.

The Nisling Range Alaskite suite forms, on Fig. 5.5, a fairly tight cluster in the quartz monzonite field. However, it should be cautioned that this is probably a result of sample bias and that more extensive sampling of this suite would define an area on the diagram that would cover much of the upper half of the granite field. Thus, Muller (1967) reports a number of modal analyses for this suite which are considerably more depleted in plagioclase than most of the samples reported here. This suite is significantly more felsic than the Nisling Range and Ruby Range granodiorites, and shows little overlap with these rocks on a modal diagram.

In the field, rocks of this suite weather to a diagnostic yellow-to-buff colour and often decompose to a crumbly, weathered surface. The accelerated weathering seems to be primarily a function

of high porosity and loose bonding of the mineral constituents in these rocks.

Textures are equigranular and fine- to coarse-grained. Most specimens contain dark, smoky, quartz crystals and brown or pink potassium feldspar. Plagioclase, mainly albite, forms smaller subhedral to euhedral crystals. The low percentage of biotite (usually less than 5%) and the absence of hornblende are diagnostic features (see Fig. 5.8, p. 109).

Muller (1967) describes a microscopic xenomorphic-granular assemblage of clear quartz and perthitic potash feldspar (with microcline twinning) with lesser plagioclase occurring as small, subhedral crystals. Micrographic intergrowths of quartz and potassium feldspar are common. Fluorite is a common and diagnostic accessory mineral.

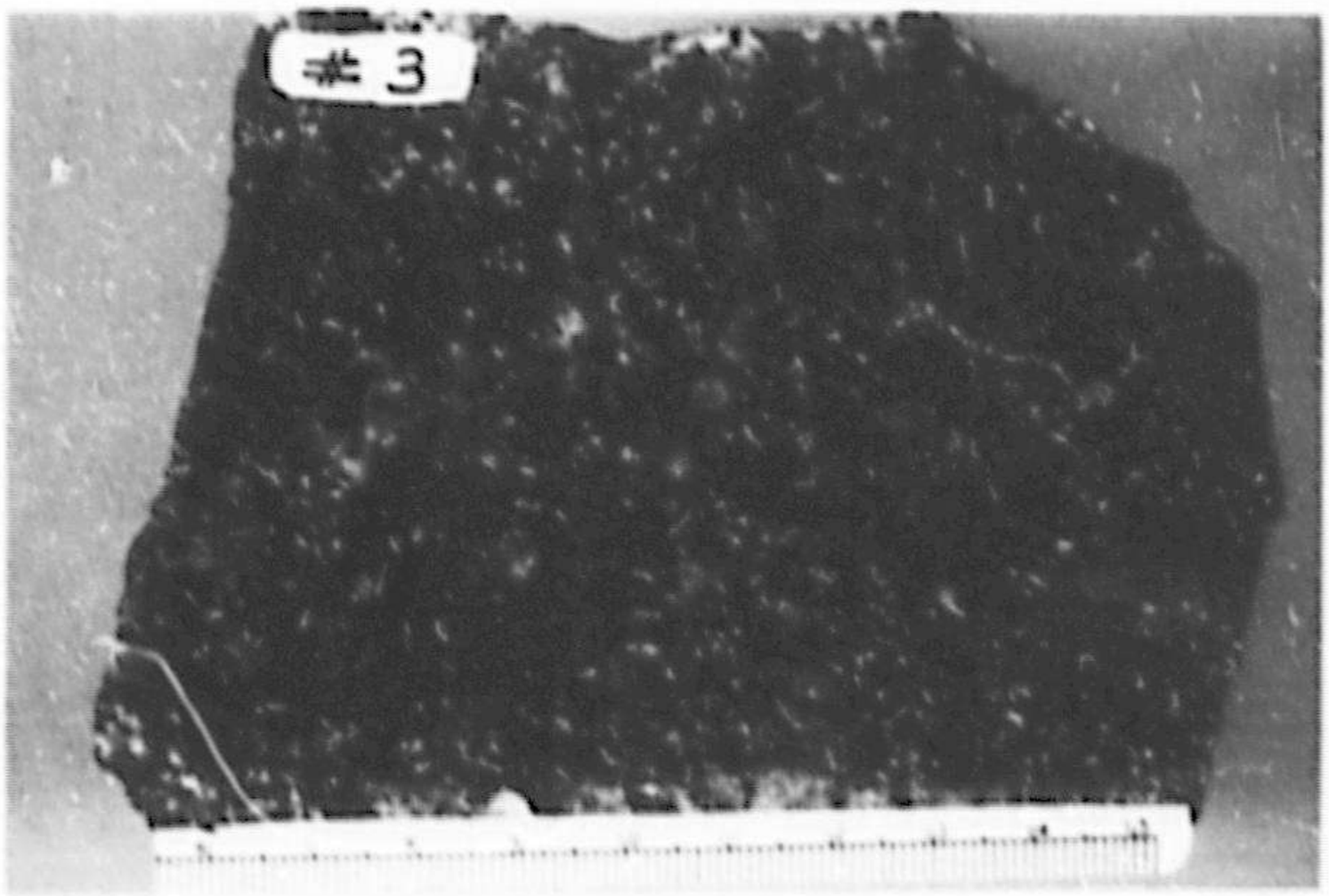
The plutonic rocks on the northeast side of the Denali-Shakwak Fault, in particular the Ruby Range granodiorites, outline virtually the same area on the quartz-plagioclase-potassium feldspar diagram as do rocks throughout the Coast Mountains in British Columbia reported by Hutchison (1970) and Roddick and Hutchison (1974). Whereas these workers regard quartz diorite and granodiorite as the most common rock-type, the specimens plotted on Fig. 5.2 show that, in the thesis area, quartz monzonite is as abundant as granodiorite. However, the writer believes that the relative abundance of quartz monzonites in the Ruby Range Batholith is partly a function

of sample bias (i.e., the easily accessible outcrops on the shore of Kusawa Lake are largely of quartz monzonite), and that the relative lack of quartz diorites may be due in part to truncation, by the Denali-Shakwak Fault, of mainly quartz dioritic rocks lying west of Moore et al.'s (1962) quartz diorite line (this possibility is discussed more fully in the following chapter).

However, in spite of possible differences in relative abundances of modal rock-types, the essential point remains that the total area defined by the Ruby Range granodiorite on the modal diagram indicates a petrographical affinity with plutonic rocks in the southern part of the Coast Plutonic Complex.

Fig. 5.6. Photographs of Nisling Range Granodiorite specimen showing texture and mineralogy with, and without, staining for potassium feldspar.

Rock is a medium- to coarse-grained, biotite-hornblende granodiorite showing hypidiomorphic-granular texture. The diagnostic mottled green appearance of these rocks is evident in the upper photograph. The large biotite flakes, also characteristic of these rocks, are best observed on fractured surfaces. The lower photograph shows that potassium feldspar tends to occur as anhedral crystals, along with quartz, in the interstices between euhedral plagioclase and mafic minerals. Scale is in millimetres.


#3

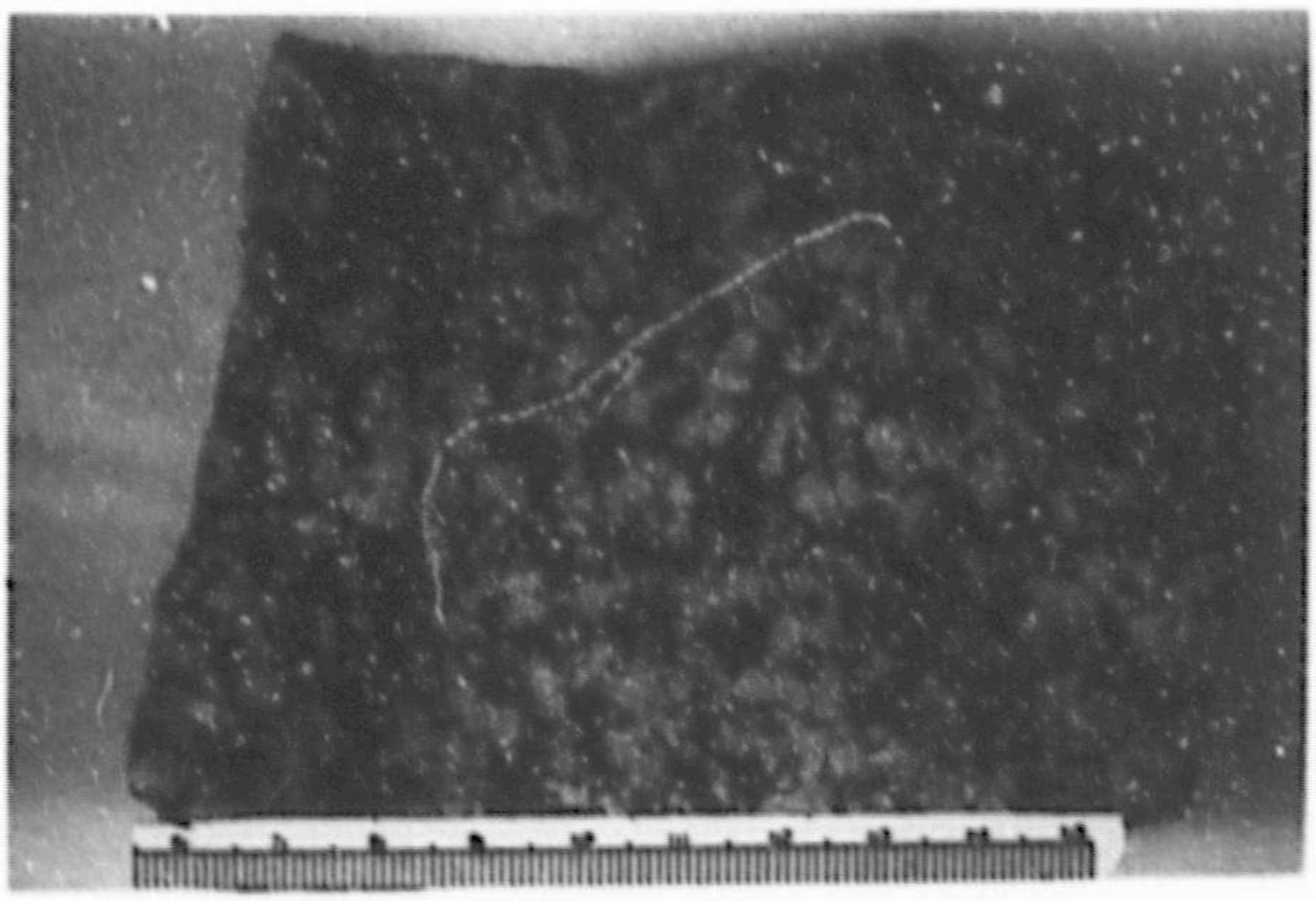
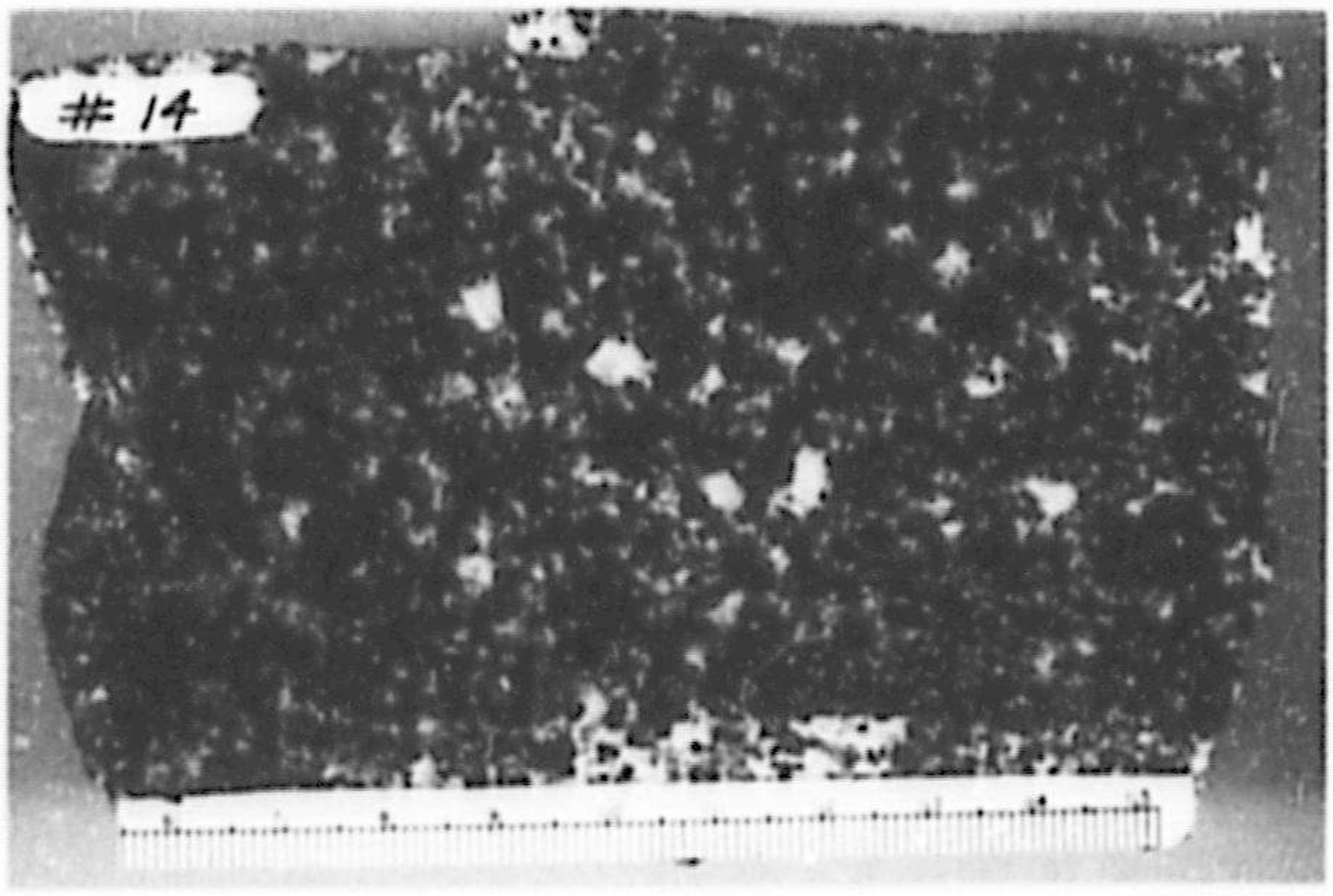


Fig. 5.7 Photographs of Ruby Range Granodiorite specimen showing texture and mineralogy with, and without, staining for potassium feldspar.

Rock is a medium-grained, equigranular, hornblende-biotite granodiorite showing hypidiomorphic-granular texture. Glassy quartz crystals form much of the dark grey areas in the upper photograph. In the lower photograph, potassium feldspar can be seen to form small, anhedral, interstitial crystals between quartz and plagioclase. Scale is in millimetres.


#14

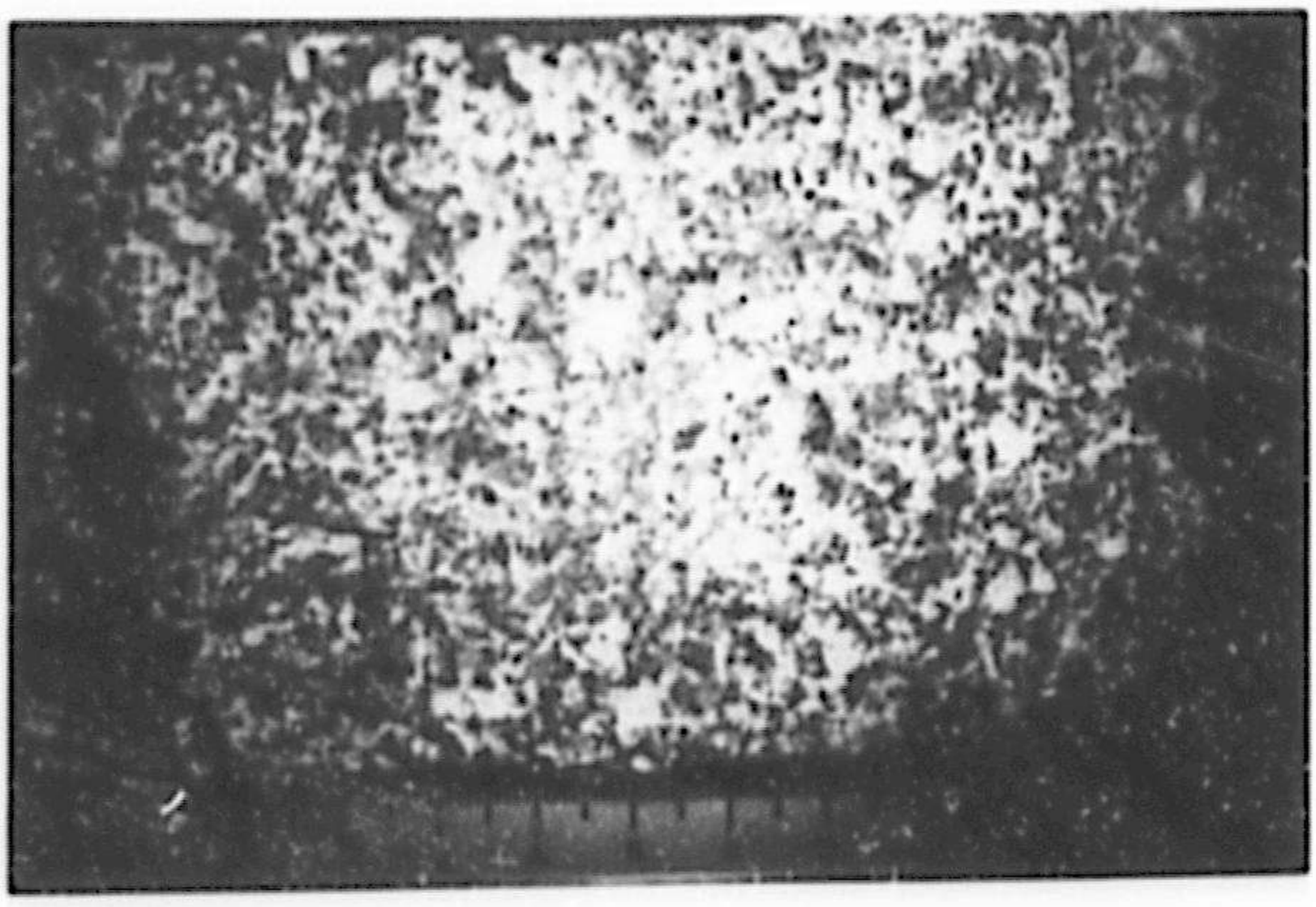
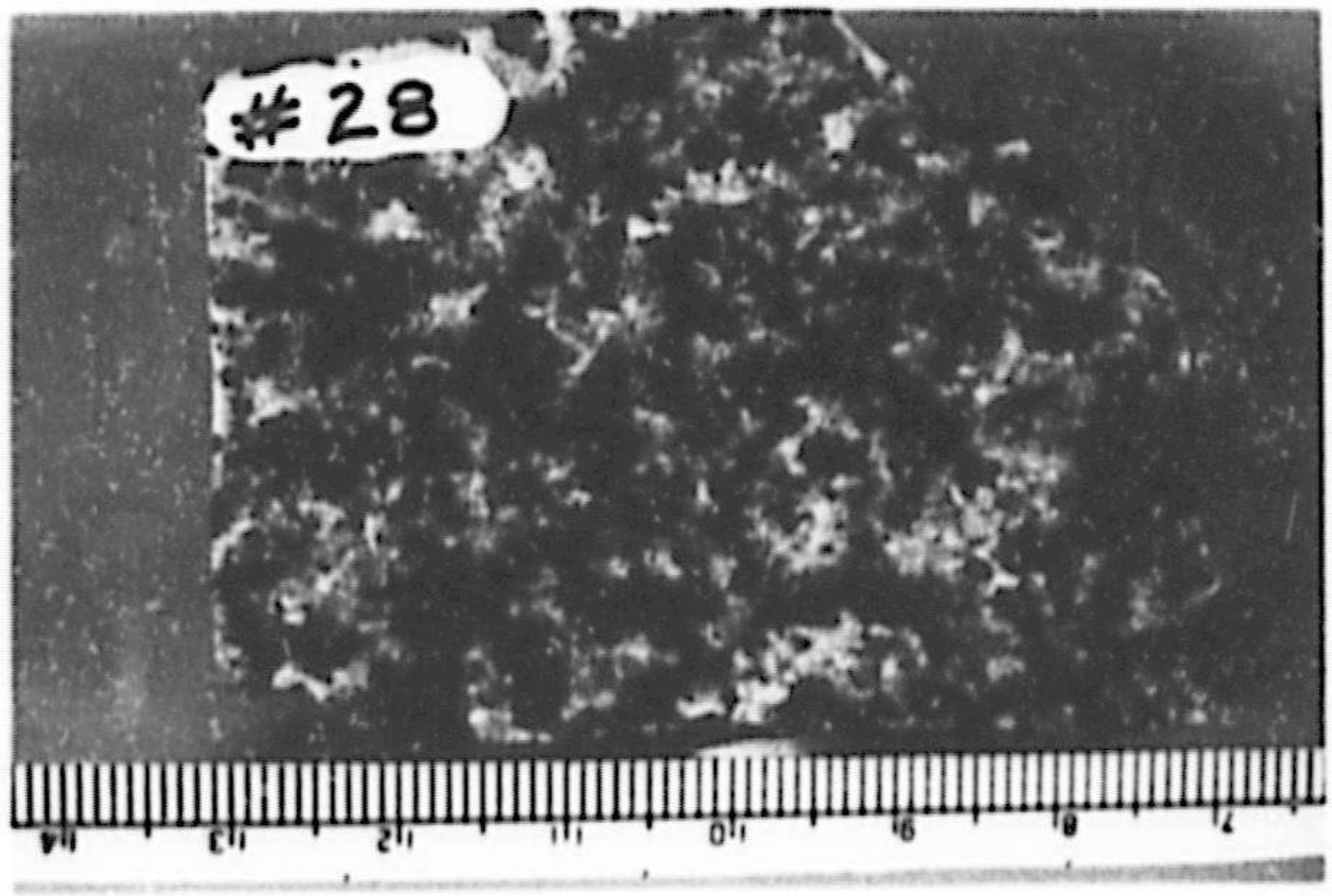


Fig. 5.8. Photographs of Nisling Range Alaskite specimen showing texture and mineralogy with, and without, staining for potassium feldspar.

Rock is a medium-grained, equigranular biotite quartz-monzonite showing hypidiomorphic granular texture. The pink potassium feldspar crystals are characteristic. The diagnostic dark, smoky, quartz crystals almost give the appearance of mafic minerals in the upper photograph but the modal analysis of this rock shows only 2% mafic minerals (all biotite) by volume. Lower photograph shows that potassium feldspar, plagioclase and quartz occur in approximately equal portions, but most specimens from this suite would show a greater relative abundance of potassium feldspar. Scale is in millimetres.


#28



CHAPTER 6

GEOCHEMISTRY OF GRANITOID PLUTONISM

6.1 Introduction

Major and minor element chemical analyses are presented in this chapter, in order to characterize further the suites of granitic rocks in southwestern Yukon. The six igneous suites described in the previous two chapters can be shown to have reasonably distinct geochemical characteristics. Numerous studies have demonstrated that suites of igneous rocks can be distinguished on conventional diagrams such as AFM and K_2O *vs* SiO_2 plots, and also through the abundances of such minor or trace elements as Rb, Sr and Ba.

Analyses were carried out in the geochemical laboratories of the Department of Geological Sciences, Queen's University. Equipment and analytical techniques used are described in Appendix A. Major oxides were determined by X-ray fluorescence, and minor elements by emission spectroscopy.

6.2 Geochemistry of Granitoid Rocks Southwest of the Denali-Shakwak Fault

Partial chemical analyses for each of the three igneous suites southwest of the Denali-Shakwak Fault are presented in Table 6.1. Oxides of major elements are shown in weight percent as determined, but were normalized to 100 percent volatile-free for

Table 6.1. Major and minor element analyses for granitic rocks southwest of Denali-Shakwak Fault.

(major elements in weight percent; minor elements in ppm)

Icefield Range Granite

Sample No.	115	127	128	132	133	134	136	138
SiO_2	54.19	68.46	55.83	6.281	48.91	72.12	63.07	47.65
Al_2O_3	17.12	15.61	17.57	14.96	14.77	14.86	16.03	16.63
CaO	7.32	2.34	5.30	2.53	12.45	1.66	1.04	11.59
K_2O	2.69	2.55	3.06	3.40	0.22	4.55	5.59	0.51
Na_2O	3.29	4.79	5.00	4.82	2.92	4.04	5.55	3.07
FeO	4.35	1.35	5.42	2.15	7.19	1.19	1.70	5.01
Fe_2O_3	2.28	0.71	2.85	1.13	3.78	0.63	0.89	2.63
MgO	2.46	0.83	2.14	0.92	6.19	0.88	0.27	5.07
TiO_2	0.96	0.31	1.61	0.52	1.56	0.27	0.35	1.41
MnO	0.14	0.04	0.13	0.05	0.14	0.17	0.08	0.12
P_2O_5	0.39	0.15	0.47	0.20	0.14	0.09	0.10	0.22
Total	95.19	97.15	99.37	93.49	98.27	100.47	94.66	93.92
Rb	105	152	121	120	N.A.	192	N.A.	20
Sr	1200	2100	440	660	N.A.	357	250	533
Ba	2500	5100	1800	2400	N.A.	1300	1200	430

Table 6.1 (cont'd.)

Kluane Range Diorite

Sample No.	105	110	111	112	113	114	119	120
SiO_2	52.11	51.06	48.41	60.11	49.26	65.16	47.55	50.61
Al_2O_3	13.22	13.24	14.69	15.17	12.11	14.01	15.99	16.99
CaO	5.95	11.66	12.73	4.65	7.99	2.69	10.62	9.53
K_2O	0.38	0.19	0.18	0.88	0.73	0.64	0.17	0.35
Na_2O	4.82	2.30	1.76	4.56	2.88	5.11	3.63	3.28
FeO	7.15	6.17	5.94	4.75	9.87	3.86	6.49	5.38
Fe_2O_3	3.76	3.24	3.12	2.49	5.19	2.03	3.41	2.82
MgO	3.52	7.57	6.58	1.40	3.49	0.51	7.38	5.86
TiO_2	1.90	0.86	1.01	0.83	2.27	0.46	0.65	0.61
MnO	0.08	0.15	0.13	0.12	0.22	0.10	0.17	0.17
P_2O_5	0.21	0.14	0.13	0.27	0.53	0.10	0.19	0.22
Total	93.09	96.59	94.68	95.24	94.54	94.67	96.25	95.82
Rb	N.A.	N.A.	N.A.	32	N.A.	N.A.	N.A.	N.A.
Sr	350	140	240	220	N.A.	340	N.A.	N.A.
Ba	760	150	200	540	N.A.	740	N.A.	N.A.

Table 6.1 (cont'd.)

Kluane Range Diorite (cont'd.)

Sample No.	121	122	123	124	125	144	167	168	125
SiO_2	48.87	54.75	43.84	41.98	47.45	41.63	56.24	69.89	54.82
Al_2O_3	17.71	16.05	17.27	17.28	16.46	15.29	16.90	14.43	18.95
CaO	10.71	7.91	13.91	13.38	11.57	12.00	6.59	1.49	8.17
K_2O	0.77	1.47	0.52	0.51	0.84	0.29	2.28	4.12	1.07
Na_2O	2.97	3.40	1.80	2.13	2.80	2.65	3.05	2.40	3.73
FeO	6.00	5.34	8.10	8.21	6.09	8.63	4.54	2.23	4.32
Fe_2O_3	3.15	2.81	4.25	4.31	3.20	4.53	2.39	1.17	2.27
MgO	4.56	4.80	6.17	7.11	6.54	7.60	3.69	0.61	2.90
TiO_2	0.78	0.83	1.21	1.32	0.90	1.70	0.75	0.38	0.71
MnO	0.17	0.16	0.15	0.12	0.12	0.21	0.14	0.08	0.11
P_2O_5	0.22	0.27	0.12	0.08	0.09	0.07	0.19	0.08	0.24
Total	95.91	97.78	97.33	96.43	96.08	94.59	96.76	96.88	97.30
Rb	N.A.	61	13	N.A.	N.A.	N.A.	80	78	49
Sr	N.A.	430	500	N.A.	N.A.	400	290	185	520
Ba	N.A.	390	600	N.A.	N.A.	200	570	2500	270

Table 6.1 (cont'd.)

Kluane Range Porphyry

Sample No.	116	117	118	140	141	143	145	146
SiO_2	71.17	69.88	73.47	69.42	68.44	68.84	61.79	64.17
Al_2O_3	13.70	13.88	15.65	15.13	14.96	15.58	15.56	12.19
CaO	2.17	2.70	3.10	2.46	2.64	2.37	4.36	3.98
K_2O	2.54	2.13	2.05	2.59	2.55	2.57	1.65	2.87
Na_2O	2.98	3.47	4.03	4.45	4.50	4.65	4.32	1.54
FeO	1.27	1.63	1.54	1.30	1.47	1.64	2.76	2.07
Fe_2O_3	0.67	0.86	0.81	0.68	0.77	0.86	1.45	1.06
MgO	0.44	0.85	0.91	0.77	0.93	0.79	2.72	1.70
TiO_2	0.27	0.27	0.33	0.33	0.37	0.33	0.76	0.37
MnO	0.03	0.01	0.03	0.06	0.05	0.05	0.00	0.16
P_2O_5	0.09	0.10	0.10	0.14	0.14	0.14	0.21	0.12
Total	95.38	95.79	102.01	97.33	96.84	97.83	95.57	90.25
Rb	60	N.A.	N.A.	77	80	69	35	91
Sr	410	N.A.	N.A.	500	521	512	760	290
Ba	1500	N.A.	N.A.	1400	1300	1400	1100	4100

Table 6.1 (cont'd.)

Kluane Range Porphyry (cont'd.)

Sample No.	147	148	149	150	153	156	161	163
SiO_2	63.66	66.41	67.50	66.80	62.96	67.14	62.88	67.68
Al_2O_3	14.38	14.47	13.94	14.58	14.31	14.99	14.47	14.21
CaO	2.40	1.59	1.44	1.99	2.61	1.55	2.02	1.96
K_2O	2.46	2.22	2.96	2.14	2.51	1.93	2.06	2.61
Na_2O	4.20	3.94	4.67	5.21	4.02	4.13	4.05	4.44
FeO	1.66	1.61	1.24	1.71	1.48	1.12	1.96	0.84
Fe_2O_3	0.87	0.85	0.65	0.90	0.78	0.59	1.03	0.44
MgO	0.94	0.62	0.40	1.01	0.81	0.55	1.41	0.63
TiO_2	0.29	0.25	0.24	0.27	0.33	0.30	0.43	0.28
MnO	0.01	0.02	0.01	0.01	0.03	0.02	0.02	0.01
P_2O_5	0.11	0.12	0.11	0.17	0.15	0.17	0.14	0.17
Total	90.99	92.10	93.15	94.80	90.00	92.48	90.47	93.29
Pb	N.A.	N.A.	N.A.	N.A.	N.A.	N.A.	N.A.	N.A.
Sr	450	440	360	560	380	620	480	400
Ba	1700	2300	2200	3100	3900	2700	1900	2900

Table 6.1 (cont'd.)

Kluane Range Porphyry (cont'd.)

Sample No.	165	166
SiO_2	64.09	64.69
Al_2O_3	14.35	13.69
CaO	3.12	2.27
K_2O	2.31	3.17
Na_2O	3.83	3.13
FeO	0.84	1.76
Fe_2O_3	0.44	0.92
MgO	0.96	0.97
TiO_2	0.35	0.28
MnO	0.02	0.01
P_2O_5	0.13	0.13
Total	90.46	91.03
Rb	N.A.	N.A.
Sr	500	370
Ba	2000	4500

use in variation diagrams. Iron was conventionally determined as ferric iron (Fe_2O_3) and converted to ferrous iron (FeO), assuming a ferric:ferrous ratio of 0.525, a value typical of quartz monzonitic and granodioritic rocks according to Nockolds (1954). Values for Rb, Sr, and Ba are reported in ppm.[1] Where a sample was not analyzed for these elements, "N.A." has been entered in the tables. Fourteen specimens were analyzed for H_2O and CO_2 and these results are reported in Appendix A.

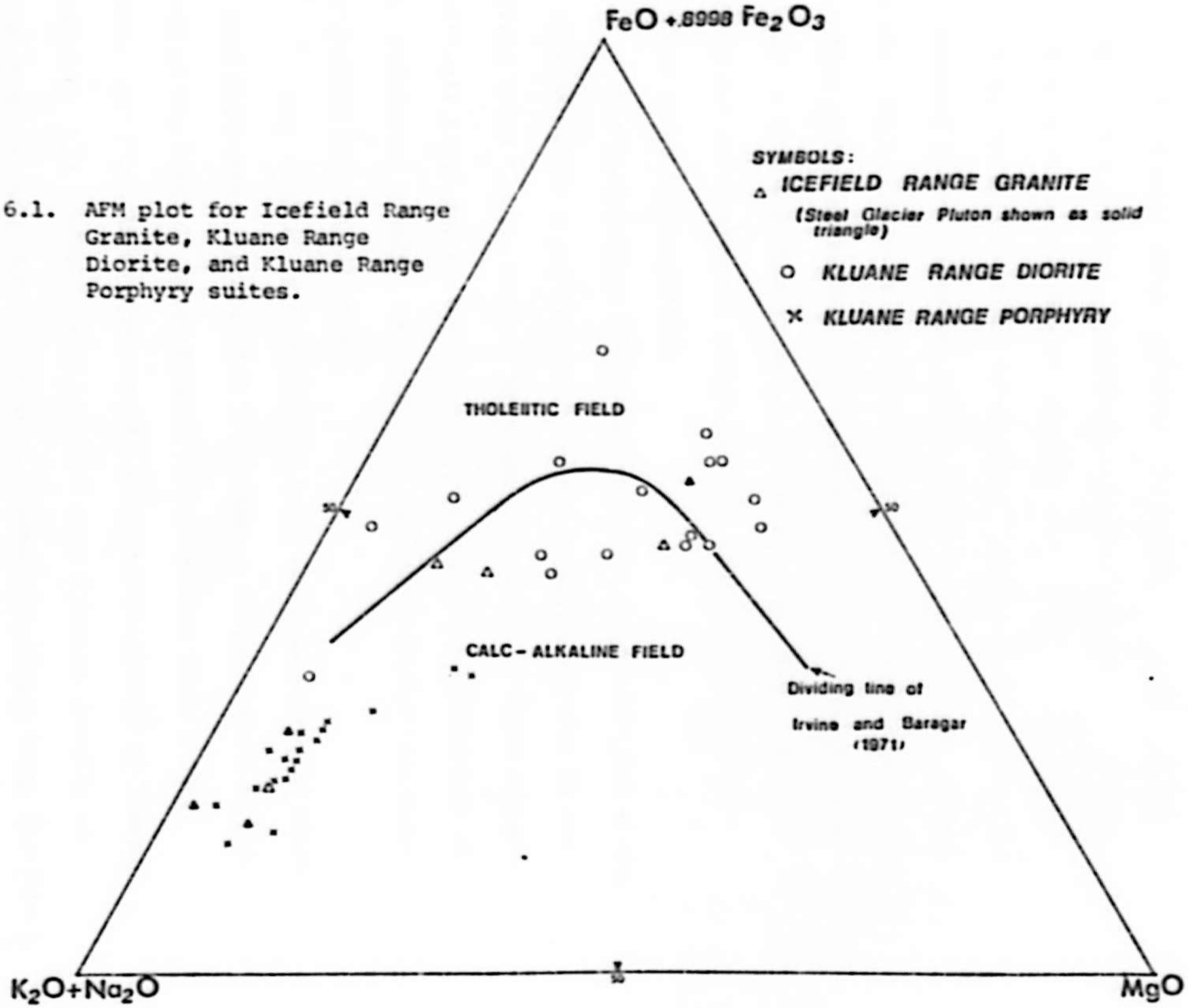
The three igneous suites are plotted on Fig. 6.1, an AFM diagram on which is drawn a dividing line proposed by Irvine and Baragar (1971) to separate tholeiitic and calc-alkaline rocks. Each suite appears to plot in a distinct area of the diagram and, for the most part, on one side or the other of this dividing line.

The Icefield Range plutonic rocks show a strong calc-alkaline trend over a wide range of total alkali values. Owing to the great difference in age between the Permian Steele Glacier pluton and the remainder of the samples in this suite, these two phases of plutonism have been identified on the diagram. The trend seems to indicate that, while two phases of plutonism can be distinguished by radiometric dating, chemical analysis does not discriminate between the older and younger bodies within this suite.

---

[1] An addendum has been prepared separately, primarily for the Department of Indian and Northern Affairs, which reports the following trace elements not considered germane to the discussion in this thesis: Cu, Pb, Zn, Ni, Cr, Co, Sn, Ga, Zr.

Fig. 6.1. AFM plot for Icefield Range Granite, Kluane Range Diorite, and Kluane Range Porphyry suites.



The Kluane Range diorites plot mainly in the tholeiitic field on the AFM diagram, although a significant number of samples lie in the calc-alkaline field. Whether these rocks can be said to show a truly tholeiitic trend is arguable. However, it is clear that when compared to the other two suites, these rocks show very strong iron enrichment. Because diorites typically have a lower ferric:ferrous ratio than quartz monzonites or granodiorites (about 0.39, compared to 0.52), a test was made to check the sensitivity of the AFM plot to different ferric:ferrous ratios in this range, and the effect was shown to be imperceptible.

The Kluane Range porphyries plot in the calc-alkaline field, but cluster within a much narrower range of alkalis compared to the Icefield Range Granite suite. The tight clustering of these rocks on chemical plots may be a function of the hypabyssal emplacement of small volumes of granitic melt, and the apparently narrow time-span during which it crystallized.

Fig. 6.2 is a K_2O vs SiO_2 plot for the same suites of rocks. The most noteworthy feature of this diagram is the divergence in the trends of the Icefield Range Granite and the Kluane Range Diorite suites. The trend lines shown on the diagram were plotted by linear regression. The Icefield Range granites show a strong increase in potash over the range 50% to 72% SiO_2, whereas the Kluane Range diorites show a much less pronounced enrichment of potash with respect to silica. As was the case with the AFM plot in Fig. 6.1, the Kluane Range

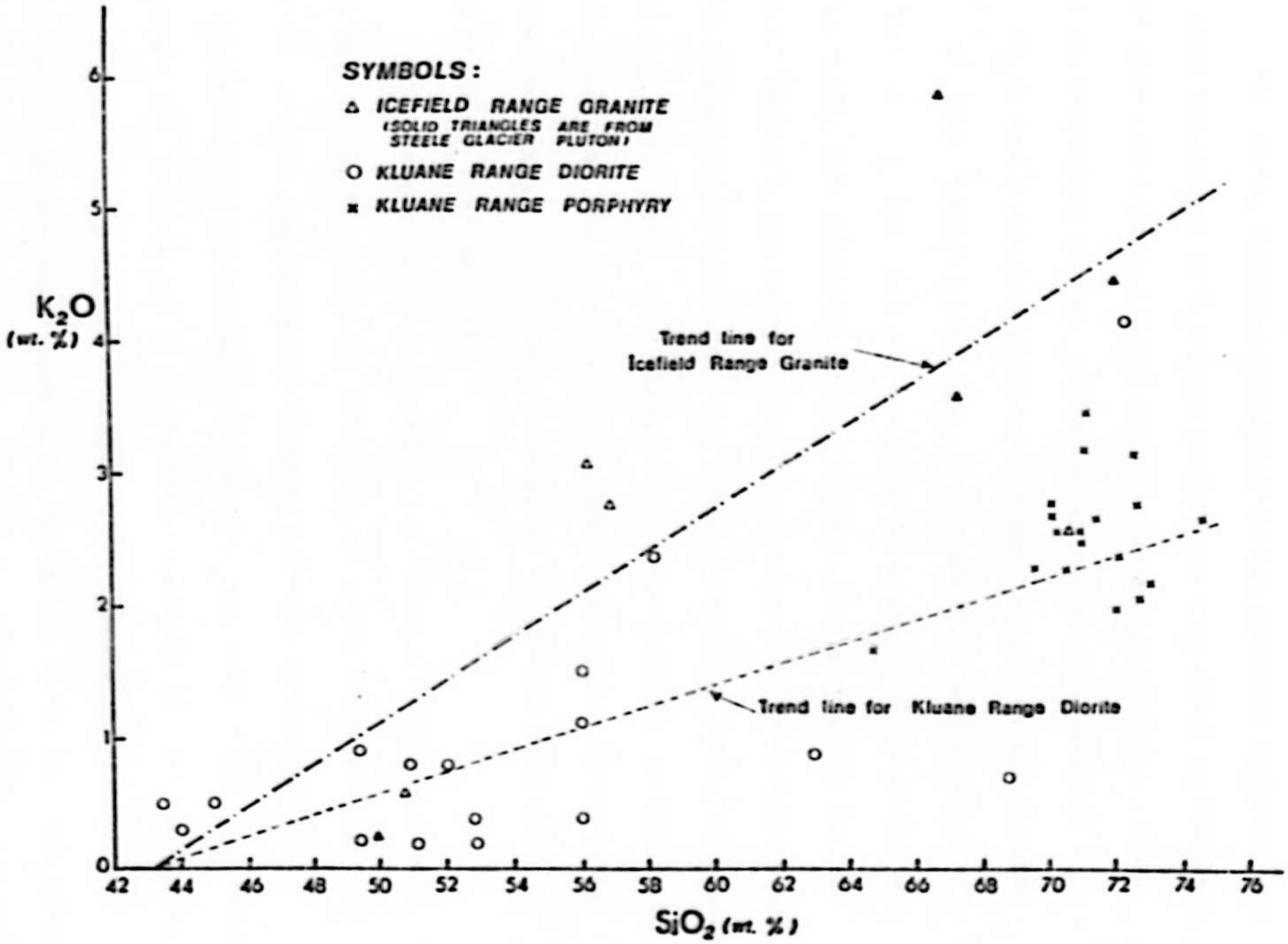


Fig. 6.2. K_2O vs SiO_2 plot for Icefield Range Granite, Kluane Range Diorite, and Kluane Range Porphyry suites.

porphyries plot in a fairly tight cluster, making it impossible to distinguish any significant co-variation of potash and silica.

The modal diagrams presented in the previous chapter, and the strong enrichment of K_2O with respect to SiO_2 shown in Fig. 6.2, suggest that the Icefield Range Granite may be an alkaline rather than a calc-alkaline suite. A diagram in which total alkalis (K_2O + Na_2O) are plotted against silica may be used to distinguish "alkaline" from "subalkaline" (i.e., calc-alkaline and tholeiitic) associations. In Fig. 6.3 the dividing line proposed by Irvine and Baragar (1971) for separating the alkaline and subalkaline fields is drawn. While a few samples from the Icefield Range Granite suite fall in the alkaline field, the trend line and the majority of points lie in the subalkaline (calc-alkaline) field. However, it should be kept in mind that the number of data points is small. As would be expected from Figs. 6.2 and 6.3, the other two suites fall well within the sub-alkaline field.

The samples were analyzed for a number of trace elements, namely Rb, Sr and Ba, with the intention of using these elements to characterize more precisely the chemistry of the igneous suites. These elements, and particularly Rb and Sr, are used in the literature to discuss the genesis and plate tectonic settings of igneous rocks.

Table 6.2 presents averaged trace element analyses, and calculated values for the ratios K/Rb, Rb/Sr and Ba/Rb for each suite. The figures in parentheses are the range of individual samples used

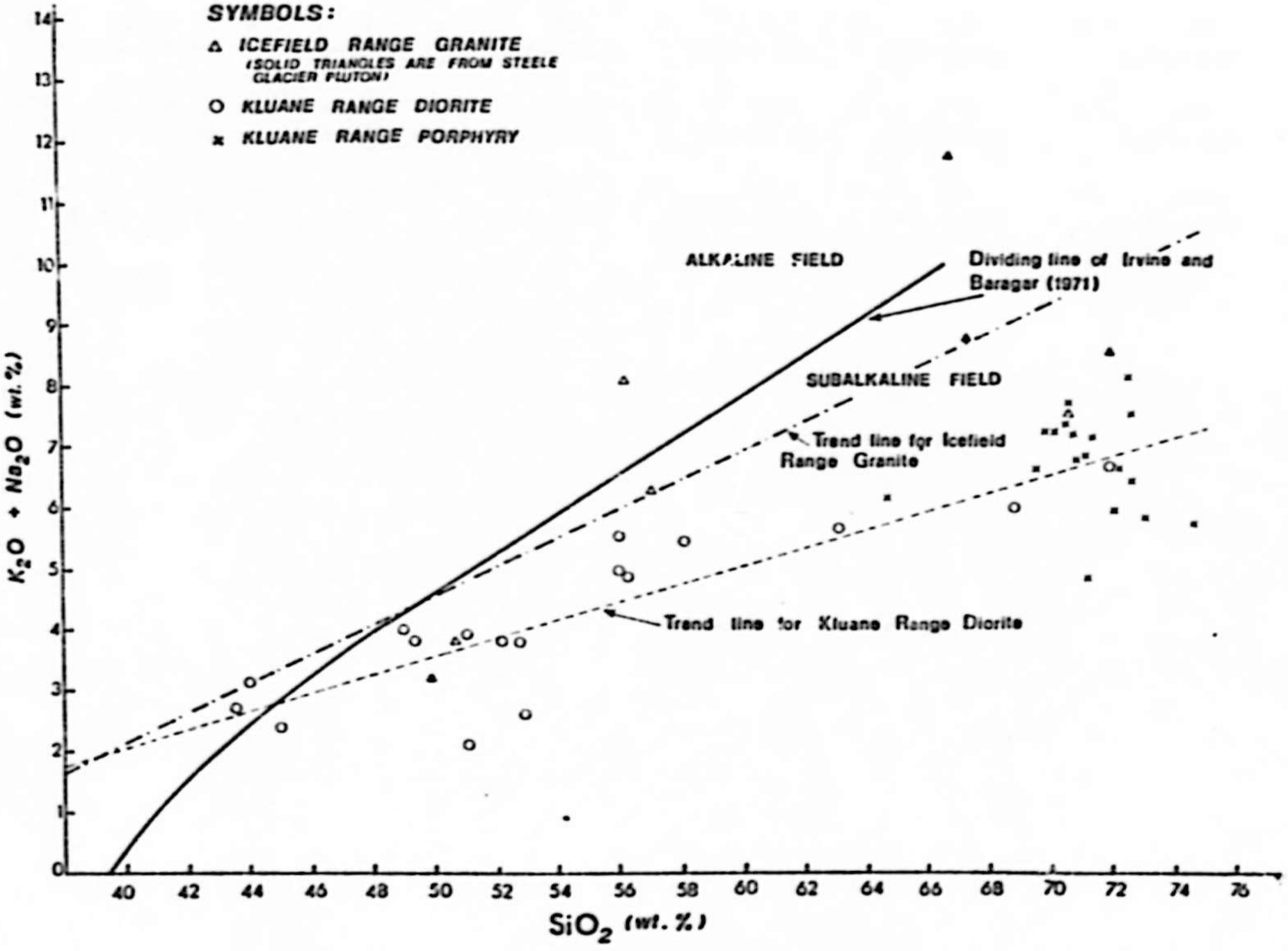


Fig. 6.3. (K_2O + Na_2O) vs SiO_2 plot for Icefield Range Granite, Kluane Range Diorite and Kluane Range Porphyry suites.

Table 6.2. Average trace element values for igneous suites southwest of the Denali-Shakwak Fault (in ppm).

Suite	n	K(%)	n	Rb	n	Sr	n	Ba	n	K/Rb	n	Rb/Sr	n	Ba/Rb
Icefield Range Granite	8	2.428 (.190-4.916)	6	118 (20-192)	7	791 (250-2100)	7	2104 (430-5100)	6	210 (144-252)	6	.20 (.04-.54)	6	20 (7-34)
Kluane Range Diorite	17	0.779 (.150-3.528)	6	52 (13-80)	11	329 (140-520)	11	629 (150-2500)	6	278 (188-452)	6	.19 (.03-.42)	6	19 (6-46)
Kluane Range Porphyry	18	2.133 (1.420-2.890)	6	69 (35-91)	16	472 (290-760)	16	2375 (1100-4500)	6	324 (274-408)	6	.16 (.05-.31)	6	26 (16-45)

to calculate the average.

The ratio K/Rb for most continental whole rocks (as opposed to oceanic rocks) is reported to lie within the fairly narrow range 160-300 (Ahrens and Taylor, 1961; Heier and Adams, 1964). Heier and Adams summarized previous work and suggested the following averages: dunites, 300; basic rocks, 270; basic-intermediate rocks, 230; crust, 229. Shaw (1968) defined a "main trend" in K/Rb in a large variety of igneous rocks, ranging from 150-300.

The K/Rb values for the igneous suites in this region fall within this "normal" range, with the exception of the Kluane Range Porphyry suite which appears to be depleted in Rb with respect to K. Shaw (1968) has suggested that the most obvious control for K/Rb ratios in ordinary igneous rocks is accumulation of biotite or crystallization and removal of hornblende to produce enrichment of Rb relative to K. Although the Kluane Range porphyries are relatively potassic (averaging about 2.1 wt.% K), they contain no modal hornblende and only minor biotite. A possible explanation for the high K/Rb ratios of these rocks is that most of the Rb and K is bound up in potassium feldspar, which typically has K/Rb values higher than biotite, and often higher than the "normal" range limit of 300.

Jakes and White (1972) report K/Rb ratios in volcanic rocks from island arcs to range from 870-1000 in tholeiites and from 340-430 in calc-alkaline rocks. Shaw (1968) suggests that the most primitive earth material available for direct analysis is abyssal

tholeiitic basalt, with KRb values as high as 3000.

The close concordance of K/Rb values for the three igneous suites southwest of the Denali-Shakwak Fault with values reported for continental whole rocks suggests that the former have evolved within a body of sialic crust, rather than in an island arc or in oceanic crust. This is consistent with the observation made in Chapter 4 that the igneous suites in the St. Elias Mountains in Yukon Territory were intruded into much older pre-existing country rocks, and were not components of evolving island arc systems with coeval calc-alkaline volcanic suites and associated ocean-floor tholeiites.

The Rb/Sr ratios for the three suites are quite consistent, ranging from 0.16-0.20. These values would be considered typical of continental sial according to Culbert (1972), but are considerably higher than those for island arc volcanic rocks of tholeiitic and calc-alkaline compsoition, which range from 0.03-0.17 (Jakes and White, 1972). The similarity in Rb/Sr values between the three suites is all the more remarkable given that Sr variation is strongly controlled by fractionation of feldspar, and in view of the markedly differing mineralogies of the igneous rock suites in the St. Elias Mountains (Chapter 5).

Ba/Rb ratios are not widely reported in the literature. The values for the three igneous suites reported here range from 19-26, somewhat higher than ratios reported by Jakes and White (1972)

for island arc volcanic rocks (9-17). Tauson and Kozlov (1972) report Ba/Rb ratios in ore-bearing granites to range from 0.03-0.26, 50-80 times smaller than ratios in neighbouring barren granites (2.5-15). None of the individual samples reported here, even those from known centres of mineralization, are in this low range.

6.3 Geochemistry of Granitoid Rocks Northeast of the Denali-Shakwak Fault

Analyses for each of the three igneous suites northeast of the Denali-Shakwak Fault are presented in Table 6.3.

The AFM plot (Fig. 6.4) shows that the Nisling Range Granodiorite, Ruby Range Granodiorite and Nisling Range Alaskite suites all follow calc-alkaline trends with no overlap into the tholeiitic field.

The Nisling Range granodiorites follow the calc-alkaline trend over a wide range of alkali values but, even within this field, show very little tendency toward iron enrichment. It is apparent on the AFM diagram that the area defined by this suite is a subset of the Ruby Range Granodiorite, indicating that this type of diagram is of limited use in distinguishing these two suites.

The Ruby Range granodiorites display a strong, continuous calc-alkaline trend over a very wide range of alkali values, but show significantly more iron enrichment than the Nisling Range granodiorites. The most siliceous members of this suite encroach

Table 6.3. Major and minor element analyses for granitic rocks northeast of Denali-Shakwak fault.

(major elements in weight percent; minor elements in ppm).

Nisling Range Granodiorite

Sample No.	1	2	3	4	23	24	25	26
SiO_2	56.71	73.77	61.61	62.40	68.35	68.27	59.61	65.84
Al_2O_3	14.47	15.45	16.38	14.71	15.51	14.98	14.08	13.41
CaO	6.30	2.10	4.57	5.87	3.60	3.44	2.59	3.29
Na_2O	3.16	3.82	3.51	2.90	3.06	3.55	1.88	3.10
FeO	4.30	1.32	2.98	2.72	2.39	2.26	3.21	2.09
Fe_2O_3	2.26	0.70	1.57	1.43	1.26	1.19	1.69	1.10
MgO	4.67	0.81	2.31	2.31	1.67	1.17	1.01	1.27
TiO_2	0.71	0.25	0.59	0.68	0.52	0.48	0.55	0.38
MnO	0.12	0.04	0.07	0.04	0.03	0.03	0.01	0.02
P_2O_5	0.19	0.07	0.17	0.15	0.21	0.20	0.25	0.20
Total	94.94	101.65	96.55	95.46	100.08	99.01	89.33	94.00
Rb	133	207	177	57	102	210	N.A.	N.A.
Sr	470	260	680	605	630	590	320	440
Ba	2400	2000	3300	3200	2400	2300	2400	4200

Table 6.3 (cont'd.)

Nisling Range Granodiorite (cont'd.)

Sample No.	27	31
SiO_2	60.64	66.85
Al_2O_3	13.67	14.19
CaO	3.23	2.06
K_2O	4.82	3.87
Na_2O	1.03	3.33
FeO	2.29	1.77
Fe_2O_3	1.20	0.93
MgO	1.18	1.02
TiO_2	0.39	0.35
MnO	0.02	0.03
P_2O_5	0.17	0.13
Total	88.65	94.52
Rb	N.A.	N.A.
Sr	350	N.A.
Ba	4800	N.A.

Table 6.3 (cont'd.)

Ruby Range Granodiorite

Sample No.	5	6	7	8	9	11	12	13
SiO_2	53.44	61.77	63.04	61.07	75.24	65.17	63.80	70.25
Al_2O_3	15.60	16.38	15.50	15.42	14.11	13.98	14.30	16.07
CaO	8.69	4.45	4.22	4.44	1.65	3.23	3.57	2.09
K_2O	1.28	2.70	3.42	2.69	4.14	3.58	3.63	5.09
Na_2O	3.68	4.11	3.72	3.94	3.63	2.84	2.93	3.42
FeO	5.08	3.10	2.92	3.05	1.13	2.32	2.45	1.49
Fe_2O_3	2.67	1.63	1.53	1.60	0.59	1.22	1.29	0.78
MgO	5.21	1.89	1.76	1.94	0.37	1.66	1.67	0.50
TiO_2	0.92	0.62	0.63	0.62	0.21	0.46	0.48	0.35
MnO	0.12	0.10	0.09	0.11	0.05	0.04	0.05	0.03
P_2O_5	0.28	0.32	0.29	0.31	0.08	0.15	0.14	0.10
Total	96.96	97.07	97.12	95.17	101.20	94.60	94.81	100.16
Rb	N.A.	185	170	166	140	N.A.	N.A.	167
Sr	N.A.	590	1300	290	130	N.A.	N.A.	420
Ba	N.A.	2900	6300	8000	1500	N.A.	N.A.	3900

Table 6.3 (cont'd.)

Ruby Range Granodiorite (cont'd.)

Sample No.	14	18	32	41	42	46	48	50
SiO_2	69.98	65.40	69.58	67.64	64.90	53.04	52.59	68.19
Al_2O_3	15.03	16.62	15.16	16.82	15.77	15.17	14.36	15.92
CaO	2.60	2.80	2.73	2.74	3.87	6.99	6.05	2.61
K_2O	3.88	3.89	3.56	2.72	2.81	1.79	2.45	3.90
Na_2O	3.49	4.01	3.07	4.87	3.76	3.34	3.63	3.93
FeO	1.61	1.65	1.79	1.61	2.37	4.65	6.49	1.99
Fe_2O_3	0.85	0.87	0.94	0.84	1.24	2.44	3.41	1.05
MgO	1.21	1.06	0.76	0.59	1.62	3.78	3.17	0.56
TiO_2	0.40	0.43	0.46	0.44	0.57	1.35	1.84	0.37
MnO	0.04	0.03	0.06	0.03	0.11	0.12	0.14	0.05
P_2O_5	0.13	0.16	0.19	0.15	0.16	0.40	0.55	0.12
Total	99.23	96.92	98.29	98.44	97.18	93.07	94.66	98.69
Rb	155	163	132	60	158	75	156	118
Sr	500	420	710	550	670	440	480	320
Ba	2900	1800	2800	2100	2500	1300	2200	3800

Table 6.3 (cont'd.)

Ruby Range Granodiorite (cont'd.)

Sample No.	52	53	54	56	57	58	59	60
SiO_2	62.99	58.94	53.72	53.81	65.98	71.83	69.52	64.51
Al_2O_3	16.63	16.37	18.02	18.22	15.14	15.65	16.28	14.85
CaO	5.20	5.70	6.46	7.80	3.04	2.16	2.83	3.27
K_2O	1.96	1.62	1.76	1.76	3.74	4.14	3.48	2.45
Na_2O	3.87	4.03	4.32	3.45	3.55	3.62	4.15	2.91
FeO	3.59	3.24	3.78	6.01	1.67	1.04	1.60	1.90
Fe_2O_3	1.89	1.70	.99	3.16	0.88	0.55	0.84	1.00
MgO	2.27	1.62	1.86	3.04	1.11	0.66	0.79	0.82
TiO_2	0.91	0.73	1.02	1.63	0.47	0.25	0.42	0.48
MnO	0.08	0.06	0.07	0.17	0.03	0.03	0.05	0.03
P_2O_5	0.29	0.25	0.33	0.49	0.16	0.07	0.15	0.16
Total	99.69	94.27	93.33	99.55	95.77	99.98	100.13	92.37
Rb	102	N.A.	63	60	180	N.A.	85	85
Sr	1100	1000	1260	820	370	N.A.	340	580
Ba	3100	3000	3700	1800	1900	N.A.	1000	2100

Table 6.3 (cont'd.)

Ruby Range Granodiorite (cont'd.)

Sample No.	61	62	64	67	68	69	70	72
SiO_2	68.77	66.67	63.19	62.09	53.40	70.46	76.19	71.57
Al_2O_3	16.12	15.29	14.76	15.18	16.41	13.46	14.37	13.37
CaO	3.49	3.24	3.74	4.09	7.50	1.23	1.62	1.26
K_2O	2.36	2.53	2.48	3.20	1.90	4.74	4.26	4.35
Na_2O	4.15	4.38	4.03	3.96	3.31	3.52	3.43	4.04
FeO	1.92	2.05	2.12	3.01	5.85	1.19	1.14	1.52
Fe_2O_3	1.01	1.08	1.11	1.58	3.07	0.63	0.60	0.80
MgO	1.25	0.93	1.81	1.84	3.66	0.06	0.32	0.54
TiO_2	0.49	0.48	0.25	0.63	1.58	0.22	0.25	0.21
MnO	0.03	0.01	0.05	0.06	0.15	0.01	0.03	0.01
P_2O_5	0.15	0.16	0.12	0.22	0.33	0.09	0.06	0.08
Total	99.74	96.80	93.66	95.86	97.17	95.60	102.28	97.74
Rb	80	N.A.	95	N.A.	114	N.A.	129	192
Sr	350	N.A.	970	710	590	290	320	300
Ba	910	N.A.	7100	3800	1600	3900	5700	3000



Table 6.3 (cont'd.)

Ruby Range Granodiorite (cont'd.)

Sample No.	73	74	75	76	77	79	81	82
SiO_2	67.08	70.83	61.85	61.67	70.51	67.41	67.25	74.44
Al_2O_3	16.33	14.12	17.18	16.92	14.19	14.16	16.11	15.05
CaO	3.85	1.34	4.36	2.68	2.26	1.73	3.47	1.63
K_2O	1.86	5.80	2.36	4.32	3.75	3.98	2.98	3.91
Na_2O	4.19	3.39	4.05	4.20	0.19	4.20	3.52	3.99
FeO	2.30	1.08	3.60	3.15	1.46	1.87	2.40	0.74
Fe_2O_3	1.21	0.57	1.89	1.66	0.77	0.98	1.26	0.39
MgO	1.43	0.15	1.94	0.58	0.56	0.54	1.32	0.41
TiO_2	0.56	0.25	0.72	0.64	0.33	0.31	0.70	0.21
MnO	0.05	0.03	0.10	0.07	0.03	0.05	0.01	0.00
P_2O_5	0.15	0.06	0.23	0.15	0.13	0.09	0.22	0.10
Total	99.00	97.61	98.29	96.03	94.20	95.32	99.24	100.86
Rb	96	206	N.A.	172	104	N.A.	123	121
Sr	512	240	610	440	460	320	680	370
Ba	750	1700	3100	9400	2800	3900	2800	1200

Table 6.3 (cont'd.)

Ruby Range Granodiorite (cont'd.)

Sample No.	83	84	85	86	87	88	90	91
SiO_2	71.47	71.41	73.25	68.78	71.33	71.69	58.69	71.06
Al_2O_3	13.64	13.64	14.39	13.29	14.37	12.97	16.30	13.91
CaO	1.45	1.44	1.74	1.19	1.62	1.38	6.19	2.08
K_2O	4.31	4.54	4.08	4.25	3.95	4.50	1.99	3.99
Na_2O	4.24	4.39	3.37	3.80	3.97	3.87	3.31	3.20
FeO	1.39	1.33	0.91	1.52	1.61	0.99	4.30	1.24
Fe_2O_3	0.73	0.70	0.48	0.80	0.85	0.52	2.26	0.65
MgO	0.11	0.60	0.34	0.40	0.53	0.15	2.91	0.39
TiO_2	0.26	0.24	0.21	0.24	0.30	0.19	1.20	0.28
MnO	0.04	0.03	0.02	0.03	0.04	0.02	0.12	0.02
P_2O_5	0.10	0.06	0.08	0.09	0.09	0.06	0.32	0.08
Total	97.76	98.37	98.88	94.37	98.65	96.36	97.58	96.91
Rb	180	206	131	N.A.	89	174	84	160
Sr	220	185	460	240	190	220	521	1600
Ba	1500	1300	320	1700	1100	1600	1300	2300

Table 6.3 (cont'd.)

Ruby Range Granodiorite (cont'd.)

Sample No.	92	93	94	95	96	97	98	99
SiO_2	70.41	71.05	71.42	69.81	71.89	71.26	68.61	61.81
Al_2O_3	13.08	14.52	14.45	14.10	13.95	14.13	13.96	16.32
CaO	1.67	2.27	2.15	1.94	2.24	2.24	2.20	4.61
K_2O	4.08	3.98	4.09	3.84	3.42	3.91	3.64	2.33
Na_2O	2.72	3.45	3.39	3.14	2.97	3.75	2.80	3.40
FeO	1.27	1.55	1.29	1.23	1.35	1.41	1.69	3.47
Fe_2O_3	0.67	0.81	0.68	0.65	0.71	0.74	0.89	1.82
MgO	0.67	0.61	0.29	0.29	0.69	0.57	0.20	1.83
TiO_2	0.24	0.35	0.32	0.25	0.27	0.29	0.30	0.72
MnO	0.02	0.11	0.03	0.01	0.05	0.04	0.03	0.10
P_2O_5	0.13	0.14	0.10	0.08	0.08	0.09	0.08	0.25
Total	94.95	98.84	98.19	95.33	97.62	98.42	94.42	96.67
Rb	N.A.	155	138	N.A.	123	207	N.A.	119
Sr	500	1400	390	390	310	420	420	420
Ba	2600	2000	2200	3200	1400	1800	340	1400

Table 6.3 (cont'd.)

Ruby Range Granodiorite (cont'd.)

Sample No.	100	101	102	103	104
SiO_2	65.15	62.08	64.50	54.28	59.92
Al_2O_3	15.44	16.18	15.77	16.55	16.69
CaO	3.24	4.73	4.20	8.93	5.70
K_2O	2.42	2.59	2.13	1.60	1.89
Na_2O	3.96	3.67	3.69	2.22	3.37
FeO	1.54	3.15	2.97	5.06	3.83
Fe_2O_3	0.81	1.65	1.56	2.66	5.01
MgO	0.57	1.61	1.37	4.23	2.82
TiO_2	0.46	0.66	0.72	1.15	0.78
MnO	0.01	0.09	0.06	0.13	0.10
P_2O_5	0.15	0.20	0.22	0.23	0.29
Total	93.76	96.60	97.18	97.04	97.40
Rb	N.A.	69	60	92	72
Sr	1100	640	690	400	770
Ba	4500	1900	1400	770	3300

Table 6.3 (cont'd.)

Nisling Range Alaskite

Sample No.	28	29	30	36	37	38	39	40
SiO_2	78.59	72.73	75.62	77.54	77.50	80.96	69.70	72.87
Al_2O_3	13.02	12.04	12.75	13.97	14.07	14.12	13.11	12.23
CaO	0.60	0.26	0.62	0.93	1.01	1.00	1.04	0.49
K_2O	4.22	4.82	4.83	4.79	4.60	4.21	4.13	4.28
Na_2O	3.62	3.05	3.28	3.64	3.42	3.78	3.59	3.76
FeO	0.71	1.14	0.43	0.94	1.07	1.06	1.76	1.08
Fe_2O_3	0.37	0.60	0.23	0.49	0.56	0.55	0.93	0.57
MgO	0.10	0.01	0.07	0.09	0.28	0.47	0.01	0.01
TiO_2	0.08	0.04	0.14	0.13	0.15	0.15	0.18	0.08
MnO	0.01	0.01	0.00	0.01	0.02	0.02	0.02	0.00
P_2O_5	0.01	0.02	0.02	0.09	0.07	0.05	0.06	0.06
Total	101.35	94.73	98.00	102.62	102.75	106.37	94.53	95.44
Rb	213	251	300	134	217	210	N.A.	N.A.
Sr	4	104	88	101	113	105	250	190
Ba	17	620	1200	810	970	590	5200	800

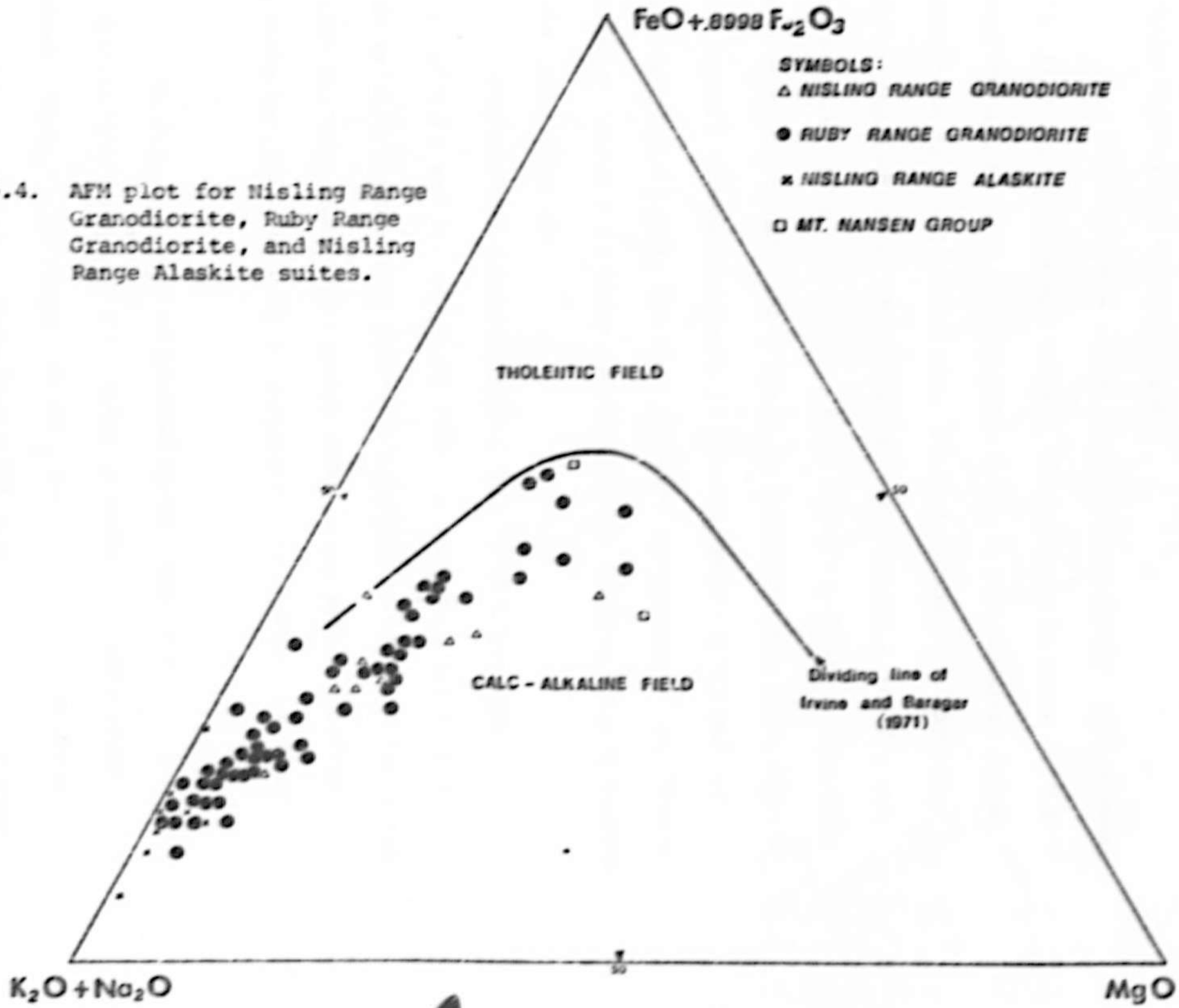


Fig. 6.4. AFM plot for Nisling Range Granodiorite, Ruby Range Granodiorite, and Nisling Range Alaskite suites.

upon the high-alkali, low-MgO part of the diagram, where rocks of rhyolitic composition typically plot.

The Nisling Range alaskites fall in a fairly tight cluster at high alkali-, and low MgO values. They appear to occur at the culmination of, or as the final product of, a calc-alkaline trend. However, this type of diagram does not discriminate well between siliceous end-members of tholeiitic and calc-alkaline trends, and so two samples of the coeval Mt. Nansen Group volcanics were also plotted on the diagram. While there is a considerable separation on the diagram between the plots of the Mt. Nansen Group and the Nisling Range alaskites, the calc-alkaline association of Mt. Nansen rocks lends credence to the proposal that the Nisling Range alaskites are also calc-alkaline.

Roddick and Hutchison (1974) report that averages for quartz diorites and granodiorites from the central Coast Mountains are tholeiitic, rather than calc-alkaline, but the lack of individual specimen analyses, and some concern about using averaged values, make their results difficult to compare to the conclusions reached here.

In Fig. 6.5, K_2O is plotted against SiO_2 for each suite. Both the Nisling Range and Ruby Range granodiorites show strong enrichment in K_2O with respect to SiO_2 but the regression lines indicate that there is no significant difference in trends between the two suites. The Nisling Range alaskites plot in a tight cluster

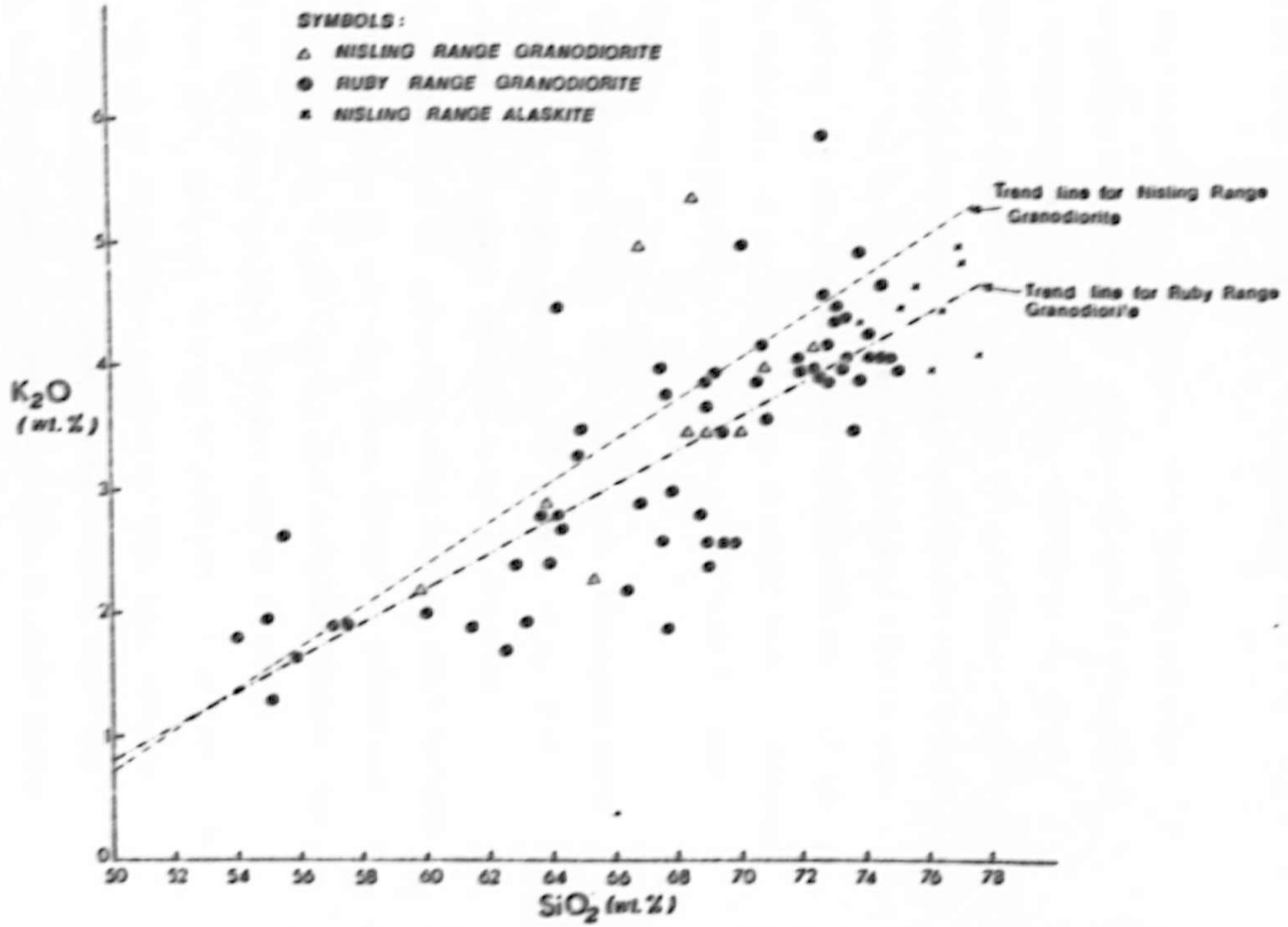


Fig. 6.5. K_2O vs SiO_2 plot for Nisling Range Granodiorite, Ruby Range Granodiorite, and Nisling Range Alaskite suites.

over a narrow range of K_2O and SiO_2, and therefore show no definable trend.

Many workers (e.g., Hutchison, 1970; Bateman and Dodge, 1970; Moore et al., 1962; Dickenson, 1970) have noted the variation in potash content across the batholiths of western North America. Fig. 6.6 shows the variation in K_2O across the Ruby and Nisling Ranges using the Denali-Shakwak Fault as a base line and surrogate for the Pacific margin. The trend line shows an increase of slightly more than 1% K_2O from the southwestern to the northeastern margin of the Ruby Range Batholith, an eastward increase in potash that is consistent in degree with those defined in other areas of the North American Pacific margin.

The effects of potash variation on modal mineralogy serve as the basis for the "quartz diorite line" of Moore et al. (1962). The line passes longitudinally down the length of the Mesozoic batholiths of North America, separating rocks lacking potash feldspar on the west, from rocks of generally quartz monzonitic composition on the east. Hutchison (1970) confirms that the quartz diorite line may be recognized along the Coast Plutonic Complex in the Prince Rupert region, B.C. However, it would be difficult, if not impossible, to extend the quartz diorite line through the Ruby Range Batholith. Even though a trend in potash content can be observed across the batholith, the potash contents of rocks along the southwest margin are sufficient to produce significant modal potash feldspar (see Fig. 6.6).

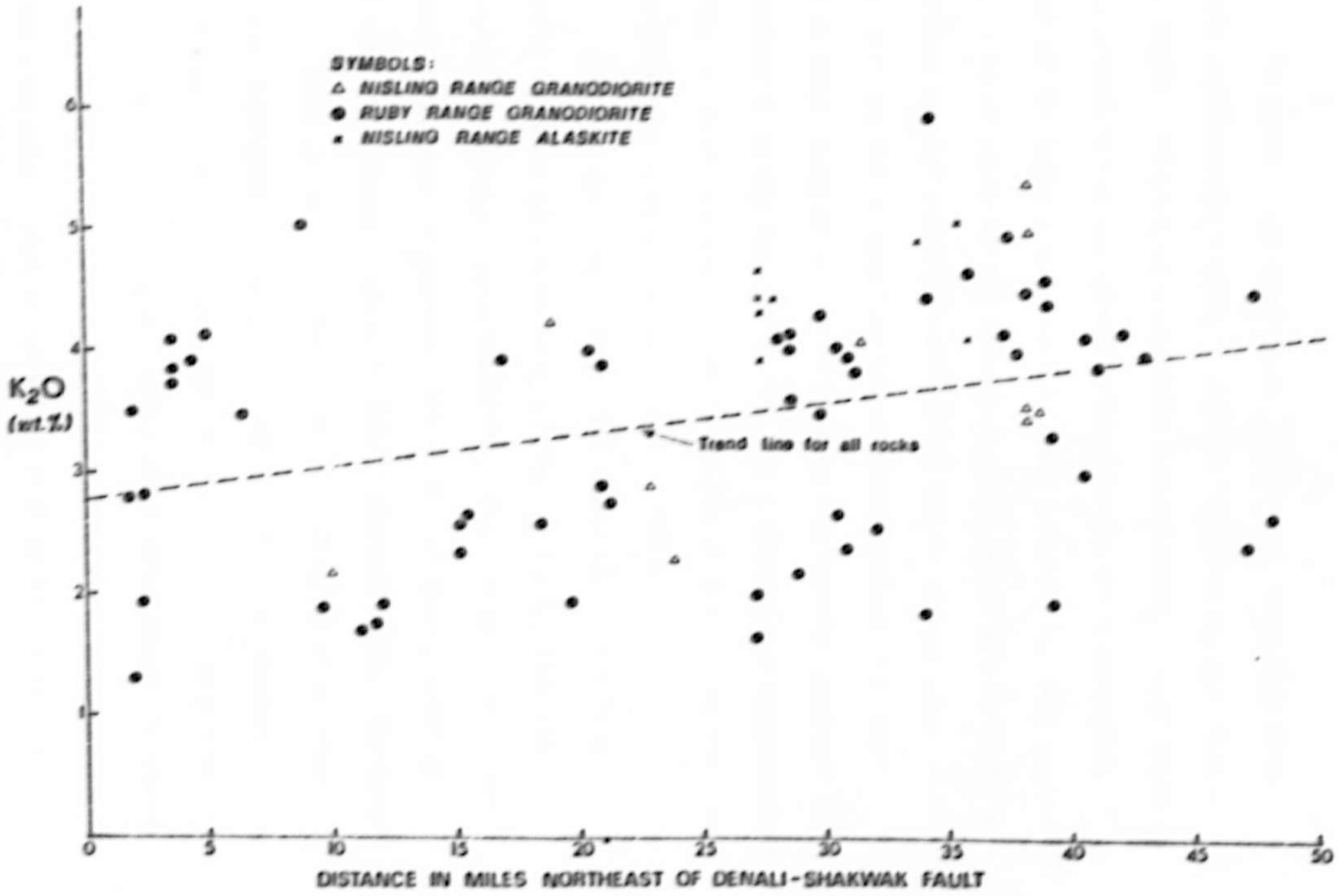


Fig. 6.6. Variation in K_2O across Ruby Range Batholith and Nisling Range.

It seems clear that parts of the Ruby Range Batholith, along its southwestern margin, have been truncated by the Denali-Shakwak Fault. Truncation could have removed mainly quartz diorites, leaving granodiorites and quartz monzonites on the southwestern boundary of the batholith. There is some evidence for this contention if one looks at parts of the batholith which do not appear to have been truncated, for example along Talbot Arm of Kluane Lake. Moving northward along Talbot Arm from the southern contact with the Kluane schists, samples no. 34 to 41 show a systematic increase in modal potash feldspar from 0% to 15% over a distance of approximately 15 miles. In this instance, it would be possible to place the quartz diorite line with some precision across Talbot Arm.

Bateman and Dodge (1970) have shown that there is a systematic increase of potash with respect to silica from west to east across the Sierra Nevada Batholith. The "potash index" used by Bateman and Dodge, $[K_2O/(SiO_2-45)] \times 10^3$, is here plotted in Fig. 6.7 against distance from the Denali-Shakwak Fault. The trend line shows that there is no significant variation in this index across the batholith. If only the samples along the traverse on Talbot Arm are considered, the same lack of variation in potash index would be observed. This implies that, while total potash increases from west to east across the batholith, silica also increases at about the same rate. Thus no variation such as that described in the Sierra Nevada Batholith is observed.

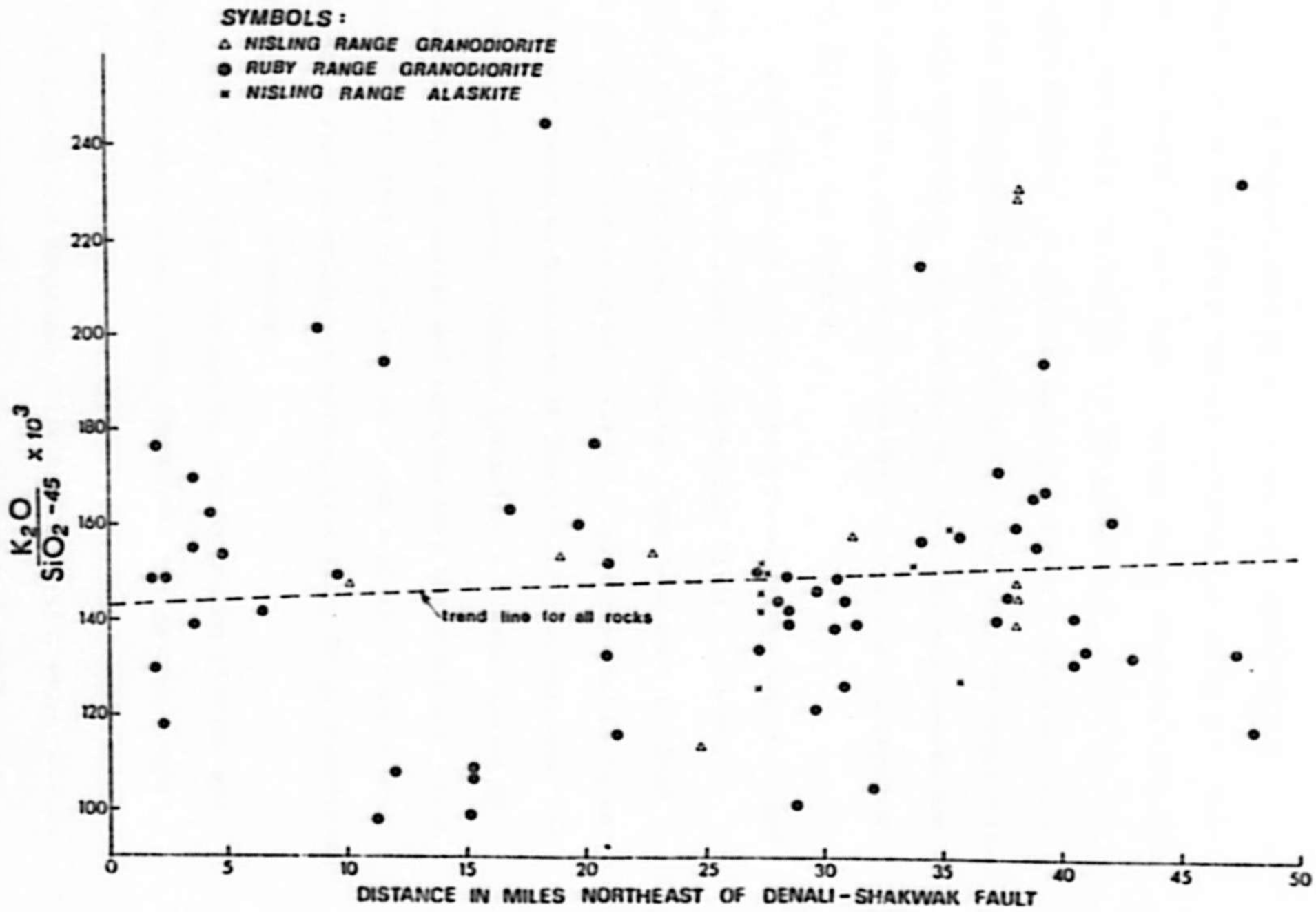


Fig. 6.7. Variation in potash index [$(K_2O/SiO_2-45) \times 10^3$] across Ruby Range Batholith and Nisling Range.

Trace element determinations for the igneous suites northeast of the fault are presented in Table 6.4, along with some figures reported by Culbert (1972) for the Coast Mountains Batholith, and data reported by Le Couteur and Tempelman-Kluit (1976) for Ruby Range granodiorites. Culbert's (op. cit.) figures were averaged in such a way (weighted by rock-type) to make them directly comparable to the data reported by this writer; that is, only his figures for quartz monzonites, granodiorites, quartz diorites and diorites were used to calculate the average.

The K/Rb ratios of the three igneous suites reported here are seen to fall within normal "continental" limits (160-300), suggesting the pre-existing continental rocks have been involved in the evolution of these rocks. The K/Rb value reported by Culbert for the Coast Mountains Batholith is significantly higher, and lies above the "normal" range. Culbert identifies a bimodal frequency distribution for K/Rb values and suggests that the anomalously high population (K/Rb >400) is related to linear tectonic features which may be relict from an earlier subduction zone along which destruction of oceanic crust was occurring.

The Rb/Sr ratios for the Nisling Range Granodiorite and Ruby Range Granodiorite are almost identical, and somewhat higher than values usually reported for typical continental crust (about 0.25). Le Couteur and Tempelman-Kluit (1976) found a value of 0.18 for the Ruby Range Granodiorite. The value of 0.06 reported by

Table 6.4. Average trace element values for igneous suites northeast of the Denali-Shakwak Fault (in ppm).

Suite	n	K(%)	n	Rb	n	Sr	n	Ba	n	K/Rb	n	Rb/Sr	n	Ba/Rb
Nisling Range Granodiorite	10	3.041 (1.808-4.510)	6	148 (57-210)	9	483 (260-680)	9	3667 (2000-8400)	6	200 (138-340)	6	.33 (.09-.80)	6	23 (10-56)
Ruby Range Granodiorite	61	2.788 (1.080-4.934)	46	128 (60-207)	56	552 (130-1400)	56	2646 (320-9400)	46	226 (124-374)	46	.34 (.05-1.11)	46	22 (2-75)
Nisling Range Alaskite	8	3.750 (3.288-4.228)	6	221 (134-300)	8	119 (4-250)	8	1276 (17-5200)	6	180 (136-290)	6	10.72 (1.33-53.25)	6	3 (0-6)
Averages for Coast Mountains Batholith (Culbert, 1972)	61	1.47 (1.05-2.20)	61	39 (30-67)	61	693 (545-795)	-		61	371 (325-390)	61	.06 (.034-.12)	-	
Ruby Range Granodiorite (Le Couteur & Tempelman-Kluit, 1976)	-		6	84 (60-107)	6	545 (341-717)	-		-		6	.18 (.08-.32)	-	

Table 6.4. Average trace element values for igneous suites northeast of the Denali-Shakwak Fault (in ppm).

Suite	n	K(%)	n	Rb	n	Sr	n	Ba	n	K/Rb	n	Rb/Sr	n	Ba/Rb
Nisling Range Granodiorite	10	3.041 (1.808-4.510)	6	148 (57-210)	9	483 (260-680)	9	3667 (2000-8400)	6	200 (138-340)	6	.33 (.09-.80)	6	23 (10-56)
Ruby Range Granodiorite	61	2.788 (1.080-4.934)	46	128 (60-207)	56	552 (130-1400)	56	2646 (320-9400)	46	226 (124-374)	46	.34 (.05-1.11)	46	22 (2-75)
Nisling Range Alaskite	8	3.750 (3.288-4.228)	6	221 (134-300)	8	119 (4-250)	8	1276 (17-5200)	6	180 (136-290)	6	10.72 (1.33-53.25)	6	3 (0-6)
Averages for Coast Mountains Batholith (Culbert, 1972)	61	1.47 (1.05-2.20)	61	39 (30-67)	61	693 (545-795)	-		61	371 (325-390)	61	.06 (.034-.12)	-	
Ruby Range Granodiorite (Le Couteur & Tempelman-Kluit, 1976)	-		6	84 (60-107)	6	545 (341-717)	-		-		6	.18 (.08-.32)	-	

Culbert (1972) for the Coast Mountains Batholith is extremely low by comparison, and more closely corresponds to figures recorded by Jakes and White (1972) for island arc basalts and andesites, ranging from 0.03-0.08.

The Rb/Sr ratio for Nisling Range alaskites reported here is very high. Le Couteur and Tempelman-Kluit (1976) report a single determination from this suite, with a similar high value of 16.94. These high Rb/Sr values easily distinguish this suite from the Nisling Range and Ruby Range granodiorites. The high Rb/Sr ratio of Nisling Range Alaskite may be a function of the fractionation of plagioclase and amphibole which would tend to increase Rb/Sr and decrease the K/Rb values relative to the other suites, which contain greater modal proportions of these two minerals.

The Ba/Rb ratios for these suites are comparable to those reported in the previous section for the suites on the southwest side of the Denali-Shakwak Fault. The exception is the Nisling Range Alaskite, which has a very low ratio in comparison. However, only one sample (no. 28) has a ratio approximating the low values reported by Tauson and Kozlov (1972) as being associated with mineralized intrusions, and this sample is not associated with known mineralization.

CHAPTER 7

TECTONIC RECONSTRUCTIONS IN SOUTHWESTERN YUKON

7.1 Introduction

In this chapter, constraints are presented which must be met by models reconstructing the tectonic history of southwestern Yukon. The writer here develops a general model which appears to satisfy the important constraints, and is based on information presented both in this thesis and the literature. The model is tentative, but is an attempt to incorporate the information derived from this study of granitoid plutonic rocks in southwestern Yukon in a way that makes it a logical conclusion to this thesis.

Over the past decade, the emergence of plate tectonic theory has forced a re-examination of traditional ideas concerning the origin of granitic rocks. Hamilton (1969a, 1969b) and Dickinson (1970) were among the first to demonstrate the relationship between calc-alkaline magmatism and underthrusting lithospheric slabs at convergent plate margins. Both drew attention to the striking array of granitoid batholiths which fringes the Pacific Ocean basin, and which is presumed to reflect present or extinct zones of subduction, largely of oceanic lithosphere.

Dickinson (1970) and other writers (e.g., Bateman and

Dodge, (1970) have demonstrated the existence of chemical variations across circum-Pacific batholiths which can be used to infer the polarity of paleo-subduction zones. Moreover, the work of Hutchison (1970) in the Central Coast Mountains in British Columbia and, more convincingly, of Farrar et al. (1970) and Clark et al. (1976) in the Central Andes of South America, has established the systematic younging of intrusive rocks away from continental margins.

In the present context, it is considered that the calc-alkaline affinity of most of the southwestern Yukon plutonic suites, demonstrated in Chapter 6, and the geochronological, petrographical and chemical data presented here, may be accepted as evidence for the previous existence of subduction zones, beneath either volcanic arcs or continental margins. This deduction should lead eventually to a more complete understanding of the tectonic evolution of this complex part of the northwestern margin of the North American continent. In this synthesis, the granitoid suites of the region, together with their host rock assemblages, will be considered in broad chronological order, and, to some extent, the two main parts of the project area, hitherto examined as separate entities, will here be incorporated into a unified scenario.

7.2 Constraints and Tectonic Reconstructions

7.2.1 Alexander Terrane and the Icefield Range Granite

The lithology, age, structure and distribution of the oldest rocks exposed southwest of the Denali-Shakwak Fault, the Kaskawulsh Group and the Greenschist Complex of the Alexander terrane, are poorly-known. The history of this heterogeneous assemblage of carbonates, metavolcanics, coarse- and fine-grained clastics, conglomerates and schists is difficult to interpret. Furthermore, when the Alexander terrane in contiguous southeastern Alaska is considered, a history of sedimentary, volcanic and metamorphic rocks ranging in age from Precambrian to Late Triassic must be accounted for.

As described in Chapter 3, a number of writers have advanced evidence to suggest that this terrane is allochthonous with respect to the North American craton, and that it has moved into its current position, as a coherent crustal fragment, through plate tectonic processes that have yet to be determined.

Ordovician and Silurian radiometric dates reported by Lanphere et al. (1965) and Churkin and Eberlein (1977) for granitic rocks at the southeastern extremity of the Alexander terrane suggest that it must have been a terrane of continental crust by at least the Silurian. Unfortunately, the geographical distribution of these dated specimens has not been accurately reported. However, since

they come from a restricted area of Chichagof, Admiralty and Prince of Wales Islands, they could yield only minimal information regarding paleo-subduction zones or plate margins, even if the early Paleozoic position of this crustal fragment were known with more accuracy.

At the northwestern extremity of the Alexander terrane, in southwestern Yukon, K/Ar ages reported in this thesis establish episodes of calc-alkaline plutonism in the Lower Permian and Middle and Upper Jurassic. Lanphere et al. (1965) report synchronous Permian plutonism in southeastern Alaska in the Alexander terrane, and Richter et al. (1975) confirm coeval Permian (actually very Late Pennsylvanian) and Jurassic plutonism in the Eastern Alaska Range, although the host rocks there appear to be part of the Taku-Skolai, rather than Alexander terrane.

The Permian and Jurassic plutonism in the Alexander terrane is so much younger than the intruded host rock that there seems no reason to associate it with plate tectonic processes that were involved in the original development of the terrane.

A regional tectonic model must consider whether the widespread (approximately 500 mi. betwsen the specimen locations reported by Richter et al. (1975) and Lanphere et al. (1965)), but essentially synchronous, episodes of Permian and Jurassic plutonism were generated in one protracted regime: for example, the subduction of a single lithospheric slab. A corollary problem is to explain why these plutonic eposides invaded Taku-Skolai terrane in eastern

Alaska but not in the St. Elias Mountains, where they are restricted to Alexander terrane. Moreover, the evidence presented here demonstrates that, in both the Eastern Alaska Range and in the St. Elias Mountains, Permian and Jurassic plutons are virtually juxtaposed, yet show no mutual intrusive contacts, and display the same southwest-to-northeast younging over a few tens of miles. Finally, there is no record of intrusive activity in the Upper Permian and through much of the Triassic.

7.2.2 The Taku-Skolai Terrane

In the St. Elias Mountains, and in the contiguous Eastern Alaska Range, rocks of the Taku-Skolai terrane are similar in age, lithology, and structural style. Two successive episodes of volcanism and shallow marine deposition, represented in the St. Elias Mountains by the Permian Cache Creek Group and the Triassic Mush Lake Group, are described in the Eastern Alaska Range by Richter and Jones (1973).

Although the serpentinized ultramafic rocks associated with the Cache Creek Group are not known to occur in the Eastern Alaska Range, they are represented farther to the west in the west-central Alaska Range, where Clark et al. (1972) have interpreted them as an ophiolitic assemblage representing fragments of oceanic crust incorporated into the continent. Clark et al. (1972) and Richter and Jones (1973) suggest that the occurrence of ophiolitic

assemblages beneath Permian volcanic and volcaniclastic rocks and limestones strongly supports the concept of a late Paleozoic volcanic arc built directly on oceanic crust. This interpretation seems entirely appropriate for the origin of the Cache Creek strata and associated ultramafic rocks in the St. Elias Mountains.

The succession of submarine basalts, andesites, and pyroclastics, and younger massive limestone and thin-bedded limestone-argillite, in the Mush Lake Group is evidence for a second episode of volcanic arc activity in the Taku-Skolai terrane in southwestern Yukon. Muller (1967) cited the interbedding of marine sediments and lavas, pillow structures, and the spilitization of volcanic flows as evidence for submarine extrusion, and postulated their deposition in a marine "eugeosynclinal" environment.

This interpretation differs significantly from that of Richter and Jones (1973). In the Eastern Alaska Range, these writers note a lack of evidence for submarine eruption in coeval volcanic flows and suggest that they were deposited as subaerial flood basalts after collapse of the Permian volcanic arc against the North American plate: "In Middle to Late Triassic time, following a general emergence of the continent, a tremendous volume of subaerial flood basalts poured over the Permian volcanic rocks and sediments along the continental margin. Removal of this vast quantity of volcanic material from the margin apparently resulted in regional subsidence. Late Triassic seas transgressed the submerged continent, depositing

thick carbonate beds and, later, thinner bedded limestone units" (op. cit., p. 418-419).

The writer questions this interpretation on the basis that the vast quantity of volcanic material removed by erosion from the continental margin must be accounted for in the stratigraphic column, perhaps as thick wedges of greywacke or arkose, not significantly younger than the Late Triassic limestones which followed their removal. However, no such rocks are known in the Eastern Alaska Range. For this reason, and in light of the evidence presented by Muller (1967), a volcanic arc origin for the Mush Lake Group seems more probable; such an arc would, of course, have comprised both submarine and subaerial strata.

The way in which the two volcanic arcs systems are separated in space and time can lead to inferences about paleo-subduction zones. The Triassic arc rocks (Mush Lake Group) followed the Permian arc rocks after a hiatus of about 25 million years (much of the Upper Permian and Lower Triassic). Although the two arc systems are clearly separated in time, they are juxtaposed everywhere by unconformity, and not by faulting, suggesting that their loci of origin were not separated spatially. This implies that the two arc systems were formed above a single subduction zone, which may have persisted for about 80 million years, from Lower Permian to Upper Triassic time, but which may have been dormant and/or become reoriented in the hiatus between the evolution of the two systems.

On the other hand, fault contact between the two systems would imply spatial separation in the development of the two systems, two possible subduction zones, and juxtaposition through collision at the site of a descending lithospheric slab.

In summary, the structure of the Permo-Triassic Taku-Skolai terrane in the St. Elias Mountains appears to be a succession of Middle and Upper Triassic volcanic arc rocks built upon an eroded Lower Permian volcanic arc system which, in turn, was built directly on oceanic crust.

Evidence for the polarity of the inferred Permo-Triassic subduction zone, within the Taku-Skolai terrane itself, is scant. No chemical data for the volcanic rocks are available and the lithological distribution of these rocks is ambiguous in terms of a tripartite trench/arc-trench gap/magmatic arc system. However, it is suggested here that the paleo-subduction zone must have been northeastward- rather than southwestward- dipping, not on the strength of observations on the rocks that it generated, but on the basis that this model avoids some awkward problems in explaining subsequent tectonic history.

For example, Richter and Jones (1973) show a south- or southwestward-dipping zone beneath Taku-Skolai terrane in the Permian in the Eastern Alaska Range (their Fig. 8). This orientation is problematic since there seems to be almost universal agreement (Hamilton, 1969b; Dickenson, 1970; Monger et al., 1972) that the

Cordillera of western North America evolved over a series of eastward-dipping subduction zones through much of the Paleozoic, Mesozoic and Tertiary. Volcanic arcs and subduction zones imply the destruction of oceanic crust and so, for southwestward- and northeastward-dipping subduction zones to have co-existed in eastern Alaska and southwestern Yukon, crust must have been generated at an oceanic ridge situated between them. However, there is no evidence for the existence of such a ridge intervening between Permian and younger rocks in the Taku-Skolai terrane and coeval rocks in the western Cordillera.

7.2.3 Interrelationships of Alexander and Taku-Skolai Terranes

Two collisional or "suturing" events must be explained by any tectonic model for this region. One is the juxtaposition by fault contact of the Alexander and Taku-Skolai terranes, and the other is the suturing of Taku-Skolai terrane to the then-western margin of the North American plate. Southwestern Yukon is perhaps the best region for interpretation of these events since all the important tectonic elements are represented there. In contrast Alexander terrane does not occur in the Eastern Alaska Range and in southeastern Alaska, the distribution and character of the Taku-Skolai terrane are poorly-known, and intense deformation and metamorphism in these rocks hamper interpretation (Berg et al., 1972).

It is proposed that the Alexander terrane became sutured with the Taku-Skolai terrane towards the end of the Lower Permian,

when the Permian (Cache Creek) volcanic arc system was in its final stages of development, and that the Alexander terrane was "rafted in" on the same lithospheric plate that was descending northeastwards beneath the arc (see Fig. 7.1).

A second important, and related, proposition is that, throughout much of the St. Elias Mountains, the Alexander terrane and Taku-Skolai terrane are juxtaposed by superposition of the former on the latter, rather than by abutment along even a shallow-dipping thrust fault. This necessitates an important revision in degree, if not in kind, in the interpretation of the nature of the Duke River Fault, considered by Muller (1967) to be a southwestward-dipping thrust fault. The Alexander terrane may be a thrust nappe representing extreme horizontal compression, perhaps as much as 50 miles, which accounts for the restricted distribution in the St. Elias Mountains of Taku-Skolai terrane (this terrane is less than 10 miles wide in the Kaskawulsh map-area) compared to the Eastern Alaska Range, where it attains 100 miles in width. This, in turn, implies that the Duke River Fault may be a zone of intense imbrication and that it should be more appropriately regarded as a horizontal boundary between tectonic elements, rather than a vertical or near-vertical boundary.

If these two propositions concerning the timing and nature of the juxtaposition of the Alexander and Taku-Skolai terranes are valid, there follow a number of attractive consequences.

Firstly, it permits the correlation of Permian and Jurassic

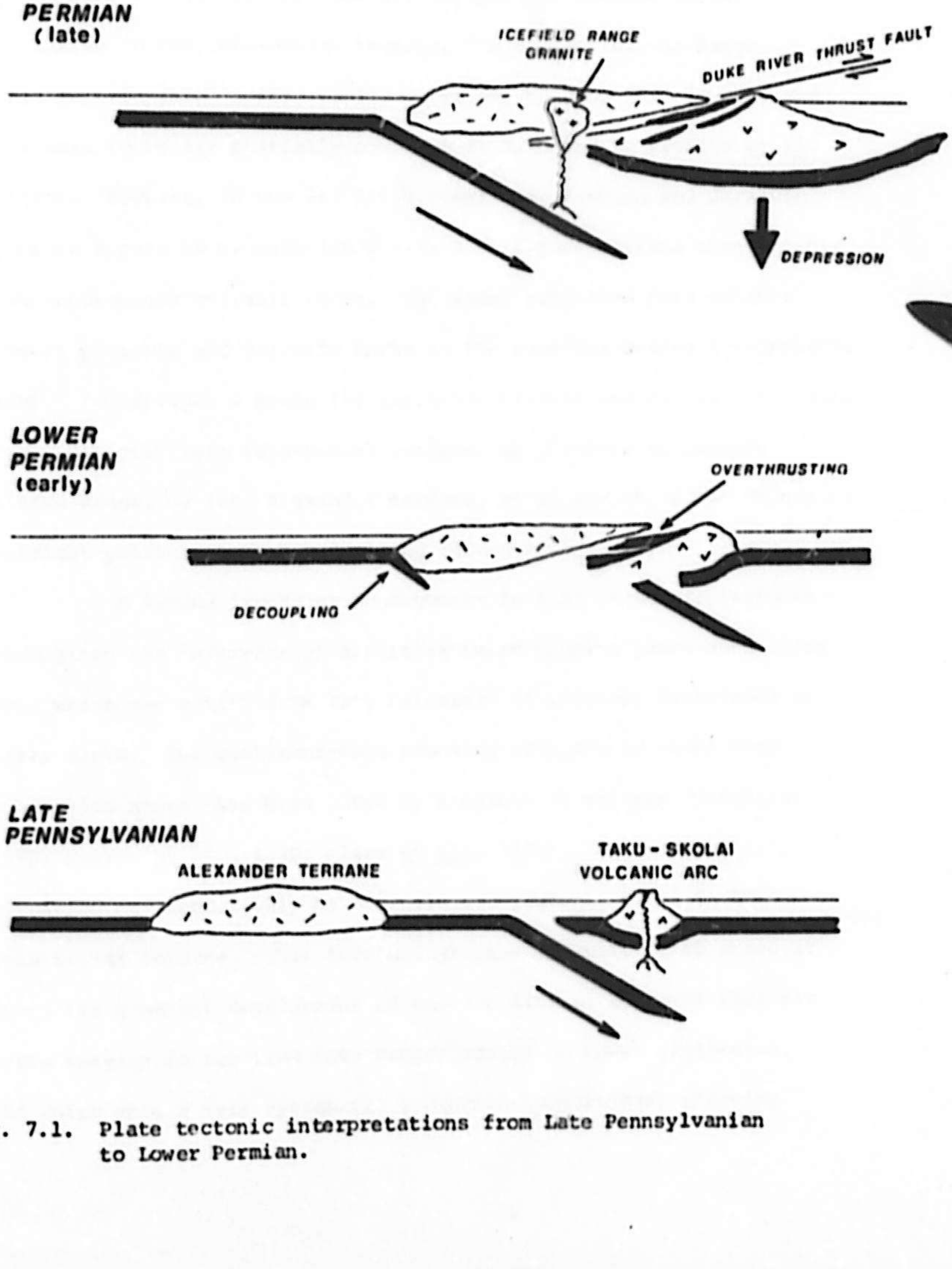


Fig. 7.1. Plate tectonic interpretations from Late Pennsylvanian to Lower Permian.

plutonic activity in the Icefield Ranges Alexander terrane (described in Chapter 4) with broadly-coeval, and perhaps consanguinous, volcanism in the Taku-Skolai terrane. In Eastern Alaska Range, this relationship is more easily observed, because the plutonic and volcanic rocks are spatially-associated, as noted by Richter et al. (1975). However, in the St. Elias Mountains, Permian and Jurassic plutons appear to be associated with a different terrane than broadly contemporaneous volcanic rocks. The model suggested here relates coeval plutonic and volcanic rocks to the same descending lithospheric slab. It provides a means for emplacing Permian and Jurassic plutonic rocks directly into Taku-Skolai terrane, as observed in Eastern Alaska Range, or into Alexander terrane, as in the St. Elias Mountains, by first passing through underlying Taku-Skolai rocks.

A second important consequence is that these propositions strengthen the inference of a northeastward-dipping paleo-subduction zone which was active from late Paleozoic to possibly Cretaceous or later times. The continent-ward younging of plutonic rocks over subduction zones, has been noted by a number of writers (Hutchison, 1970; Farrar et al., 1970; Clark et al., 1976). An analogous situation may tentatively be advanced for plutonic rocks in the Taku-Skolai terrane. This terrane, perhaps 100 miles wide where it shows its greatest development in eastern Alaska, contains plutonic rocks ranging in age from Late Pennsylvanian to Lower Cretaceous, and which show a very systematic southwest-to-northeast younging.

The "age gradient", in Eastern Alaska Range at least, is remarkably similar to that observed in the Central Coast Mountains of B.C., and, most strikingly, in the Central Andes. In the St. Elias Mountains, the "age gradient" for Permian to Cretaceous plutonic rocks is somewhat steeper, occurring over a distance of about 50 miles, and may be related, in part, to further post-plutonic horizontal compression (see below).

Two ancillary observations may be made, which arise from this sequence of postulated events, and which may explain differences in the interpretations of the environments of formation of Permo-Triassic volcanic rocks by Muller (1967) and Richter and Jones (1973). One is that the ultramafic or oceanic-crustal rocks observed in the St. Elias Mountains, but not the Eastern Alaska Range, may be imbricate slices directly attributable to Permian collision of Alexander and Taku-Skolai terrane. This explains their absence farther to the northwest in contiguous Alaska. The second observation concerns the nature of Triassic volcanism which, in the St. Elias Moutains, Muller (1967) described as submarine and, in Eastern Alaska Range, Richter and Jones (1973) described as sub-aerial. In the present study area, the superposition of Alexander terrane on Permian arc rocks could have depressed the crust behind the arc providing a submarine environment for the deposition of later Triassic volcanic arc rocks. In eastern Alaska, however, the addition of a second volcanic pile to a previously-formed arc may have built a positive

area, so that much of the Triassic volcanic rocks were deposited subaerially. However, the writer does not agree with Richter and Jones' (1973) account of this event, as stated previously.

7.2.4 Post-Triassic Events at the Continental Margin

Interpretations of the tectonic history subsequent to the development of Taku-Skolai terrane seem to follow on well from the postulations and events described to this point. Plutonic activity occurred through most of the Jurassic in the southwestern part of the Taku-Skolai terrane, although volcanic activity had apparently waned. The Permo-Triassic magmatic arc system was probably uplifted, perhaps in the Middle Jurassic, when it began to shed detrital material into the marine basin along the northeast flank of the arc. Eisbacher (1976) suggests that these clastic sediments, which constitute the Dezadeash Group, were deposited on a broad sub-sea fan system, and spread eastward over a relatively deep submarine plain (see Fig. 7.2).

From at least Lower Jurassic times, the Taku-Skolai terrane must have been "connected" to the North American craton by a lithospheric plate which was being consumed at the continental margin along a northeastward-dipping subduction zone, as shown by Monger et al. (1972, see Fig. 3.3); this was probably sub-parallel to the subduction zone which was presumably still active under the Taku-Skolai terrane.

The marine basin between the encroaching Taku-Skolai

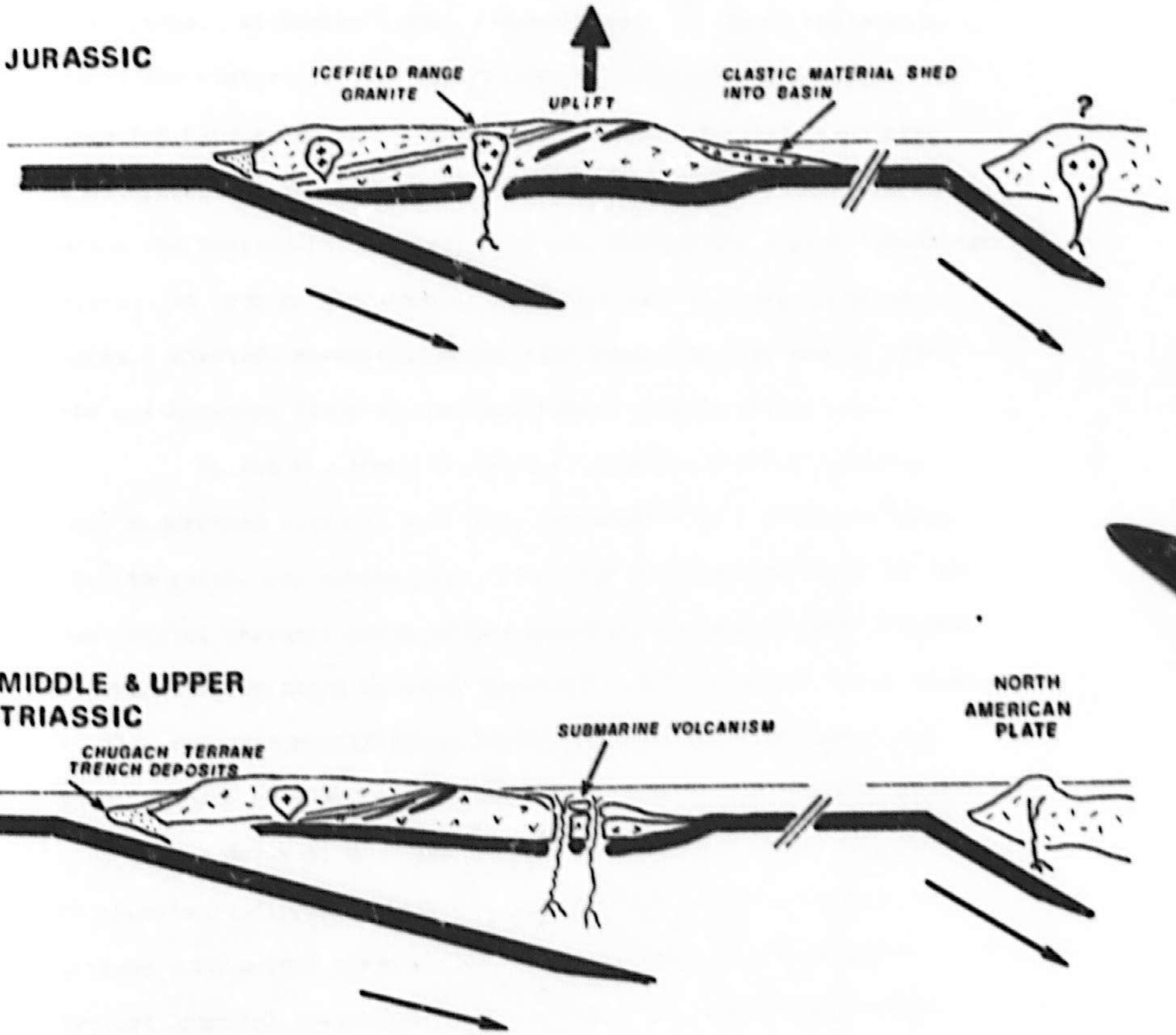


Fig. 7.2. Plate tectonic interpretations from Middle Triassic to Jurassic.

terrane and the continent must have begun to close by the Upper Cretaceous. Eisbacher (1976) suggests that, in latest Cretaceous time, the eastern part of the Dezadeash Group was metamorphosed to form the Kluane Schist. Perhaps the metamorphism (to greenschist and amphibolite facies) was brought about by burial at the trench along the continental margin. However, blueschist mineral assemblages, typical of such an environment, are not known to occur in these rocks. Instead, metamorphism may have taken place by burial along the northeastern flank of the Taku-Skolai terrane (Fig. 7.3).

During the lower Cretaceous, from about 120 to 110 m.y. ago, widespread plutonic activity, represented by the Kluane Range Diorite suite, was taking place along the northeastern flank of the Taku-Skolai terrane; rocks of the Dezadeash Group were also invaded. Synchronous intrusion by ultramafic rocks into Dezadeash Group rocks is also reported by Eisbacher (1976), but coeval volcanism is not known to have occurred with either the dioritic or ultramafic suites.

A derivation of the Kluane Range Diorite suite from the northeastward-dipping subduction zone beneath the Taku-Skolai terrane (see above) seems possible, but may be too simplistic. Typical chemical variations observed elsewhere would suggest that these rocks should be more potassic than the older Icefield Range granites closer to the consuming plate margin, southwest of the Taku-Skolai terrane. Instead, these rocks are low in potash, and display tholeiitic rather than calc-alkaline affinities. Moreover, the

spatial association with contemporaneous ultramafic rocks suggests the possible involvement of oceanic crustal rocks in their evolution.

It is very tentatively suggested here that the nature of this Cretaceous plutonism may reflect interaction between the descending lithospheric slabs beneath the Taku-Skolai terrane, which had long been active, and the slab subducted beneath the continental margin, by now not far distant. However, exactly how these slabs could have interacted to produce the Cretaceous plutonism in Taku-Skolai terrane and Dezadeash Group rocks is not clear. A schematic representation of how this may have come about is shown in Fig. 3. Indirect evidence that the two plates were beginning to merge may be reflected in uplift of the terrane to the southwest of the marginal ocean basin as indicated by the subsequent deposition of continental sediments of the Paleocene Amphitheatre Formation.

It was argued in Chapter 4 that the Ruby Range Batholith was emplaced at the beginning of the Paleocene, about 65 m.y. ago, but that some undefined "tectonic event" at the beginning of the Eocene, about 55 m.y. ago, caused rapid uplift of the batholith, moving it through the argor retention isotherm, and that the same event also led to the intrusion of the Nisling Range Alaskite and the eruption of the Mt. Nansen volcanics.

That argument will be further developed here by suggesting that: 1. the Ruby Range Batholith was generated through plate subduction in the final stages of the closure of the ocean basin

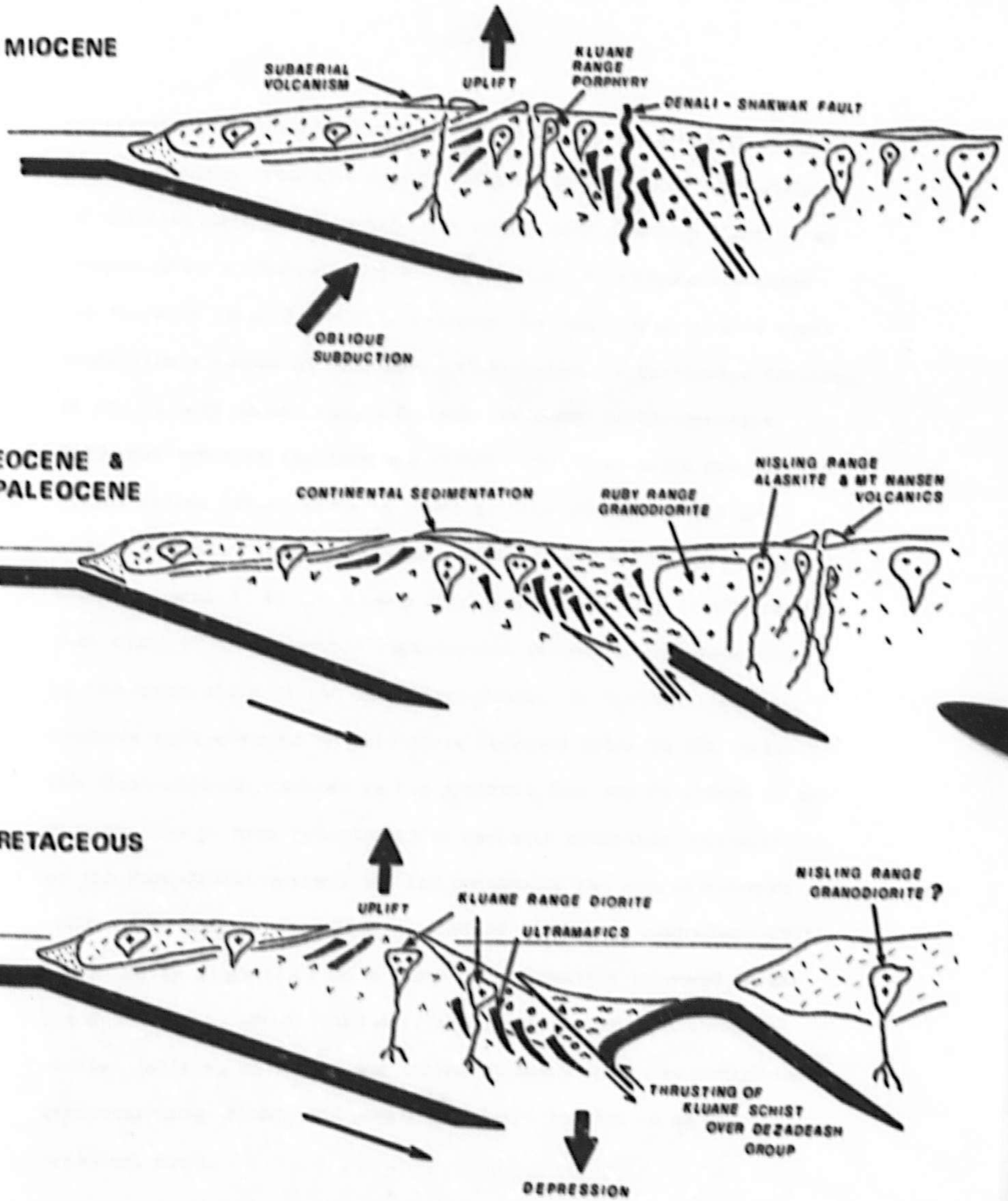


Fig. 7.3. Plate tectonic interpretations from Cretaceous to Miocene.

separating the North American continent and the Taku-Skolai terrane; and 2. that the "tectonic event" referred to above was the collision of the Alexander and Taku-Skolai terranes and Dezadeash Group rocks against the continental margin. In addition to radiometric dates for the Ruby Range Batholith, evidence for the timing of this event comes from a number of deformational features, in particular faulting. In the Eastern Alaska Range, Richter and Jones (1973) describe different types of faulting and state: "The high-angle reverse and normal faults offset rocks as young as Late Cretaceous and are probably related largely to a late Mesozoic and early Cenozoic tectonic event." In the Kluane Lake map-area, Muller (1967) notes that rocks of the Paleocene Amphitheatre Formation are overridden by the upper plate of the Duke River Fault. He further cites evidence that movement on this fault occurred twice in the Tertiary: the first episode occurred in the interval from the Paleocene to the Miocene, and is here interpreted as probably recording collision of the Taku-Skolai terrane and the continent; the second movement occurred in post-Miocene time. In broad agreement, Eisbacher (1976) has recently suggested that a stage of deformation occurred in the Dezadeash Group, about 70-60 m.y. ago, represented by high-angle reverse faulting of the Kluane Schist westward onto unmetamorphosed Dezadeash Group rocks, and possibly related to closure of the Dezadeash Basin.

The origin of the Cretaceous Nisling Range Granodiorite

suite is uncertain. Tempelman-Kluit (1976) does not describe this suite in his description of the evolution of the Yukon Crystalline Terrane, and yet its evolution may be related to events that took place there. Its very limited distribution in the Nisling Range in southwestern Yukon would tend to argue against its derivation from the same descending lithospheric slab which generated such widespread calc-alkaline magmatism in the Ruby Range Batholith. The polarity in ages would also be anomalous in that case. Furthermore, Le Couteur and Tempelman-Kluit (1976) report initial Sr^{87}/Sr^{86} ratios which suggest that the Nisling Range Granodiorite was intruded through Precambrian continental crust and that the Ruby Range Granodiorite was not.

In the Miocene, extensive subaerial volcanism represented by the Wrangell Lavas (St. Clare Group) covered much of the St. Elias Mountains and contiguous eastern Alaska. Perhaps these rocks represent the youngest material in this region to be derived from an underthrusting lithospheric plate. Shortly after the extrusion of these rocks, Richter and Jones (1976) suggest that a change in direction and rate of Pacific plate motion caused underthrusting to cease, but initiated transform faulting along the suture between the collapsed Taku-Skolai terrane and the paleo-continental margin, along the present trace of the Denali-Shakwak Fault (Fig. 7.3).

Reconstructions of movement along the Denali-Shakwak Fault by Forbes et al. (1973), Turner et al. (1974), and Eisbacher

(1976), based on the restoration of similar truncated rock units on opposite sides of the fault, indicate a dextral displacement of about 200 to 250 miles.

Richter and Jones (1973) consider that compressional stresses caused by the motion of the Pacific plate have been accommodated by uplift, which may explain the height of the St. Elias Mountains and the rapid erosion of the Wrangell Lavas noted by Souther and Stanciu (1975), and also by movement along the Denali-Shakwak Fault from the Miocene to perhaps the Pleistocene. In the Pleistocene, the development of the Totschunda Fault deactivated that portion of the Denali-Shakwak Fault lying southeast of their juncture, including the portion in southwestern Yukon.

7.3 Summary

The tectonic reconstruction model proposed here is consistent, in its major aspects, with known geological relationships in southwestern Yukon and contiguous parts of Alaska. Although other models cannot be precluded, the present reconstruction may represent an improvement over previously-proposed models.

The work of Berg et al. (1972), which was so important in identifying tectonic terranes in this region, is the only general model applicable to this part of the western North American continent and it appears to have a number of weaknesses which the authors admit.

These writers suggest that the difficulty in fitting their tectonic terranes, in particular, the Gravina-Nutzotin belt, into a typical trench/arc-trench gap/magmatic arc assemblage is due mainly to the presence of the Alexander terrane adjacent to the Gravina-Nutzotin belt for much of its length. About their model they state: "Our view that the Gravina-Nutzotin belt represents an ancient volcano-plutonic arc genetically linked with subduction in the Chugach trench faces some difficulty due mainly to differences between the belt and other modern and ancient volcanic arcs. The deep-marine deposition of most of the Gravina-Nutzotin sedimentary rocks and their great thickness imply rapid depression of a long, linear belt [and] hence, much of the belt was primarily a negative feature, not positive as expected in a volcanic arc..... In our view also, the differences between present models of magmatic arcs and the Gravina-Nutzotin belt...may be due to the presence there of the Alexander terrane...." (p. D20-D21).

The writer suggests that, according to the model presented here, that the Alexander terrane has had little influence on post-Permian tectonic events in the region northeast of it, and has not measurably affected the lithology, structure and distribution of the Gravina-Nutzotin belt (Dezadeash Group in southwestern Yukon). Rather, the difficulty with the model of Berg et al. (1972) is the failure to recognize the second northeastward-dipping subduction zone, northeast of the Taku-Skolai terrane at the continental margin,

which was so important in determining post-Jurassic tectonic events including the provision of a deep-marine environment for Gravina-Nutzotin rocks prior to collision of the Alexander and Taku-Skolai terranes with the North American plate.

BIBLIOGRAPHY

Ahrens, L. H. and Taylor, S. R., 1961. Spectrochemical Analysis (2nd ed.), Addison-Wesley.

Bateman, P. C. and Dodge, F. C. W., 1970. Variations of major chemical constituents across the Central Sierra Nevada Batholith. G.S.A. Bull., v. 81, no. 2, p. 409-420.

Berg, H. C., Jones, D. L., and Richter, D. H., 1972. Gravina Nutzotin belt - tectonic significance of an Upper Mesozoic sedimentary and volcanic sequence in southern and southeastern Alaska, U.S.G.S. Prof. Paper 800D, p. D1-D24.

Bostock, H. S., 1936. Carmacks district, Yukon. Geol. Surv. Can., Mem. 189.

_____ 1948. Physiography of the Canadian Cordillera, with special reference to the area north of the fifty-fifth parallel. Geol. Surv. Can., Mem. 247.

_____ 1952. Geology of the northwest Shakwak Valley, Yukon Territory. Geol. Surv. Can., Memoir 267.

Cairnes, D. D., 1914. Geology of a portion of the Yukon-Alaska boundary between Porcupine and Yukon Rivers. Geol. Surv. Can., Sum. Rept. 1912, p. 9-11.

_____ 1915a. Exploration in southwestern Yukon. Geol. Surv. Can., Sum. Rept. 1914, p. 10-33.

_____ 1915b. Upper White River district, Yukon. Geol. Surv. Can., Mem. 50, p. 12-28.

Campbell, R. B. and Dodds, C. J., 1975. Operation Saint Elias. Geol. Surv. Can., Paper 75-1, Part A, p. 51-52.

Carson, D. J. T., 1973. The plutonic rocks of Vancouver Island. Geol. Surv. Can. Paper 72-44.

Chayes, F., 1956. Petrographic modal analysis - an elementary statistical appraisal; John Wiley and Sons, Inc.

Christopher, P. C., White, W. H. and Harakal, J. E., 1972. K/Ar dating of the 'Cork' (Burwash Creek) Cu-Mo prospect, Burwash Landing area, Yukon Territory; Can. Jour. Earth Sci., v. 9, p. 918-921.

Churkin, M. and Eberlein, G. C., 1977. Ancient borderland terranes of the North American Cordillera: correlation and microplate tectonics. G.S.A. Bull., v. 88, p. 769-786.

Clark, A. L., Clark, S. H. B. and Hawley, C. C., 1972. Significance of upper Paleozoic oceanic crust in the Upper Chulitna District, west-central Alaska Range; U.S.G.S. Prof. Paper 800-C, p. C95-C101.

Clark, A. H., Farrar, E., Caelles, J. C., Haynes, S. J., Lortie, R. B., McBride, S. L., Quirt, G. S., Robertson, R. C. R. and Zentilli, M., 1976. Longitudinal variations in the metallogenetic evolution of the Central Andes: a progress report. Geol. Assoc. Canada, Spec. Paper no. 14, p. 23-58.

Clark, K. F., 1972. Stockwork molybdenum deposits in the western cordillera of North America. Econ. Geol., v. 67, no. 6, p. 731-758.

Cockfield, W. E., 1928. Dezadeash Lake Area, Yukon, Geol. Surv. Can., Sum. Rept. 1927, pt. A, p. 1-7.

_____ 1927. Aishihik Lake District, Yukon. Geol. Surv. Can. Sum. Rept. 1926, pt. A, p. 1-13.

Culbert, R. R., 1972. Abnormalities in the distribution of K, Rb, and Sr in the Coast Mountains batholith, British Columbia. Geochimica et Cosmochimica Acta, v. 36, no. 10, p. 1091-1100.

Dalrymple, G. B. and Lanphere, M. A., 1969. Potassium-Argon Dating (Principles, Techniques and Applications to Geochronology); W. H. Freeman and Company.

Dickinson, W. R., 1970. Relations of andesites, granites and derivative sandstones to arc-trench tectonics. Reviews of Geophsics and Space Physics, v. 8, no. 4, p. 813-860.

Eisbacher, G. H., 1976. Sedimentology of the Dezadeash flysch and its implications for strike-slip faulting along the Denali Fault, Yukon Territory and Alaska; Can. Jour. Earth Sci., v. 13, no. 11, p. 1495-1513.

Farrar, E., Clark, A. H., Haynes, S. J., Quirt, G. S., Conn, H. and Zentilli, M., 1970. K/Ar evidence for the post-Paleozoic migration of granitic intrusion foci in the Andes of northern Chile. Earth Plan. Sci. Lett., v. 9, p. 17-28.

Fernald, A. T., 1962. Radiocarbon dates relating to a widespread volcanic ash deposit, eastern Alaska; U.S.G.S. Prof. Paper 450-B, p. 29-30.

Forbes, R. B., Turner, D. L., Stout, J. and Smith, T. E., 1973. Cenozoic offset along the Denali Fault, Alaska. (abs.) Eos, v. 54, p. 495.

Hamilton, W., 1969a. The volcanic central Andes, a modern model for the Cretaceous batholiths and tectonics of western North America. Oreg. Dept. Geol. Miner. Ind. Bull. 65, p. 175-184.

_____ 1969b. Mesozoic California and the underflow of Pacific mantle. Geol. Soc. Amer. Bull., v. 80, p. 2409-2430.

Hassard, F. R. and Trigg, C. M., 1971. A Report on Diamond Drilling Geological and Geochemical Surveys, Max Claim Group, Rhyolite Creek Area (61°N, 138°W). Trigg-Woollett and Associates Ltd.

Heier, K. S. and Adams, J. A. S., 1964. The geochemistry of the alkali metals; Phys. Chem. Earth, v. 5, p. 253-382.

Hutchison, W. W., 1970. Metamorphic framework and the plutonic styles in the Prince Rupert region of the central) Coast Mountains, British Columbia. Can. Jour. Earth Sci., v. 7, no. 2, p. 376.

Irvine, T. N. and Baragar, W. R. A., 1971. A guide to the chemical classification of the common volcanic rocks, Can. Jour. Earth Sci., v. 8, no. 5, p. 523-548.

Jakes, P. and White, A. J. R., 1970. K/Rb ratios of rocks from island arcs. Geochimica et Cosmochimica Acta, v. 34, no. 8, p. 849-856.

_____ 1972. Major and trace element abundances in volcanic rocks of orogenic areas. Geol. Soc. Am. Bull., v. 83. no. 1, p. 24-40.

Jones, D. L., Irwin, W. P. and Ovenshine, A. T., 1972. Southeastern Alaska - A displaced continental fragment? U.S.G.S. Prof. Paper 800B, p. B211-B217.

Kindle, E. D., 1952. Dezadeash map-area, Yukon Territory; Geol. Surv. Can. Mem. 268.

Lanphere, M. A. and Eberlein, G. D., 1966. K/Ar ages of magnetite-bearing ultramafic complexes in southeastern Alaska; Geol. Soc. Am. Spec. Paper 87, p. 94.

Lanphere, M. A., Loney, R. A. and Brew, D. A., 1965. Potassium-argon ages of some plutonic rocks, Tenakee area, Chichagof Island, southeastern Alaska, in Geological Survey Research 1965: U.S.G.S. Prof. Paper 525-B, p. B108-B111.

Lanphere, M. A., MacKevett, E. M. and Stern, T. W., 1964. Potassium-argon and lead-alpha ages of plutonic rocks, Bokan Mountain area, Alaska; Science, v. 145, no. 3633, p. 705-707.

Lanphere, M. A. and Reed, B. L., 1973. Timing of Mesozoic and Cenozoic plutonic events in circum-Pacific North America. Geol. Soc. Am. Bull., v. 84, p. 3773-3782.

Lathram, E. H., 1964. Apparent right-lateral separation on Chatham Strait Fault, southeastern Alaska; Geol. Soc. Am. Bull., v. 75, no. 3, p. 249-252.

LeCouteur, P. C. and Tempelman-Kluit, D. J., 1976. Rb/Sr ages and profile of initial Sr^{87}/Sr^{86} ratios for plutonic rocks across the Yukon Crystalline Terrane; Can. Jour. Earth Sci., v. 13, p. 319-330.

Loney, R. A., Brew, D. A. and Lanphere, M. A., 1967. Post-Paleozoic ratiometric ages and their relevance to fault movements, northern southeastern Alaska; Geol. Soc. Am. Bull., v. 78, no. 4, p. 54-526.

Lowden, J. A., 1960. Age determinations by the Geological Survey of Canada (Report 1 Isotopic Ages); Geol. Surv. Can., Paper 60-17.

_____ 1961. Age determinations by the Geological Survey of Canada (Report 2 Isotopic Ages); Geol. Surv. Can., Paper 61-17.

Lowden, J. A., Stockwell, C. H., Tipper, H. W. and Wanless, R. K., 1963. Age determinations and geological studies. Geol. Surv. Can. Paper 62-17.

MacKevett, E. M., 1971. Stratigraphy and general geology of the McCarthy C-5 Quadrangle, Alaska; U.S.G.S. Bull. 1323.

Monger, J. W. H. and Ross, C. A., 1971. Distribution of fusulinaceans in the western Canadian Cordillera. Can. Jour. Earth Sci., v. 8, no. 2, p. 259-278.

Monger, J. W. H., Souther, J. G. and Gabrielse, H., 1972. Evolution of the Canadian Cordillera: a plate tectonic model, Am. Jour. Sci., v. 272, p. 577-602.

Moore, J. G., Grantz, A. and Blake, M. C., 1962. The quartz diorite line in northwestern North America. U.S.G.S. Prof. Paper 450-E, p. 89-93.

Muller, J. E., 1967. Kluane Lake map area, Yukon Territory, Geol. Surv. Can. Mem. 340.

McConnell, R. G., 1905. The Kluane mining district, southwest Yukon. Geol. Surv. Can., Ann. Rept. 1904, v. 16, p. 1A-18A.

Nockolds, S. R., 1954. Average chemical compositions of some igneous rocks; Geol. Soc. Am. Bull., v. 65, p. 1007-1032.

Ovenshine, A. T. and Brew, D. A., 1972. Separation and history of the Chatham Strait Fault, southeastern Alaska, North America (abs.), Internat. Geol. Cong., 24th, Montreal, Canada, Proc.

Peto, P. 1974. Plutonic evolution of the Canadian Cordillera. Geol. Soc. Am. Bull., v. 85, p. 1269-1276.

Plafker, G., 1972. New data on Cenozoic displacements along the Fairweather fault system, Alaska. in Faults, fractures, lineaments, and related mineralization in the Canadian Cordillera. Geol. Assoc. Canada, Cordilleran Section, Program and abstracts, p. 30.

Quirt, G. S., 1972. A potassium-argon geochronological investigation of the Andean mobile belt of north-central Chile. Ph.D. thesis, Queen's University.

Read, P. B., 1976. Operation Saint Elias, Yukon Territory: Pre-Cenozoic volcanic assemblages in the Kluane Ranges. Geol. Surv. Can., Paper 76-1A.

Richter, D. H. and Jones, D. L., 1973. Structure and stratigraphy of Eastern Alaska Range, Alaska, in Arctic Geology, Am. Assoc. Petrol. Geol., Mem. 19, p. 408-420.

Richter, D. H., Lanphere, M. A. and Matson, N. A., 1975. Granitic plutonism and metamorphism, Eastern Alaska Range, Alaska. Geol. Soc. Am. Bull., v. 86, p. 819-829.

Roddick, J. C., 1970. The geochronology of the Tulameen and Hedley complexes, B.C., unpubl. M.Sc. thesis, Queen's University.

Roddick, J. A. and Hutchison, W. W., 1974. Setting of the Coast Plutonic Complex, British Columbia. Pacific Geology, v. 8, p. 91-108.

Sharp, R. P., 1943. Geology of the Wolf Creek area, St. Elias Range, Yukon Territory, Canada. Bull. Geol. Soc. Am. v. 54, p. 625-649.

Shaw, D. M., 1968. A review of K-Rb fractionation trends by covariance analysis. Geochimica et Cosmochimica Acta, v. 32, no. 6, p. 573-601.

Smith, J. G. and MacKevett, E. M., 1970. The Skolai Group in the McCarthy B-4, C-4 and C-5 Quadrangles, Wrangell Mountains, Alaska. U.S.G.S. Bull. 1274-Q.

Souther, J. G. and Stanciu, C., 1975. Operation Saint Elias, Yukon Territory: Tertiary Volcanic Rocks. Geol. Surv. Can., Paper 75-1, Part A, p. 63-70.

Tauson, L. V. and Kozlov, V. D., 1972. Distribution functions and ratios of trace-element concentrations as estimators of the ore-bearing potential of granites; in Geochemical Exploration 1972; Proceedings of the Fourth International Geochemical Exploration Symposium, London, 1972. Ed. E. M. Jones, p. 37-44.

Tempelman-Kluit, D. J., 1974. Reconnaissance geology of Ashihik Lake, Snag and part of Stewart River map areas, west-central Yukon; Geol. Surv. Can. Paper 73-41.

Tempelman-Kluit, D. J., 1976. The Yukon Crystalline Terrane: Enigma in the Canadian Cordillera. Geol. Soc. Am. Bull., v. 87, p. 1343-1357.

_____ and Wanless, R. K., 1975. Potassium-argon age determinations of metamorphic and plutonic rocks in the Yukon Crystalline Terrane. Can. Jour. Earth Sci., v. 12, p. 1895-1909.

Turner, D., Smith, T. E. and Forbes, R. B., 1974. Geochronology of offset along the Denali Fault system in Alaska. (abs.) Geol. Soc. Am. Cordillera Sec. Meet. Abstr., p. 268.

Van Eysinga, F. W. B., 1975. Geologic time table. Elsevier Scientific Publishing Co., 3rd Edition, Amsterdan.

Wheeler, J. O., 1963. Kaskawulsh map-area, Yukon Territory. Geol. Surv. Can., Map 1134A.

APPENDIX A

ANALYTICAL METHODS

A-1 X-ray fluorescence ---------- p. 179

A-2 Measurement of volatiles ---------- p. 180

A-3 Emission spectrograph ---------- p. 182

A-4 Modal analyses ---------- p. 184

ANALYTICAL METHODS

A-1 X-ray Fluorescence

Preparation of sample by fusion technique.

1) On glazed paper weigh: a) 1.600 g lithium tetraborate

b) 0.4000 g sample

c) 0.300 g lanthanum oxide

2) Place weighed powder in a numbered graphite crucible and carefully mix powders with a small spatula for one minute.

3) Place crucible in a metal tray and put in a preheated (1,000°C) furnace for 10 minutes.

4) After sample has cooled remove bead from crucible and place on glazed paper. Add sufficient Avicel so that the weight of the bead plus Avicel equals 2.600 g.

5) Place the bead and Avicel mixture in a tungsten carbide vial. Cap the vial and put in a Pitchford Industries Inc. mixer. Grind and homogenize the sample by shaking the vial for five minutes on the mixer.

6) Put fine crystalline boric acid into a pre-numbered aluminum cap (Spex Industries catalogue number 3619), so that the cap is approximately one-third full and has a flat surface.

7) Pour the ground sample into the boric acid backing, and smooth out the sample to obtain a relatively flat surface. Ensure that the boric acid backing does not show through the sample material.

8) Pelletize the sample by placing it in a tungsten carbide die for 30 seconds at a pressure of 4,800 p.s.i. The top cap of the die and plunger must be cleaned with acetone after each sample is pelletized.

9) Standards for calibration purposes are prepared in the same manner.

Equipment and calibration

The fused sample pellets were analyzed for SiO_2, Al_2O_3, MgO, Na_2O, K_2O, and P_2O_5 using a Seimens Model VRS Vacuum X-ray Spectrograph and Fe_2O_3 (as total Fe), MnO, CaO, and TiO_2 using a Philips Model 52530 Vacuum X-ray Spectrograph. Precision was monitored by the analysis of duplicate samples. Accuracy was controlled by calibration with U.S.G.S. rock standards BCR, PCC, AGV, GSP and G-2.

A-2 Measurement of Volatiles

Fourteen specimens were selected for the determination of volatile content. The results are shown in the table below (figures in weight percent).

8) Pelletize the sample by placing it in a tungsten carbide die for 30 seconds at a pressure of 4,800 p.s.i. The top cap of the die and plunger must be cleaned with acetone after each sample is pelletized.

9) Standards for calibration purposes are prepared in the same manner.

Equipment and calibration

The fused sample pellets were analyzed for SiO_2, Al_2O_3, MgO, Na_2O, K_2O, and P_2O_5 using a Seimens Model VRS Vacuum X-ray Spectrograph and Fe_2O_3 (as total Fe), MnO, CaO, and TiO_2 using a Philips Model 52530 Vacuum X-ray Spectrograph. Precision was monitored by the analysis of duplicate samples. Accuracy was controlled by calibration with U.S.G.S. rock standards BCR, PCC, AGV, GSP and G-2.

A-2 Measurement of Volatiles

Fourteen specimens were selected for the determination of volatile content. The results are shown in the table below (figures in weight percent).

Sample No.	H_2O	CO_2	$H_2O + CO_2$	Loss on Ignition
18	1.1	0.05	1.15	1.4
25	2.6	2.2	4.8	5.1
27	2.4	2.8	5.2	4.7
39	0.3	<0.1	<0.4	0.8
46	1.1	<0.1	<1.2	2.2
46 (duplicate)	1.0	0.15	1.1	0.7
77	0.5	<0.1	<0.6	0.6
90	0.8	<0.1	<0.9	1.0
116	3.1	<0.1	<3.2	4.1
120	1.0	<0.1	<1.1	0.8
127	0.7	<0.1	<0.8	0.6
134	0.1	<0.1	<0.2	0.7
153	1.3	2.0	3.3	3.3
168	1.6	<0.1	<1.7	1.8

H_2O is determined by heating 1 gm of the sample (pre-dried at 110°C for 4 hours) in a Pyrex test tube with sodium tungstate as a flux. The water is condensed onto a piece of pre-weighed filter paper in the upper part of the test tube, which is cooled by an ice- or water-jacket. After heating the tube at full heat with a burner for 5 minutes, the filter paper is removed and quickly transferred to a sealed weighing tube of known weight. The tube and filter paper are weighed and the absorbed H_2O is calculated by subtraction.

CO_2 is determined volumetrically by measuring the amount of gas evolved from a sample, upon treatment with acid, in a 150 mm test tube to which is attached, at an acute angle, a calibrated side arm to trap evolved CO_2. Sample powder, solid mercuric chloride, mercuric chloride solution, paraffin oil, and HCl are added to the carbon dioxide tube and the sample is decomposed by heating the lower part of the tube, for 5 minutes, in a heating bath which is maintained at 115° to 120°C. The percent CO_2 in the sample is calculated by multiplying the gas-column length in the side-arm by a factor derived by decomposing a standard of known CO_2 content by the same method.

Loss on ignition is determined by placing a 1 gm sample (pre-dried at 110°C for 4 hours) in a porcelain crucible of known weight and heating at 1,000°C in a furnace for 1 hour. The sample and crucible are then placed into a dessicator to cool for 30 minutes and then reweighed, the volatile content being determined by subtraction.

A-3 Emission Spectrograph

Preparation of sample and Standards

Weigh with a torsion balance 50 mg (±.5 mg) of silicate rock sample in a plastic vial, weigh also 50 mg (±.5 mg) of graphite internal standard mixture, close the vial and mix for 1 minute with the "wig-l-bug" mixture without ball, then insert ball and shake for 1 minute.

Weigh from this mixture obtained, 15 mg in an electrode S-14 using a small plastic funnel and tap the material to the bottom. Place the electrodes in a stand, add one drop of sugar solution in the cavity and place the electrodes on the hot plate using a hard asbestos stand and heat the electrodes slowly at 200°C for 5 minutes (warm up time included), then switch to high for 8 minutes, remove electrodes from hot plate; the sample is now completely sealed in the electrode cavity.

Summary of method

The ground samples (100 mesh) are mixed with graphite 50:50, (the graphite is salted to contain 0.0050 percent paladium). The mixture is weighed in a cup electrode, sealed, and excited with a D.C. constant current arc:

1. 24-second exposure in an Argon atmosphere.
2. exposure of remainder in an Argon-oxygen atmosphere 60/40, for total consumption.

The spectra are recorded on Eastman Kodak spectrographic plates S.A. No. 3, analytical and internal standard lines (paladium), are measured on a microdensitometer.

Transmittance measurements are converted into intensity ratios utilizing a calculation board. Concentration is obtained by referring intensity ratios of the unknowns to analytical curves prepared with standard rock samples or made up rock samples of known content. Precision is monitored by the analysis of duplicate samples.

Equipment

1) Excitation source Tomorrow Enterprises Model 3060 constant current D.C. arc power supply, with electronically regulated output 0-30 amps. with timers and arc programming mechanism.

2) Spectrograph: 3.4 M. Ebert, Jarrell Ash.
Grating: 590 Grooves/mm, Blaze angle 5.1°, 3000 A.
Reciprecal linear dispersion 5 A/mm.

3) Spex enclosed Stallwood jet, watercooled.

4) Microdensitometer-Baird Atomic R.C.II, with recorder attached.

A-4 Modal Analyses

Modal analyses were carried out on smooth rock slabs which were stained for feldspars by the commonly used technique of etching in HF, staining potassium feldspar in sodium cobaltinitrate solution, and staining plagioclase in alazarin red solution following rinse by barium chloride.

The slabs were mounted on a moving stage attached to a point counter and viewed through a reflected-light microscope.

Accuracy was controlled by using Chayes' (1956) replication schedules to maintain average major mineral analytical error less than 2.45. The replication schedules are a means of relating the grain size of a rock to the measurement area to ensure that fine- and coarse-grained rocks are compared on an equivalent basis. The

coarser the grain of a rock, the larger the measurement area which must be analyzed to ensure a representative modal composition.

VITA

Name:	Dana Clark Way
Place and Year of Birth:	Ottawa, 1947.
Education:	Ontario primary and secondary schools; completed Grade XIII in 1966.
	Queen's University, Faculty of Applied Science, 1967-1971; awarded B.Sc. (Eng.) with honours standing.
	Queen's University, School of Business, 1974-1976; awarded Master's degree in Business Administration (M.B.A.).
	Queen's University, Faculty of Graduate Studies and Research, 1971-1977; present program, M.Sc. in Geological Sciences.
Experience:	Geological assistant, Department of Indian and Northern Affairs, 1970 and 1971 field seasons.
	Teaching assistant, Queen's University, 1971-1974.
	Geologist and Party Chief, Canada Tungsten Mining Corporation Ltd., 1974 and 1975 field seasons.
	Commerce Officer, Resource Industries Branch, Department of Industry, Trade and Commerce, 1976 to present.
Awards:	Department of Indian and Northern Affairs research grant, 1972.
	Reinhardt Fellowship, 1972.
	D. I. McLeod Scholarship, 1974.

Professional Associations: Association of Professional Engineers of Ontario.

Publications: with A. H. Clark and E. Farrar; Age relationships of granitoid plutonism in southwestern Yukon Territory: a reconnaissance study; abstract presented at 4th meeting of the Circum-Pacific Plutonism Project, Vancouver, August, 1975.

Labour Relations and Manpower Constraints in the Canadian Steel Industry; in The Canadian Steel Industry in a Competitive World Environment; Costs and Performance, v. 2, Dr. D. F. Barnett ed.; Dept. Industry, Trade and Commerce, 1977.

The Cost Impact of Pollution Control in the Canadian Steel Industry; in The Canadian Steel Industry in a Competitive World Environment; Markets and Trade, v. 3, Dr. D. F. Barnett ed.; Dept. Industry, Trade and Commerce, 1977.

ADDENDUM*

Trace Element Analyses

copyright © Dana Clark Way, 1977

* To accompany: Way, D. C., 1977. A reconnaissance study of granitoid plutonism in southwestern Yukon Territory; M.Sc. Thesis, Queen's University.

Trace Element Analyses

(in parts per million)

Sample Number	Cu	Pb	Zn	Ni	Cr	Co	Sn	Ga	Zr	Sr	Ba	Rb
1	22	19	18	36	112	92	Tr	16	112	470	2400	133
2	2	28	36	ND	12	126	Tr	12	74	260	2000	207
3	22	20	54	6	30	107	9	18	84	680	3300	177
4	3	17	36	7	18	71	Tr	14	101	605	3200	57
5	NA	NA	NA	NA	NA	NA	NA	NA	NA	NA	NA	NA
6	13	26	81	8	24	126	6	19	112	590	2900	185
7	17	25	59	7	19	98	Tr	13	140	1300	6300	170
8	10	19	249	8	7	138	Tr	26	300	290	8000	166
9	ND	25	88	ND	1	172	ND	14	106	130	1500	140
11	NA	NA	NA	NA	NA	NA	NA	NA	NA	NA	NA	NA
12	NA	NA	NA	NA	NA	NA	NA	NA	NA	NA	NA	NA
13	3	26	52	6	8	270	10	18	92	420	3900	167
14	9	26	101	ND	11	27	ND	18	42	500	2900	155
18	4	28	72	5	7	126	7	21	66	420	1800	163
23	133	13	32	5	12	153	ND	14	101	630	2400	102
24	190	13	66	6	11	230	ND	15	70	590	2300	210
25	>200	15	65	ND	18	44	ND	22	80	320	8400	NA
26	>200	16	72	ND	15	75	ND	16	77	440	4200	NA
21	>200	15	68	ND	16	38	ND	15	63	350	4800	NA
28	2	30	135	ND	6	156	7	37	105	4	17	213
29	5	24	70	ND	ND	36	ND	21	158	104	620	251
30	7	23	165	ND	ND	39	6	16	129	88	1200	300
31	NA	NA	NA	NA	NA	NA	NA	NA	NA	NA	NA	NA
32	ND	26	123	ND	10	29	ND	19	99	710	2800	132
36	19	28	48	4	5	230	9	16	76	101	810	134
37	9	30	65	5	5	290	9	18	87	113	970	217
38	11	28	46	ND	5	204	Tr	16	64	105	590	210

Trace Element Analyses (cont'd.)

Sample Number	Cu	Pb	Zn	Ni	Cr	Co	Sn	Ga	Zr	Sr	Ba	Rb
39	13	16	215	ND	ND	45	Tr	25	134	250	5200	NA
40	35	26	165	ND	ND	51	Tr	21	73	190	800	NA
41	3	24	92	6	10	131	7	21	112	550	2100	60
42	ND	23	120	8	19	30	ND	18	59	670	2500	158
46	25	14	120	23	83	53	Tr	21	137	440	1300	75
48	12	17	95	ND	15	47	Tr	17	125	480	2200	156
50	4	24	77	5	14	112	6	20	136	320	3800	118
52	7	15	83	5	25	113	Tr	17	115	1100	3100	102
53	5	9	98	ND	14	35	ND	15	76	1000	3000	-1
54	5	8	104	ND	14	22	ND	18	129	1260	3700	63
56	5	18	200	ND	25	32	9	24	80	820	1800	60
57	6	30	55	9	20	27	ND	18	74	370	1900	180
58	NA	NA	NA	NA	NA	NA	NA	NA	NA	NA	NA	NA
59	2	23	50	7	14	158	7	18	106	340	1000	85
60	5	18	69	11	27	48	ND	16	92	580	2100	85
61	4	16	74	7	17	174	8	17	53	350	910	80
62	NA	NA	NA	NA	NA	NA	NA	NA	NA	NA	NA	NA
64	12	9	43	16	75	29	ND	12	74	970	7100	95
67	8	17	69	ND	15	34	ND	16	62	710	3800	NA
68	10	21	76	ND	55	29	ND	5	112	590	1600	114
69	Tr	25	74	ND	12	47	ND	13	80	290	3900	NA
70	100	23	28	ND	5	140	Tr	13	83	320	5700	129
72	11	19	57	ND	20	48	ND	17	88	300	3000	192
73	12	14	80	9	10	154	8	16	106	512	750	96
74	ND	34	55	ND	ND	19	Tr	6	129	240	1700	206
75	38	18	124	ND	23	28	ND	14	196	610	3100	NA
76	6	24	58	9	ND	25	ND	21	409	440	9400	172
77	ND	21	59	ND	10	36	ND	17	31	460	2800	104
79	5	10	23	ND	16	21	ND	20	206	320	3900	NA

Trace Element Analyses (cont'd.)

Sample Number	Cu	Pb	Zn	Ni	Cr	Co	Sn	Ga	Zr	Sr	Ba	Rb
81	ND	26	110	ND	ND	26	Tr	28	161	680	2800	123
82	6	29	68	4	5	167	Tr	16	46	370	1200	121
83	ND	29	64	ND	ND	36	Tr	26	126	220	1500	180
84	ND	31	109	ND	ND	23	Tr	27	56	185	1300	206
85	ND	34	96	ND	16	37	ND	16	60	460	320	131
86	4	17	72	7	10	43	Tr	17	133	240	1700	NA
87	ND	23	100	ND	10	98	7	19	129	190	1100	89
88	ND	38	65	ND	ND	33	Tr	27	43	220	1600	174
90	8	31	100	ND	28	24	ND	22	31	521	1300	84
91	ND	39	75	ND	ND	32	Tr	24	164	1600	2300	160
92	7	23	50	ND	13	66	Tr	14	118	500	2600	NA
93	ND	33	89	ND	ND	31	Tr	24	210	1400	2000	155
94	ND	33	52	ND	ND	28	Tr	24	50	390	2200	138
95	3	21	61	ND	11	27	Tr	16	134	390	3200	NA
96	32	19	65	ND	7	154	5	29	112	310	1400	123
97	ND	36	54	ND	ND	33	Tr	6	43	420	1800	207
98	5	16	39	ND	13	49	Tr	13	91	420	340	NA
99	5	22	112	7	12	168	7	25	97	420	1400	119
100	4	17	158	ND	12	37	ND	20	73	1100	4500	NA
101	ND	30	84	ND	11	26	ND	22	98	640	1900	69
102	5	17	107	6	10	142	9	20	90	690	1400	60
103	13	19	89	11	54	30	ND	16	49	400	770	92
104	7	19	69	ND	29	72	ND	15	74	770	3300	72
105	198	ND	30	ND	ND	48	ND	13	120	350	760	NA
110	77	22	77	87	250	95	7	10	32	140	150	NA
111	112	ND	32	81	120	40	ND	8	63	240	200	NA
112	9	10	63	ND	ND	30	ND	18	76	220	540	32
113	NA	NA	NA	NA	NA	NA	NA	NA	NA	NA	NA	NA

Trace Element Analyses (cont'd.)

Sample Number	Cu	Pb	Zn	Ni	Cr	Co	Sn	Ga	Zr	Sr	Ba	Rb
114	26	ND	51	ND	ND	39	ND	11	168	340	740	NA
115	15	13	67	8	17	57	ND	12	118	1200	2500	105
116	6	12	40	ND	25	17	ND	12	118	410	1500	60
117	NA	NA	NA	NA	NA	NA	NA	NA	NA	NA	NA	NA
118	NA	NA	NA	NA	NA	NA	NA	NA	NA	NA	NA	NA
119	NA	NA	NA	NA	NA	NA	NA	NA	NA	NA	NA	NA
120	NA	NA	NA	NA	NA	NA	NA	NA	NA	NA	NA	NA
121	NA	NA	NA	NA	NA	NA	NA	NA	NA	NA	NA	NA
122	108	9	71	46	182	101	ND	11	64	430	390	61
123	36	ND	82	19	33	46	ND	10	42	500	600	13
124	NA	NA	NA	NA	NA	NA	NA	NA	NA	NA	NA	NA
125	NA	NA	NA	NA	NA	NA	NA	NA	NA	NA	NA	NA
127	8	33	33	ND	6	105	Tr	13	126	2100	5100	152
128	7	17	71	ND	ND	20	ND	22	181	440	1800	121
132	6	19	43	ND	ND	47	ND	23	123	660	2400	120
133	NA	NA	NA	NA	NA	NA	NA	NA	NA	NA	NA	NA
134	ND	23	74	ND	5	64	ND	11	21	357	1300	192
136	3	19	67	ND	ND	27	ND	56	161	250	1200	NA
138	12	Tr	67	10	150	80	ND	12	42	533	430	20
140	ND	18	40	8	13	23	ND	5	59	500	1400	77
141	Tr	19	32	10	13	15	ND	5	50	521	1300	80
143	2	17	40	8	13	84	ND	12	77	512	1400	69
144	180	ND	51	ND	ND	44	ND	15	67	400	200	NA
145	69	8	25	20	13	41	Tr	13	106	760	1100	35
146	53	34	132	23	56	18	ND	13	104	290	4100	91
147	>200	Tr	154	16	23	23	ND	14	120	450	1700	NA
148	>200	Tr	28	17	27	32	ND	18	87	440	[illegible]	NA
149	>200	Tr	30	14	18	28	ND	14	104	360	2200	NA

Trace Element Analyses (cont'd.)

Sample Number	Cu	Pb	Zn	Ni	Cr	Co	Sn	Ga	Zr	Sr	Ba	Rb
150	81	Tr	25	16	19	53	ND	12	90	560	3100	NA
153	6	Tr	50	15	21	23	ND	14	98	380	3900	NA
156	30	Tr	26	14	21	31	ND	17	94	620	2700	NA
161	>200	Tr	55	17	21	33	ND	19	126	480	1900	NA
163	90	Tr	28	12	17	26	ND	14	81	400	2900	NA
165	29	Tr	59	14	19	35	ND	15	83	500	2000	NA
166	>200	Tr	85	15	17	54	ND	17	105	370	4500	NA
167	38	11	48	21	36	96	7	15	83	290	570	80
168	3	11	77	ND	6	168	ND	12	119	185	2500	78
169	42	Tr	62	7	8	120	9	16	87	520	270	49

Notes

(1) Analyses by emission spectroscopy. See Way (1977) for analytical methods and sample locations.

(2) Symbols: NA - not analyzed

ND - not detectable

Tr - trace (at or slightly below detection limit)

(3) Detection limits (in ppm).

Cu - 2	Cr - 3	Zr - 7
Pb - 4	Co - 3	Sr - .3
Zn - 3	Sn - 3	Ba - 2
Ni - 3	Ga - 2	Rb - 3

(4) Samples were also analyzed for Au and Ag but no values greater than 1 ppm were observed.

(5) The following specimens were taken from known mineralized showings:

#23 - 27 - Max Claims

#36 - 40 - Talbot Prospect

#144-166 - Cork Claims

ADDENDUM*

Trace Element Analyses

copyright © Dana Clark Way, 1977

---

* To accompany: Way, D. C., 1977. A reconnaissance study of granitoid plutonism in southwestern Yukon Territory; M.Sc. Thesis, Queen's University.

Trace Element Analyses

(in parts per million)

Sample Number	Cu	Pb	Zn	Ni	Cr	Co	Sn	Ga	Zr	Sr	Ba	Rb
1	22	19	18	36	112	92	Tr	16	112	470	2400	133
2	2	28	36	ND	12	126	Tr	12	74	260	2000	207
3	22	20	54	6	30	107	9	18	84	680	3300	177
4	3	17	36	7	18	71	Tr	14	101	605	3200	57
5	NA	NA	NA	NA	NA	NA	NA	NA	NA	NA	NA	NA
6	13	26	81	8	24	126	6	19	112	590	2900	185
7	17	25	59	7	19	98	Tr	13	140	1300	6300	170
8	10	19	249	8	7	138	Tr	26	300	290	8000	166
9	ND	25	88	ND	1	172	ND	14	106	130	1500	140
11	NA	NA	NA	NA	NA	NA	NA	NA	NA	NA	NA	NA
12	NA	NA	NA	NA	NA	NA	NA	NA	NA	NA	NA	NA
13	3	26	52	6	8	270	10	18	92	420	3900	167
14	9	26	101	ND	11	27	ND	18	42	500	2900	155
18	4	28	72	5	7	126	7	21	66	420	1800	163
23	133	13	32	5	12	153	ND	14	101	630	2400	102
24	190	13	66	6	11	230	ND	15	70	590	2300	210
25	>200	15	65	ND	18	44	ND	22	80	320	8400	NA
26	>200	16	72	ND	15	75	ND	16	77	440	4200	NA
21	>200	15	68	ND	16	38	ND	15	63	350	4800	NA
28	2	30	135	ND	6	156	7	37	105	4	17	213
29	5	24	70	ND	ND	36	ND	21	158	104	620	251
30	7	23	165	ND	ND	39	6	16	129	88	1200	300
31	NA	NA	NA	NA	NA	NA	NA	NA	NA	NA	NA	NA
32	ND	26	123	ND	10	29	ND	19	99	710	2800	132
36	19	28	48	4	5	230	9	16	76	101	810	134
37	9	30	65	5	5	290	9	18	87	113	970	217
38	11	28	46	ND	5	204	Tr	16	64	105	590	210

Trace Element Analyses (cont'd.)

Sample Number	Cu	Pb	Zn	Ni	Cr	Co	Sn	Ga	Zr	Sr	Ba	Nb
39	13	16	215	ND	ND	45	Tr	25	134	250	5200	NA
40	35	26	165	ND	ND	51	Tr	21	73	190	800	NA
41	3	24	92	6	10	131	7	21	112	550	2100	60
42	ND	23	120	8	19	30	ND	18	59	670	2500	158
46	25	14	120	23	83	53	Tr	21	137	440	1300	75
48	12	17	95	ND	15	47	Tr	17	125	480	2200	156
50	4	24	77	5	14	112	6	20	136	320	3800	118
52	7	15	83	5	25	113	Tr	17	115	1100	3100	102
53	5	9	98	ND	14	35	ND	15	76	1000	3000	-1
54	5	8	104	ND	14	22	ND	18	129	1260	3700	63
56	5	18	200	ND	25	32	9	24	80	820	1800	60
57	6	30	55	9	20	27	ND	18	74	370	1900	180
58	NA	NA	NA	NA	NA	NA	NA	NA	NA	NA	NA	NA
59	2	23	50	7	14	158	7	18	106	340	1000	85
60	5	18	69	11	27	48	ND	16	92	580	2100	85
61	4	16	74	7	17	174	8	17	53	350	910	80
62	NA	NA	NA	NA	NA	NA	NA	NA	NA	NA	NA	NA
64	12	9	43	16	75	29	ND	12	74	970	7100	95
67	8	17	69	ND	15	34	ND	16	62	710	3800	NA
68	10	21	76	ND	55	29	ND	5	112	590	1600	114
69	Tr	25	74	ND	12	47	ND	13	80	290	3900	NA
70	100	23	28	ND	5	140	Tr	13	83	320	5700	129
72	11	19	57	ND	20	48	ND	17	88	300	3000	192
73	12	14	80	9	10	154	8	16	106	512	750	96
74	ND	34	55	ND	ND	19	Tr	6	129	240	1700	206
75	38	18	124	ND	23	28	ND	14	196	610	3100	NA
76	6	24	58	9	ND	25	ND	21	409	440	9400	172
77	ND	21	59	ND	10	36	ND	17	31	460	2800	104
79	5	10	23	ND	16	21	ND	20	206	320	3900	NA

Trace Element Analyses (cont'd.)

Sample Number	Cu	Pb	Zn	Ni	Cr	Co	Sn	Ga	Zr	Sr	Ba	Nb
81	ND	26	110	ND	ND	26	Tr	28	161	680	2800	123
82	6	29	68	4	5	167	Tr	16	46	370	1200	121
83	ND	29	64	ND	ND	36	Tr	26	126	220	1500	180
84	ND	31	109	ND	ND	23	Tr	27	56	185	1300	206
85	ND	34	96	ND	16	37	ND	16	60	460	320	131
86	4	17	72	7	10	43	Tr	17	133	240	1700	NA
87	ND	23	100	ND	10	98	7	19	129	190	1100	89
88	ND	38	65	ND	ND	33	Tr	27	43	220	1600	174
90	8	31	100	ND	28	24	ND	22	31	521	1300	84
91	ND	39	75	ND	ND	32	Tr	24	164	1600	2300	160
92	7	23	50	ND	13	66	Tr	14	118	500	2600	NA
93	ND	33	89	ND	ND	31	Tr	24	210	1400	2000	155
94	ND	33	52	ND	ND	28	Tr	24	50	390	2200	138
95	3	21	61	ND	11	27	Tr	16	134	390	3200	NA
96	32	19	65	ND	7	154	5	29	112	310	1400	123
97	ND	36	54	ND	ND	33	Tr	6	43	420	1800	207
98	5	16	39	ND	13	49	Tr	13	91	420	340	NA
99	5	22	112	7	12	168	7	25	97	420	1400	119
100	4	17	158	ND	12	37	ND	20	73	1100	4500	NA
101	ND	30	84	ND	11	26	ND	22	98	640	1900	69
102	5	17	107	6	10	142	9	20	90	690	1400	60
103	13	19	89	11	54	30	ND	16	49	400	770	92
104	7	19	69	ND	29	72	ND	15	74	770	3300	72
105	198	ND	30	ND	ND	48	ND	13	120	350	760	NA
110	77	22	77	87	250	95	7	10	32	140	150	NA
111	112	ND	32	81	120	40	ND	8	63	240	200	NA
112	9	10	63	ND	ND	30	ND	18	76	220	540	32
113	NA	NA	NA	NA	NA	NA	NA	NA	NA	NA	NA	NA

Trace Element Analyses (cont'd.)

Sample Number	Cu	Pb	Zn	Ni	Cr	Co	Sn	Ga	Zr	Sr	Ba	Nb
114	26	ND	51	ND	ND	39	ND	11	168	340	740	NA
115	15	13	67	8	17	57	ND	12	118	1200	2500	105
116	6	12	40	ND	25	17	ND	12	118	410	1500	60
117	NA	NA	NA	NA	NA	NA	NA	NA	NA	NA	NA	NA
118	NA	NA	NA	NA	NA	NA	NA	NA	NA	NA	NA	NA
119	NA	NA	NA	NA	NA	NA	NA	NA	NA	NA	NA	NA
120	NA	NA	NA	NA	NA	NA	NA	NA	NA	NA	NA	NA
121	NA	NA	NA	NA	NA	NA	NA	NA	NA	NA	NA	NA
122	108	9	71	46	182	101	ND	11	64	430	390	61
123	36	ND	82	19	33	46	ND	10	42	500	600	13
124	NA	NA	NA	NA	NA	NA	NA	NA	NA	NA	NA	NA
125	NA	NA	NA	NA	NA	NA	NA	NA	NA	NA	NA	NA
127	8	33	33	ND	6	105	Tr	13	126	2100	5100	152
128	7	17	71	ND	ND	20	ND	22	181	440	1800	121
132	6	19	43	ND	ND	47	ND	23	123	660	2400	120
133	NA	NA	NA	NA	NA	NA	NA	NA	NA	NA	NA	NA
134	ND	23	74	ND	5	64	ND	11	21	357	1300	192
136	3	19	67	ND	ND	27	ND	56	161	250	1200	NA
138	12	Tr	67	10	150	80	ND	12	42	533	430	20
140	ND	18	40	8	13	23	ND	5	59	500	1400	77
141	Tr	19	32	10	13	15	ND	5	50	521	1300	80
143	2	17	40	8	13	84	ND	12	77	512	1400	69
144	180	ND	51	ND	ND	44	ND	15	67	400	200	NA
145	69	8	25	20	13	41	Tr	13	106	760	1100	35
146	53	34	132	23	56	18	ND	13	104	290	4100	91
147	>200	Tr	154	16	23	23	ND	14	120	450	1700	NA
148	>200	Tr	28	17	27	32	ND	18	87	440	2300	NA
149	>200	Tr	30	14	18	28	ND	14	104	360	2200	NA

Trace Element Analyses (cont'd.)

Sample Number	Cu	Pb	Zn	Ni	Cr	Co	Sn	Ga	Zr	Sr	Ba	Nb
150	81	Tr	25	16	19	53	ND	12	90	560	3100	NA
153	6	Tr	50	15	21	23	ND	14	98	380	3900	NA
156	30	Tr	26	14	21	31	ND	17	94	620	2700	NA
161	>200	Tr	55	17	21	33	ND	19	126	480	1900	NA
163	90	Tr	28	12	17	26	ND	14	81	400	2900	NA
165	29	Tr	59	14	19	35	ND	15	83	500	2000	NA
166	>200	Tr	85	15	17	54	ND	17	105	370	4500	NA
167	38	11	48	21	36	96	7	15	83	290	570	80
168	3	11	77	ND	6	168	ND	12	119	185	2500	78
169	42	Tr	62	7	8	120	9	16	87	520	270	49

Notes

(1) Analyses by emission spectroscopy. See Way (1977) for analytical methods and sample locations.

(2) Symbols: NA - not analyzed

ND - not detectable

Tr - trace (at or slightly below detection limit)

(3) Detection limits (in ppm).

Cu - 2	Cr - 3	Zr - 7
Pb - 4	Co - 3	Sr - .3
Zn - 3	Sn - 3	Ba - 2
Ni - 3	Ga - 2	Nb - 3

(4) Samples were also analyzed for Au and Ag but no values greater than 1 ppm were observed.

(5) The following specimens were taken from known mineralized showings:

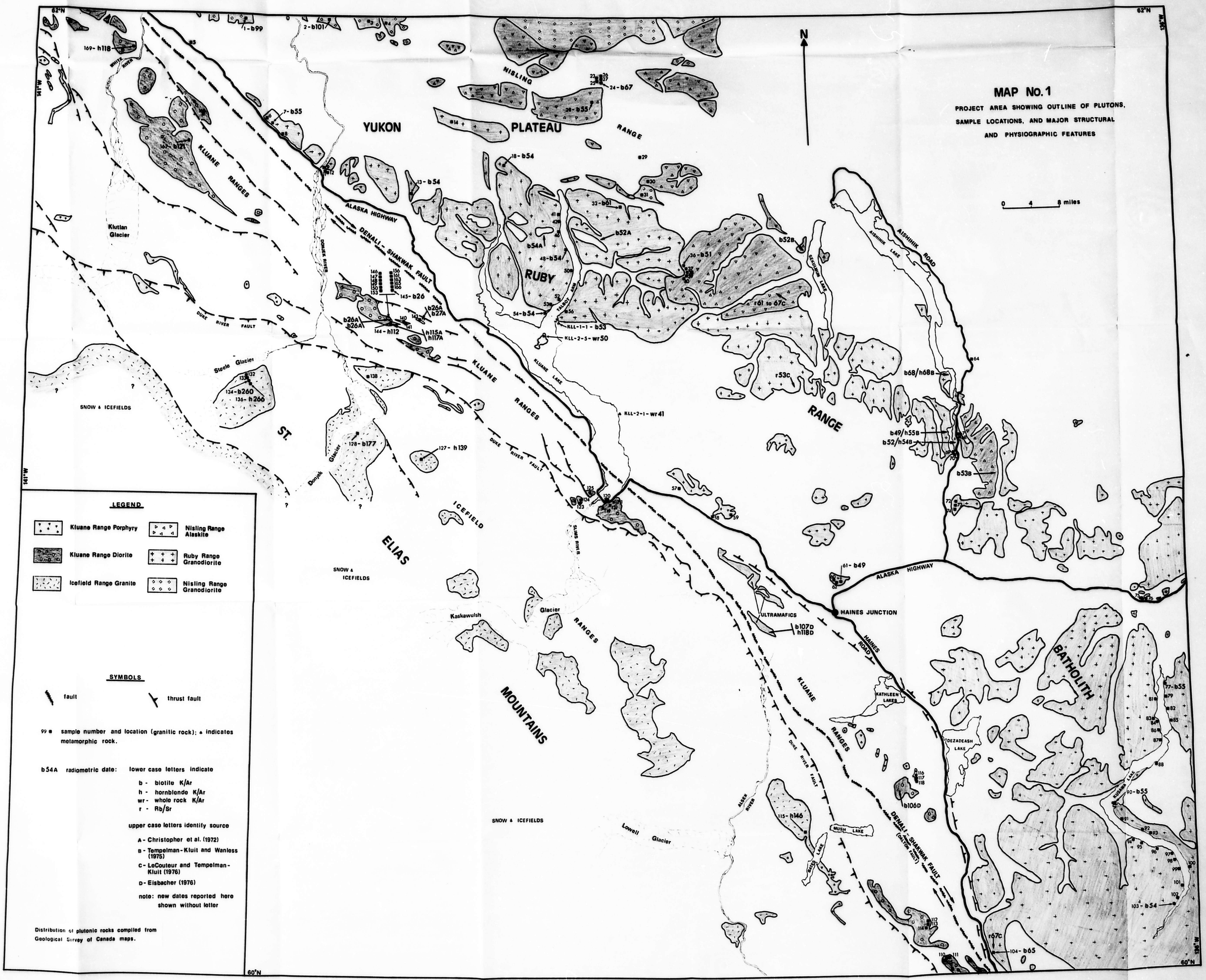
#23 - 27 - Max Claims

#36 - 40 - Talbot Prospect

#144-166 - Cork Claims

MAP No. 1

PROJECT AREA SHOWING OUTLINE OF PLUTONS, SAMPLE LOCATIONS, AND MAJOR STRUCTURAL AND PHYSIOGRAPHIC FEATURES



LEGEND

- Kluane Range Porphyry
- Kluane Range Diorite
- Icefield Range Granite
- Nisling Range Alaskite
- Ruby Range Granodiorite
- Nisling Range Granodiorite

SYMBOLS

- fault
- thrust fault

99 ● sample number and location (granitic rock); ▲ indicates metamorphic rock.

b54A radiometric date: lower case letters indicate

- b - biotite K/Ar
- h - hornblende K/Ar
- wr - whole rock K/Ar
- r - Rb/Sr

upper case letters identify source

- A - Christopher et al. (1972)
- B - Tempelman-Kluit and Wanless (1975)
- C - LeCouteur and Tempelman-Kluit (1976)
- D - Eisbacher (1976)

note: new dates reported here shown without letter

Distribution of plutonic rocks compiled from Geological Survey of Canada maps.